

Stationarity Analysis and Supervised Machine Learning
Techniques for Energy Management Forecasting

by

Hmeda Najemeddin Musbah

Submitted in partial fulfillment of the requirements
for the degree of Doctor of Philosophy

Dalhousie University

Halifax, Nova Scotia

April 2023

© Copyright by Hmeda Najemeddin Musbah, 2023

Dedication

To my Lord, Allah; to my dear mother, Aisha; and my honored father, Najemeddin. To my lovely wife, Hajer; my beloved sons, Anas and Aows; and my daughter, Asawer. To my respected brothers and sister; to my honest friends and colleagues; to all my teachers; and to those who wish me success.

TABLE OF CONTENTS

LIST OF TABLES	vi
LIST OF FIGURES	vii
ABSTRACT.....	ix
LIST OF ABBREVIATIONS AND SYMBOLS USED.....	x
ACKNOWLEDGEMENTS.....	xi
Chapter 1. Introduction.....	1
1.1 Background and Motivation.....	1
Power output.....	2
speed, and temperature	2
Power output.....	2
1.2 Thesis Objectives.....	2
1.2.1 Part 1:.....	3
1.2.2 Part 2:.....	4
1.3 Thesis Contribution	4
1.4 Thesis Outline.....	5
Chapter2. Identifying Seasonality in a Time Series by Applying Fast Fourier Transform [15].....	7
2.1 Introduction	7
2.2 Literature Review	8
2.3 Methods and Results	9
2.4 Autocorrelation Function (ACF)	14
2.5 Conclusion.....	15
2.6 SARIMA Forecasting Model of Short-Term Electric Load Data Enhanced by Fast Fourier Transform-based Seasonality Detection [16]	16
2.7 Introduction	16

2.8 Methodology and Material	17
2.9 Results and Discussion	19
2.10 CONCLUSION.....	22
Chapter3. A Proposed Novel Adaptive DC Technique for Non-Stationary Data Removal	24
3.1 Introduction	24
3.2 Literature Review	26
3.3 Removing Non-Stationarity.....	28
3.3.1 Differencing Technique	30
3.3.2 Proposed Adaptive DC Technique.....	33
3.4 Results and Discussion	36
3.5 Conclusion.....	39
Chapter4. Energy Management of Hybrid Energy System Sources Based on Machine-Learning Classification Algorithms	40
4.1 Introduction	40
4.2 Literature Review	42
4.3 Machine Learning.....	44
4.3.1 Random Forest (RF).....	45
4.3.2 Gaussian Naive Bayes (Gaussian NB)	46
4.3.3 Decision Tree (DT) algorithm	47
4.3.4 K-Nearest Neighbor (KNN)	47
4.4 Evaluating Metrics.....	48
• Precision.....	48
• Recall.....	48
• F1 Score.....	49
4.5 Data Analysis and Hybrid Energy System Description	49
4.6 Focus of the Present Research.....	52

4.7 Results and Discussion	52
4.8 Conclusion	57
Chapter5. Energy Management Using Multi-Criteria Decision Making and Machine-Learning Classification Algorithms for Intelligent Systems	58
5.1 Introduction	58
5.2 Literature Review	60
5.2.1 Power Management.....	60
5.2.2 Multi-Criteria Decision-Making (MCDM)	61
5.2.3 Machine Learning.....	63
5.3 Methodology.....	64
5.3.1 TOPSIS	64
5.3.2 Analytic Hierarchy Method (AHP).....	66
5.3.3 Fuzzy Analytic Hierarchy Method (F-AHP)	67
5.3.4 LightGBM Algorithm.....	68
5.3.5 Random Forest	69
5.4 Case Study	70
5.5 Proposed Model Framework	72
5.6 Results and Discussion	72
5.7 Conclusion	80
Chapter6. Conclusions & Future Work	81
6.1 Conclusions	81
6.2 Future Work	82
Bibliography	83
Appendix A.....	99
Appendix B.....	100
Appendix C.....	101

LIST OF TABLES

<i>TABLE 1.1 HES VARIABLES.....</i>	<i>2</i>
<i>TABLE 2.1 SUGGESTED MODELS AND THEIR AIC AND BIC.....</i>	<i>21</i>
<i>TABLE 3.1 SAMPLING OF STUDIES THAT APPLY COMMON TOOLS TO IDENTIFY AND REMOVE STATIONARITY. 28</i>	
<i>TABLE 3.2 RESULTS OF STATISTICAL TESTS OF TIME SERIES.....</i>	<i>37</i>
<i>TABLE 3.3 RESULTS OF STATISTICAL TESTS AFTER APPLYING DIFFERENCING TECHNIQUE.....</i>	<i>37</i>
<i>TABLE 3.4 RESULTS OF STATISTICAL TESTS AFTER APPLYING THE ADAPTIVE DC TECHNIQUE.</i>	<i>38</i>
<i>TABLE 4.1 ENCODED VALUES FOR DIFFERENT CLASSES.....</i>	<i>49</i>
<i>TABLE 4.2 OVERALL ACCURACY OF ALGORITHMS.....</i>	<i>52</i>
<i>TABLE 5.1 SCALE OF RELATIVE IMPORTANCE.....</i>	<i>67</i>
<i>TABLE 5.2 RANDOM CONSISTENCY OF A RANDOMLY GENERATED PAIRWISE COMPARISON MATRIX.....</i>	<i>67</i>
<i>TABLE 5.3 COMPARISON BETWEEN LIGHTGBM AND OTHER CLASSIFICATION ALGORITHMS.....</i>	<i>70</i>
<i>TABLE 5.4 COMPARISON BETWEEN RANDOM FOREST AND OTHER CLASSIFICATION ALGORITHMS.</i>	<i>70</i>
<i>TABLE 5.5 DIFFERENT ALTERNATIVES OF HYBRID ENERGY SOURCES.....</i>	<i>72</i>
<i>TABLE 5.6 DECISION MATRIX AT 34.2 KW.....</i>	<i>72</i>
<i>TABLE 5.7 NORMALIZED MATRIX.....</i>	<i>73</i>
<i>TABLE 5.8 PAIRWISE COMPARISON MATRIX.....</i>	<i>74</i>
<i>TABLE 5.9 NORMALIZED PAIRWISE COMPARISON MATRIX.....</i>	<i>74</i>
<i>TABLE 5. 10 PERFORMANCE SCORE OF HYBRID ENERGY SOURCES BASED ON AHP.....</i>	<i>75</i>
<i>TABLE 5.11 PAIRWISE COMPARISON MATRIX IN FUZZY NUMBERS.....</i>	<i>75</i>
<i>TABLE 5.12 FUZZY GEOMETRIC MEAN FOR EACH CRITERION.....</i>	<i>76</i>
<i>TABLE 5.13 FUZZY WEIGHT OF THE ITH CRITERION.....</i>	<i>76</i>
<i>TABLE 5.14 DE-FUZZIFICATION OF THE FUZZY WEIGHT OF THE ITH CRITERION.....</i>	<i>76</i>
<i>TABLE 5.15 PERFORMANCE SCORE OF HYBRID ENERGY SOURCES BASED ON F-AHP.....</i>	<i>77</i>

LIST OF FIGURES

<i>FIGURE 1.1 BOX-JENKINS APPROACH.</i>	3
<i>FIGURE 1.2 BREAKDOWN SUMMARY OF THESIS CONTRIBUTIONS.</i>	5
<i>FIGURE 2.1 A) TIME SERIES OF DAILY TEMPERATURE DATA. B) FFT OUTPUT OF MEAN DAILY TEMPERATURE.</i>	10
<i>FIGURE 2.2 A) TIME SERIES OF MONTHLY WIND DATA. B) RESULTS OF RUNNING FFT.</i>	10
<i>FIGURE 2.3 A) TIME SERIES OF HOURLY INTERNET TRAFFIC DATA. B) OUTPUT OF FFT FOR THE TIME SERIES OF HOURLY INTERNET TRAFFIC DATA.</i>	11
<i>FIGURE 2.4 A) TIME SERIES OF MONTHLY SUTTER COUNTY WORKFORCE. B) COMPONENT THAT FORMS THE TIME SERIES OF THE MONTHLY SUTTER COUNTY WORKFORCE.</i>	12
<i>FIGURE 2.5 A) MONTHLY CIVILIAN LABOUR FORCE. B) RESULTS OF RUNNING FFT.</i>	12
<i>FIGURE 2.6 A) TIME SERIES OF MONTHLY NIGERIAN POWER CONSUMPTION. B) RESULTS OF APPLYING FFT TO THE TIME SERIES OF MONTHLY NIGERIAN POWER CONSUMPTION.</i>	13
<i>FIGURE 2.7 A) TIME SERIES OF ANNUAL UNEMPLOYMENT. B) OUTPUT OF APPLYING FFT TO THE TIME SERIES OF ANNUAL UNEMPLOYMENT.</i>	13
<i>FIGURE 2.8 OUTPUT OF ACF FOR THE TIME SERIES OF MONTHLY WIND SPEED.</i>	14
<i>FIGURE 2.9 OUTPUT OF ACF FOR THE TIME SERIES OF AN ELECTRICAL LOAD.</i>	15
<i>FIGURE 2.10 HOURLY ELECTRICAL LOAD DATA.</i>	19
<i>FIGURE 2.11 TIME SERIES OF ELECTRIC LOAD DATA IN FREQUENCY DOMAIN.</i>	20
<i>FIGURE 2.12 RESIDUAL PLOTS OF ELECTRICAL LOAD DATA.</i>	21
<i>FIGURE 2.13 FORECASTING 24 HOURS OF ELECTRICAL LOAD DATA.</i>	22
<i>FIGURE 3.1 VARIOUS CASES OF NON-STATIONARY DATA. A) TIME DEPENDENT MEAN. B) TIME DEPENDENT VARIANCE.</i>	25
<i>FIGURE 3.2 FLOWCHART OF BOX-JENKINS STEPS.</i>	25
<i>FIGURE 3.3 FLOWCHART SHOWING THE FIRST STAGE IN THE BOX-JENKINS APPROACH.</i>	26
<i>FIGURE 3.4 HOURLY DIESEL PRICES.</i>	29
<i>FIGURE 3.5 HOURLY GASOLINE PRICES.</i>	29
<i>FIGURE 3.6 DAILY TEMPERATURE.</i>	29
<i>FIGURE 3.7 HOURLY LOAD.</i>	30
<i>FIGURE 3.8 THE NUMBER OF INTERNET USERS.</i>	30
<i>FIGURE 3.9 DIFFERENCING OF THE TIME SERIES OF DIESEL PRICE.</i>	31
<i>FIGURE 3.10 DIFFERENCING OF THE TIME SERIES OF DIESEL PRICE.</i>	31
<i>FIGURE 3.11 DIFFERENCING OF THE TIME SERIES OF TEMPERATURE.</i>	32
<i>FIGURE 3.12 DIFFERENCING OF THE TIME SERIES OF LOAD.</i>	32
<i>FIGURE 3.13 DIFFERENCING OF THE TIME SERIES OF THE NUMBER OF INTERNET USERS.</i>	33

<i>FIGURE 3.14 ADAPTIVE DC TECHNIQUE FLOWCHART.</i>	34
<i>FIGURE 3.15 ADAPTIVE DC TECHNIQUE OF DIESEL.</i>	34
<i>FIGURE 3.16 ADAPTIVE DC TECHNIQUE OF GASOLINE.</i>	35
<i>FIGURE 3.17 ADAPTIVE DC TECHNIQUE OF TEMPERATURE.</i>	35
<i>FIGURE 3.18 ADAPTIVE DC TECHNIQUE OF LOAD.</i>	36
<i>FIGURE 3.19 ADAPTIVE DC TECHNIQUE OF THE NUMBER OF INTERNET USERS.</i>	36
<i>FIGURE 3.20 2ND DIFFERENCING OF THE TIME SERIES OF THE NUMBER OF INTERNET USERS.</i>	38
<i>FIGURE 4.1 COMMON METHODOLOGY.</i>	41
<i>FIGURE 4.2 TWO MAIN STEPS IN ACHIEVING ML ALGORITHMS</i>	45
<i>FIGURE 4.3 MAIN STEPS INVOLVED IN THE RANDOM FOREST (RF) ALGORITHM.</i>	46
<i>FIGURE 4.4 GAUSSIAN NAIVE BAYES ALGORITHM FLOWCHART.</i>	46
<i>FIGURE 4.5 THE FLOWCHART OF DT ALGORITHM.</i>	47
<i>FIGURE 4.6 GRAPHICAL DISTRIBUTION OF TEMPERATURE.</i>	50
<i>FIGURE 4.7 GRAPHICAL DISTRIBUTION OF LOAD.</i>	50
<i>FIGURE 4.8 GRAPHICAL DISTRIBUTION OF THE AVAILABILITY OF SUN.</i>	51
<i>FIGURE 4.9 GRAPHICAL DISTRIBUTION OF THE AVAILABILITY OF WIND.</i>	51
<i>FIGURE 4.10 PRECISION METRIC.</i>	53
<i>FIGURE 4.11 RECALL METRIC.</i>	53
<i>FIGURE 4.12 F1-SCORE METRIC.</i>	54
<i>FIGURE 4.13 PRECISION METRIC: KNN ALGORITHM PERFORMANCE POST-DATASET STANDARDIZING.</i>	55
<i>FIGURE 4.14 RECALL METRIC: KNN ALGORITHM PERFORMANCE POST-DATASET STANDARDIZING.</i>	55
<i>FIGURE 4.15 F1 SCORE METRIC: KNN ALGORITHM PERFORMANCE POST-DATASET STANDARDIZING.</i>	56
<i>FIGURE 4.16 CONFUSION MATRIX OF THE ALGORITHMS.</i>	56
<i>FIGURE 5.1 HIERARCHICAL TREE OF CRITERIA FOR AHP ANALYSIS.</i>	66
<i>FIGURE 5.2 OVERALL PROCESS OF PROPOSED EM OF THE HES MODEL.</i>	73
<i>FIGURE 5.3 RANK OF THE HES AT 23 kW.</i>	78
<i>FIGURE 5.4 RANK OF THE HES AT 66 kW.</i>	78
<i>FIGURE 5.5 RANK OF THE HES AT 76 kW.</i>	79
<i>FIGURE 5.6 CONFUSION MATRIX.</i>	80

ABSTRACT

One of the most realistic solutions to the problem of power outages in remote areas is hybrid energy sources (HES). Forecasting is necessary because HES uses renewable energy sources, which are often either intermittent or insufficient. By directly influencing planning and management techniques, forecasting plays a crucial part in energy systems. Due to electronic devices shutting down as a result of generating unwanted harmonics that degrade the system's quality, inaccurate forecasting can lead businesses to lose money. Choosing a trustworthy and efficient forecasting model is crucial.

In this thesis, regression and classification are the two supervised machine learning techniques used for prediction of renewables. There are two sections to the thesis. The regression using the ARIMA model is covered in the first section. Three studies on ARIMA are presented in order to examine the stationarity of a time series. The third study suggests a novel technique that involves moving non-stationary data to a domain that deals with it as a stationary time series. The first two studies provide a new technique to test stationarity. The thesis' second section, on classification, focuses on a new approach to energy management. To create a new dataset that may be used to anticipate energy management (EM), the new technique advises gathering the outcomes of energy management from many decision-making procedures throughout a range of time periods.

LIST OF ABBREVIATIONS AND SYMBOLS USED

1 st diff	First Differencing
ACF	Autocorrelation Function
ADF	Augmented Dickey Fuller
AHP	Analytic Hierarchy Process
ARIMA	Autoregressive Integrated Moving Average
AR	Autoregressive
DT	Decision Tree
EM	Energy Management
EMS	Energy Management Strategy
HES	Hybrid Energy System(s)
F-AHP	Fuzzy Analytic Hierarchy Process
FFT	Fast Fourier Transform
KNN	K-Nearest Neighbor
MA	Moving Average
MCDM	Multiple-Criteria Decision-Making
ML	Machine learning
NB	Gaussian Naive Bayes
RF	Random Forest
SARIMA	Seasonal Autoregressive Integrated Moving Average
SAR	Seasonal Autoregressive
SMA	Seasonal Moving Average

ACKNOWLEDGEMENTS

I want to express my gratitude to God, Allah, for his help and mercy in completing this thesis. I am deeply indebted to everyone who contributed to this work, especially my supervisors, Dr. Tim Little, and Dr. Hamed Aly, for their valuable advice and unwavering belief in the success of this work.

I would like to extend my special thanks to the Libyan Ministry for Higher Education for its financial assistance in the form of scholarships.

Finally, I owe a great deal of thanks to my mother, brothers, and sister for their support throughout my personal and professional education.

Most importantly, I am deeply grateful to my wife, Dr. Hajer Ramadan, who provided me with constant encouragement, support, and love throughout my PhD work.

Chapter 1. Introduction

1.1 Background and Motivation

Electricity is one of the most critical factors affecting the growth of developing nations, but 17% of the world's population still has no access to reliable electrical power [1]. The main sources of electricity for people living in remote areas are diesel and gasoline generators [2]. Aboriginal Affairs and Northern Development Canada (AANDC) has reported that the negative impacts of using diesel and gasoline generators fall under the three main categories of environmental, social, and economic sustainability. Lumos Energy stated that these impacts could be mitigated by using renewable energy sources [3], yet renewables also have some disadvantages. For example, some renewable energy sources such as wind and solar may be insufficient and only sporadically available [4]. Overcoming these issues can be achieved by using Hybrid energy sources HES [5].

HES contain one or more sources of renewable energy and can also be combined with one or more conventional energy sources. All these sources work in standalone or grid-connected mode [6]. Solar and wind energy are the main hybrid sources that combine with other sources to form HES in remote areas. Numerous studies have been conducted on HES, covering different topics such as forecasting and Energy Management EM. Forecasting plays a vital role in HES, as it gives designers a clear idea about the behavior of HES variables, such as weather conditions and load over short time periods. Table (1.1) shows the typical number of variables usually predicted when studying HES.

One of the biggest concerns that should be considered when building HES is the continuity of electricity flowing to the load. This concern can be solved by the application of a robust Energy Management Strategy (EMS), as it increases the lifetime of the components and protects them from overload damage [7]. The common methods employed to achieve EMS are linear programming, software, and artificial intelligence (AI), such as differential evolution algorithm, particle swarm optimization, genetic algorithm, and artificial neural networks [8].

Table 1.1 HES Variables

Reference	Year	Variables	Method	HES
[8]	2014	Solar irradiance, wind Speed, and fuel price	Empirical Mode Decomposition (EMD), Cascade-Forward Neural Network (CFNN)	Wind farm, solar farm, fuel cell and conventional thermal power plant
[9]	2014	Power output	Autoregressive Moving Average model with Exogenous inputs (ARMAX)	Grid-connected photovoltaic system
[10]	2015	Solar irradiance, wind speed, and temperature	Autoregressive (AR) model	Solar and wind energy system
[11]	2017	Wind speed	Model combining Fourier series and Autoregressive Moving Average (ARMA)	Nuclear power plant, wind farm, battery storage, natural gas boiler, and chemical plant
[12], [13]	2019	Solar radiation, ambient temperature, and wind speed	Artificial Neural Network (ANN)	Solar and wind energy system
[14]	2022	Power output	IDGC-GRNN and IDGC-RBFNN	Solar and wind

1.2 Thesis Objectives

This thesis provides a comprehensive study of HES, covering renewable energy sources (solar and wind energy) and traditional sources (gasoline and diesel generators). The work is divided into two main parts. The first part focuses on studying the initial step in the Box-Jenkins approach, as illustrated in Figure (1.1). This step contains two processes, namely detection and transformation. The detection process, which includes autocorrelation function (ACF) and statistical tests, checks to see whether the time series is stationary.

If it is stationary, we proceed to the Box-Jenkins's approach. Otherwise, the time series is transformed to stationary in the transformation process. The transformation can be done using the differencing method or the logarithmic transformation approach based on the used data. These processes could be done in more than one step. In thesis a novel technique is proposed to convert nonstationary data to stationary from the first step and compared with previous work done. The second part of this thesis shines new light on EM by proposing a novel concept for achieving an energy management strategy. The new concept suggests collecting EM results from conventional

methods to form a new dataset that can be used in forecasting EM, instead of relying on the other methods.

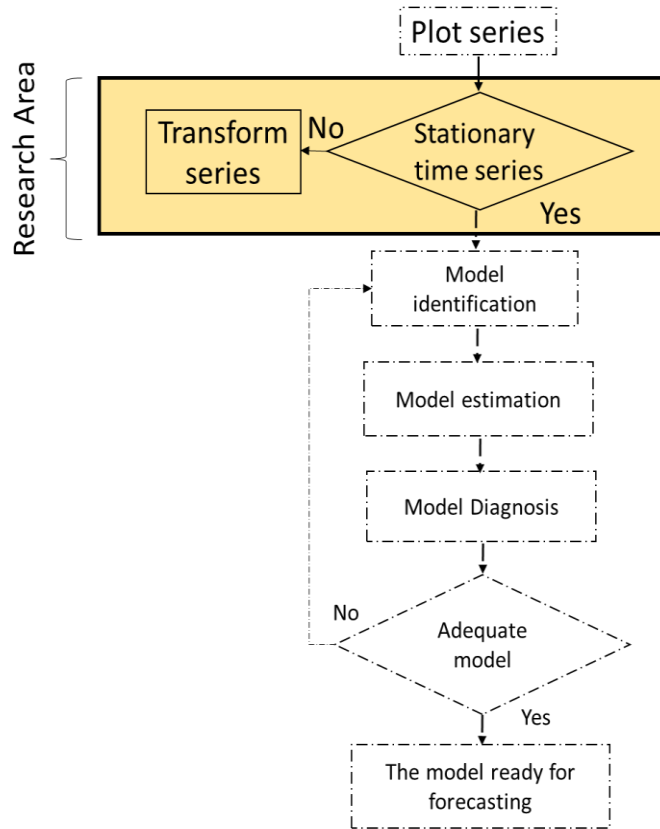


Figure 1.1 Box-Jenkins approach.

The objectives of this thesis are listed below.

1.2.1 Part 1:

1. Leveraging the Fast Fourier Transform (FFT) concept to detect trends and seasonal components in a time series.
2. Applying FFT instead of Autocorrelation Function (ACF) in a Box-Jenkins's algorithm.
3. Comparing FFT results to those of ACF.
4. Introducing a new technique to remove the trend and seasonal components from the first step and compare it to other techniques to validate the proposed work.

1.2.2 Part 2:

1. Developing a HES consisting of renewable and traditional energy sources based on machine-learning algorithms.
2. Proposing an optimal HES that is based on the technique for order of preference by similarity to the ideal solution (TOPSIS), using different combinations to minimize fossil fuel emissions and the overall cost.
3. Calculating five criteria based on the time series load data to evaluate different combinations of sources.
4. Synthesizing the dataset from the TOPSIS method results, which can then be used in forecasting the sources that should be connected to the load.
5. Validating the proposed work by using different intelligent approaches.

1.3 Thesis Contribution

Achieving the thesis objectives has already resulted in several contributions, including two conference papers [15] [16] and three published journal articles [17] [7], [18]. A summary of the contributions is given below:

- The work in [15] proposes using the FFT technique for detecting trend and seasonal components in a time series. The results are compared to the ACF to evaluate its performance. The results show that the proposed FFT outperforms ACF in most cases. Electrical load data is used as a case study in [16].
- The work in [17] proposes a novel adaptive DC technique to improve the forecasting of any nonlinear datasets like most renewables to enhance the system's reliability. This technique removes the trend component from a time series and makes it a stationary time series. The results of the proposed technique are compared with the differencing technique as a way to validate the proposed work, proving its effectiveness. To evaluate the performance of the proposed technique in removing the trend, ACF is used for both methods.
- The work in [7] proposes a new methodology to achieve EMS based on machine-learning classification algorithms such as Random Forest (RF), Decision Tree (DT), Gaussian Naive

Bayes (Gaussian NB), and K-Nearest Neighbors (KNN). The new methodology is applied to a dataset that was collected from a common method. It is found that the DT algorithm achieved the best performance compared to the RF and Gaussian NB algorithms, while the KNN algorithm presents a weak performance, especially over class 3. After standardizing the dataset, the KNN algorithm is able to compete with RF and Gaussian NB algorithms in some of the classes.

- The proposed work in [18] presents energy management using multi-criteria decision-making and machine-learning classification algorithms for intelligent systems. The work is divided into two stages. In the first stage, a historical load dataset is used to model and calculate the five criteria. TOPSIS method results are combined with the five criteria and the load dataset to synthesize an artificial dataset. In the second stage, machine-learning algorithms, namely random forest (RF) and light gradient boosted machine (LightGBM) are used to predict the combination of the energy sources to validate the proposed work. Evaluating the algorithms shows the superiority of the RF algorithm, with an accuracy of 81.81%, over LightGBM, with an accuracy of 68.6% respectively.

A breakdown summary of the thesis contributions is illustrated in Figure 1.2.

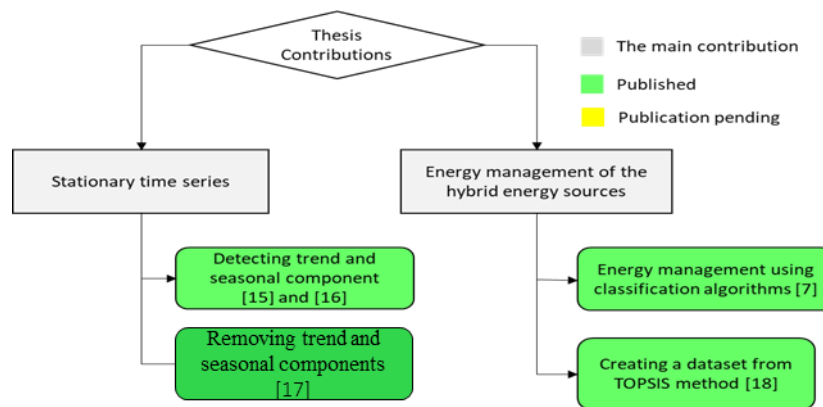


Figure 1. 2 Breakdown summary of thesis contributions.

1.4 Thesis Outline

The thesis is organized into six chapters, as detailed below:

- Chapter 2 introduces an overview of a non-stationary time series and evaluates the performance of the Fast Fourier Transform (FFT) in detecting the trend and seasonal components in the time series. The FFT is used to enhance the SARIMA model to forecast short-term electrical load data.
- Chapter 3 proposes a new method to remove the trend component. The method is validated by comparing its results with those in the relevant literature.
- Chapter 4 presents an energy management strategy hybrid energy systems sources based on machine-learning classification algorithms.
- Chapter 5 presents an energy management strategy that uses multi-criteria decision-making and machine-learning classification algorithms for intelligent systems.
- Chapter 6 provides the conclusions for the thesis and suggests future research directions.

Chapter2. Identifying Seasonality in a Time Series by Applying Fast Fourier Transform [15]

(The materials presented in this chapter are based on conference papers published in IEEE Canada Electric Power Conference, EPEC 2019 [15], and the Canadian Conference on Electrical and Computer Engineering, CCECE 2019 [16].)

Abstract

Studying time series characteristics is essential, as most forecasting models assume that time series must be stationary. In addition, non-stationary time series can cause unexpected behaviors or create a non-existent relationship between two variables. This chapter aims to shine new light on the Fast Fourier Transform (FFT) technique by examining its efficiency in identifying trends and seasonality and applying it to different time series, these series were recorded over different time scales. A comparison between FFT and the Autocorrelation Function (ACF) is conducted. The results show that FFT successfully identifies trends and seasonality. The most obvious observation is that, unlike the FFT technique, ACF has limitations in determining the exact seasonality time that repeats itself.

2.1 Introduction

Several studies have been conducted on time series because of their importance in planning and decision-making. Researchers are interested in studying and analyzing the time series, along their trend, seasonal, cycle, and random components. Understanding the behavior of these components helps build a successful model that can clarify the data to allow for prediction. A stationary time series [19] occurs when the mean, variance, and autocorrelation are constant along a period of the time series. A stationary time series is especially crucial to understand, as a non-stationary time series can be very difficult to predict, and therefore cannot be modeled or forecasted. The results gathered from a non-stationary time series can be false or misleading, in particular when there is a non-existent relationship between two variables. Also, some models and approaches, such as the Box-Jenkins approach [19], assume that the time series should be stationary [20].

Trend and seasonal components can turn a stationary time series into a non-stationary one. These two components occur when the mean and variance fluctuate over time. Therefore, many

researchers have looked for ways to detect whether there is a trend or seasonal component in a time series.

In this chapter, the Fast Fourier Transform algorithm has been applied to different datasets to evaluate its performance in detecting seasonal components. ACF is used to validate the results of FFT.

2.2 Literature Review

In [21], four graphical techniques, a run sequence plot, a seasonal sub-series plot, multiple box plots, and an autocorrelation plot were used to detect the seasonality in a time series. The authors stated that to employ a seasonal subseries plot and box plot, the seasonal periods must be known. Likewise, [22] mentioned that the time plot of the whole series could be used to identify the seasonality by determining whether there are repeated peaks and troughs in regular periods, that have similar magnitude.

The Buys Ballot table has been used to detect the presence of trends and seasonal effects in time series [23]. Several graphics that were proposed by the Buys Ballot table were employed to check the existence of seasonality [24]. Besides graphical techniques, other statistical tests could be used to identify seasonality. These tests were summarized in [21] into three groups: the χ^2 Goodness-of-Fit test, the Kolmogorov-Smirnov goodness-of-fit test, and the Nonparametric test. The authors applied different types of tests to the row variances of the Buys Ballot table, with the Student t -test and Wilcoxon Signed-Ranks test showing promising results in the detection of seasonality. Wind speed in winter and summer have been compared to study seasonality by applying various signal processing techniques. Continuous Wavelet Transform [25] identified the seasonality of wind speeds in winter and summer time series.

In [26], the historical rainfall data at Ilorin, North Central Nigeria was studied. The authors used Mann-Kendell trend analysis, the Augmented Dickey-Fuller (ADF) test, and ACF to identify the trend component. The results showed that the observed data was non-stationary. Additionally, they used Fourier Transform to convert the historical rainfall data from the time domain to the frequency domain to detect seasonality. The authors stated that the historical rainfall data showed seasonality every 12, 6, and 4 months.

In [27], the Box-Jenkins's algorithm was used for forecasting. This study focused on building a statistical model for forecasting the monthly average surface temperature in Ghana's Brong-Ahafo region to understand the dynamics of the events. The authors used ACF and decomposing to determine the seasonality. All these approaches confirmed the presence of seasonality. ACF plays a vital role in the Box-Jenkins algorithm, which is considered the main tool for identifying trend and seasonal components. In [28], the researchers affirmed that seasonality must be significant; otherwise, the ACF tool cannot detect it.

2.3 Methods and Results

FFT is used widely in signal processing and data analysis. This technique is a way to convert the time series from a time domain to a frequency domain. The number of computations in FFT is less than in Discrete Fourier Transform (DFT), because FFT reduces the complexity of computing by using the factor $N/2 \log N$, where N is the number of points [29]. The FFT algorithm is also useful for identifying seasonality in a time series [26].

Figures (2.1a), (2.2a) show mean daily temperature and monthly wind data, respectively, plotted as a time series. The time series of mean daily temperature has a low frequency of regular pattern showing small rough edges throughout the sine wave. The time series of monthly wind has a smooth regular pattern up and down. The most important concept regarding output of FFT is the significant spikes and their locations. Figure (2.1b) shows the FFT output of mean daily temperature. The time series is formed from one frequency that is represented by a significant spike, indicating a seasonality. The time series tends to repeat itself every 365 days. In contrast, Figure (2.2b) shows the results of running the FFT technique. The significant spike located at $3.445 \times 10^{-8} \text{ Hz}$ means the time series of wind speed tends to iterate itself every 12 months. Neither the mean daily temperature times series nor the monthly wind the time series needs to apply FFT or any other techniques, as the presence of seasonality is obvious. However, FFT is still required to determine the time in which the series repeats itself.

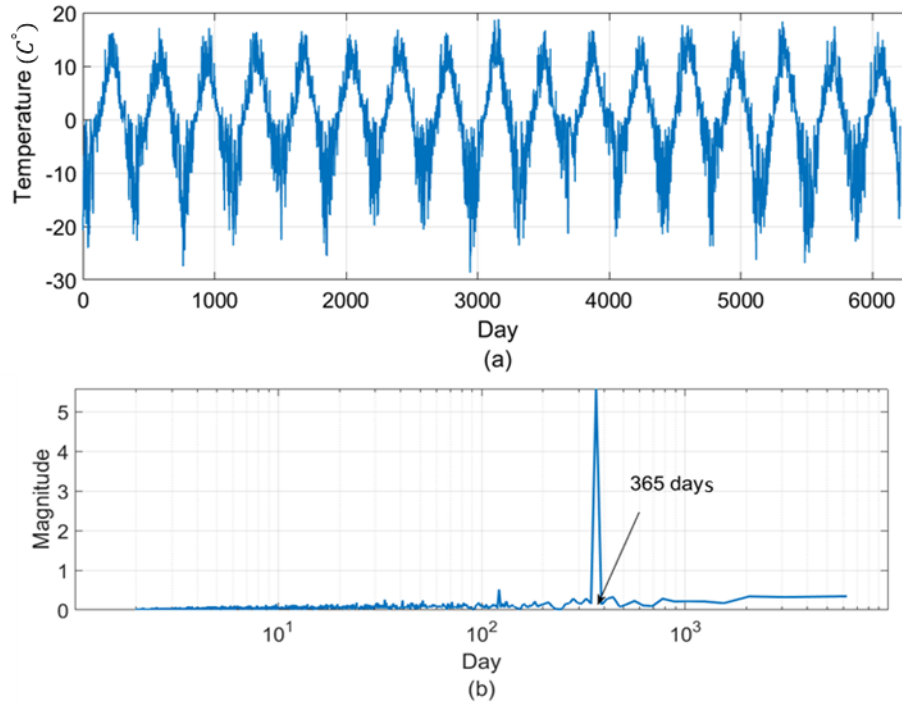


Figure 2.1 a) Time series of daily temperature data. b) FFT output of mean daily temperature.

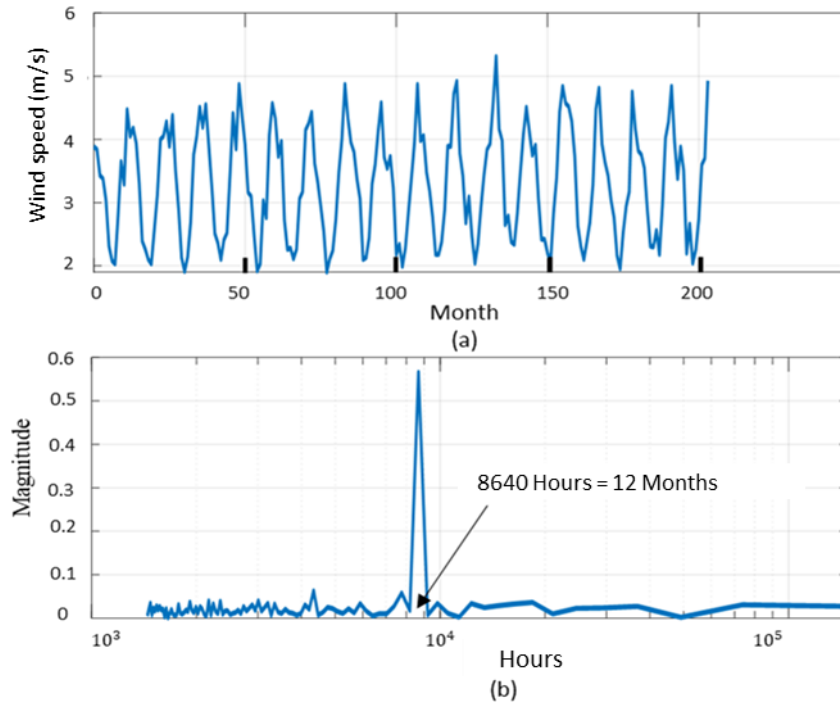


Figure 2.2 a) Time series of monthly wind data. b) Results of running FFT.

Figure (2.3a) shows the time series of hourly internet traffic data, with noticeable protrusions of seasonality. This is illustrated in the frequency domains, as shown in Figure (2.3b). The significant spike tends to repeat itself every 23 hours, and there are harmonics and noise components.

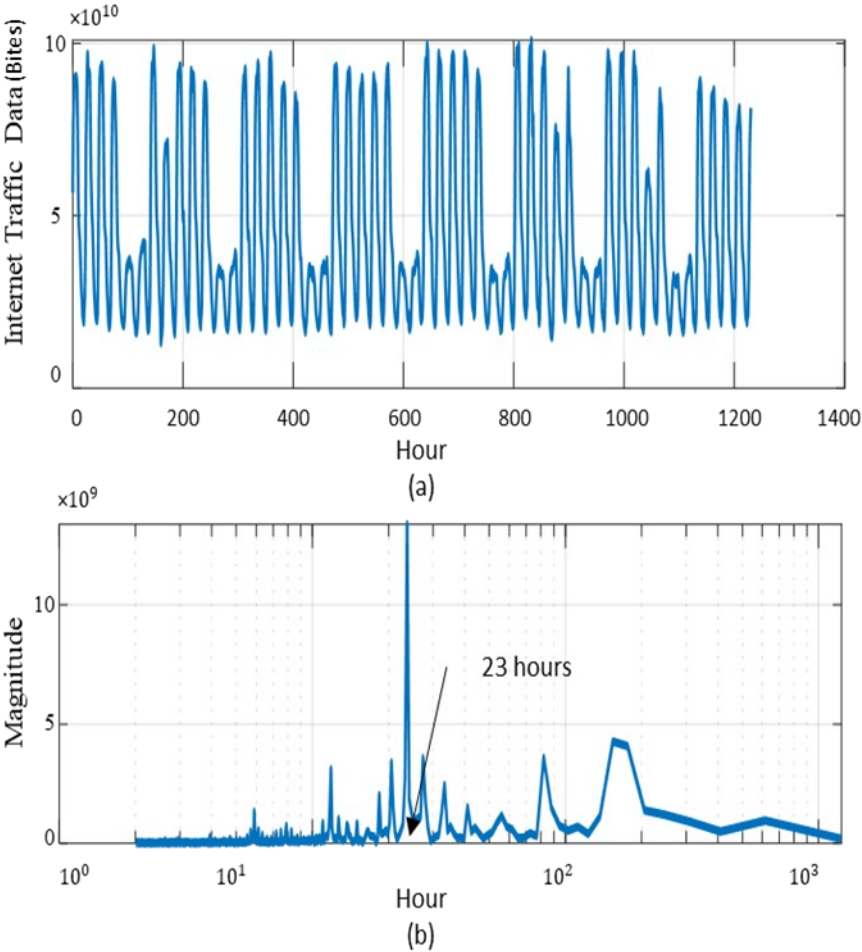


Figure 2.3 a) Time series of hourly internet traffic data. b) Output of FFT for the time series of hourly internet traffic data.

Figure (2.4a) displays the time series of the monthly Sutter County workforce, while Figure (2.4b) illustrates several spikes located at different times. The significant spike indicates that the time series of the monthly Sutter County workforce exhibits seasonality that repeats itself every 12 months. Figures (2.5a) and (2.6a) show the time series of the monthly civilian labor force and Nigerian power consumption, respectively. Without a doubt, the FFT results demonstrate that there

is no seasonality in both time series, civilian labor force and Nigerian power consumption, as shown in Figures (2.5b) and (2.6b), respectively.

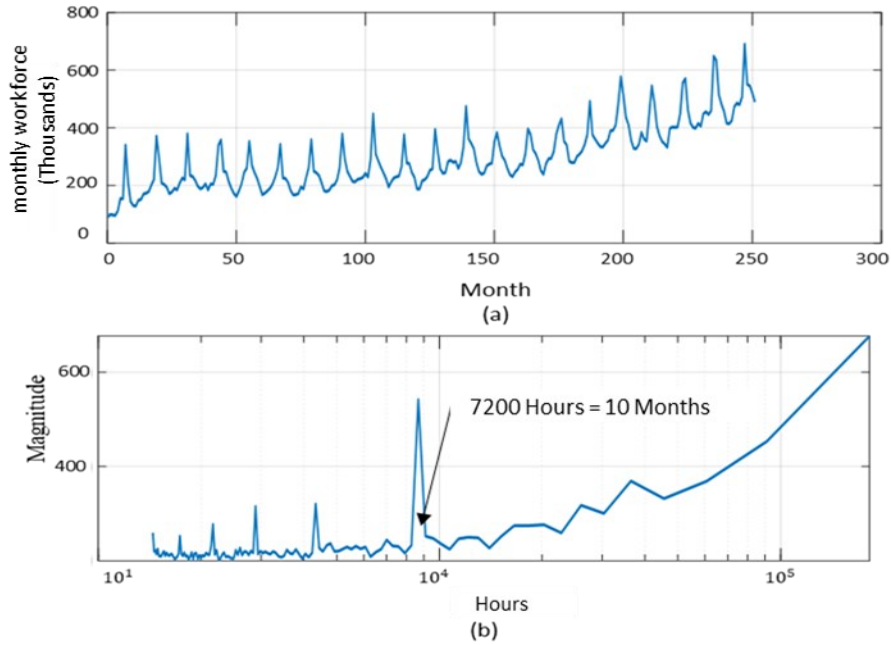


Figure 2.4 a) Time series of monthly Sutter County workforce. b) Component that forms the time series of the monthly Sutter County workforce.

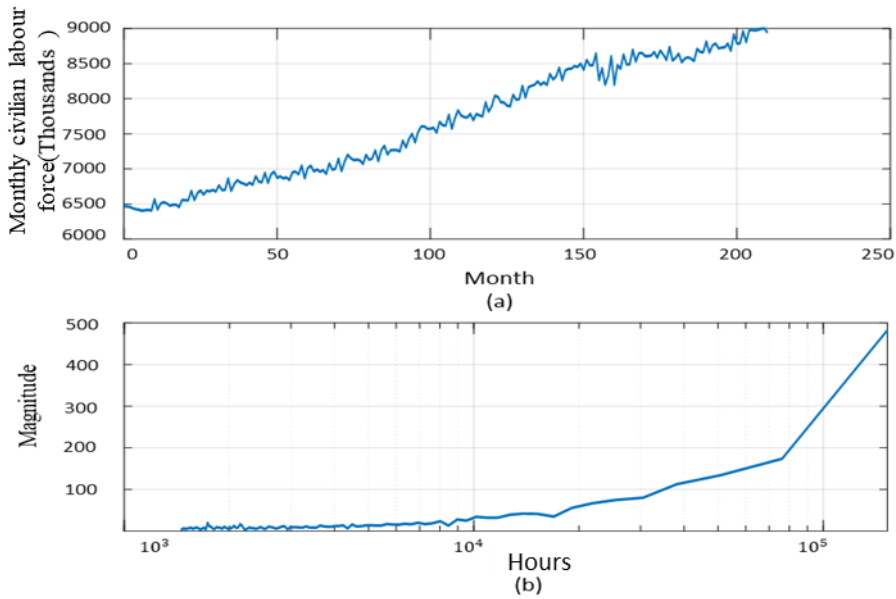


Figure 2.5 a) Monthly civilian labour force. b) Results of running FFT.

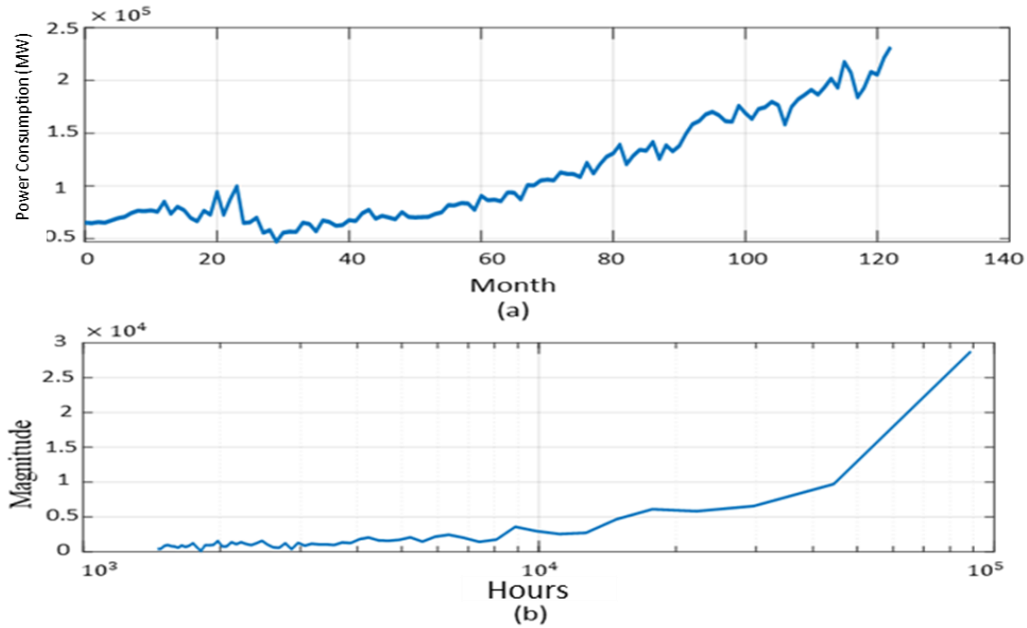


Figure 2.6 a) Time series of monthly Nigerian power consumption. b) Results of applying FFT to the time series of monthly Nigerian power consumption.

Figure (2.7a) shows time series of annual unemployment. The output of running FFT displays insignificant spikes, as shown in Figure (2.7b). From this figure, we can see that the time series of annual unemployment does not include a seasonal component.

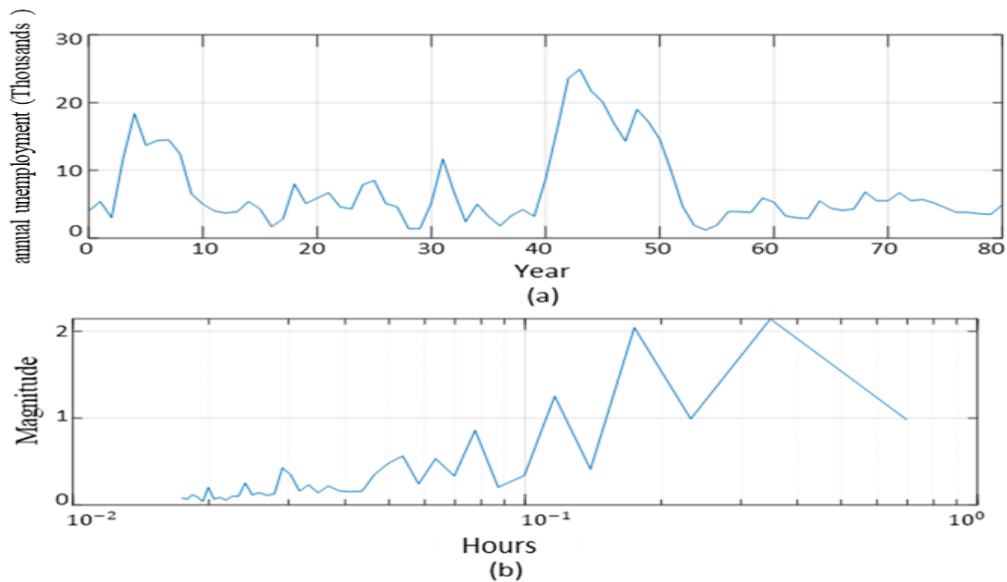


Figure 2.7 a) Time series of annual unemployment. b) Output of applying FFT to the time series of annual unemployment.

2.4 Autocorrelation Function (ACF)

ACF measures the relation between every two consecutive observations in a time series. The ACF coefficient $r_1, r_2, r_3, \dots, r_h$ measures the relationship between x_t and x_{t-1} , x_t and x_{t-2} , x_t and $x_{t-3} \dots x_n$ and x_{t-n} , respectively. The coefficient of r_h can be written as:

$$r_h = \frac{\text{Autocovariance function at lag } h}{\text{Variance of the time series}} = \frac{\sum_{t=1}^{n-h} (x_t - \bar{x})(x_{t+h} - \bar{x})}{\sum_{t=1}^n (x_t - \bar{x})^2} \quad (2.1)$$

Where x_t is the observation at any time, \bar{x} is the mean of the time series, and h is the difference of two moments in time, called a lag. The lag can be calculated as:

$$h = t - s \quad (2.2)$$

Several studies have used ACF to determine whether the time series is stationary or not and to identify the existence of seasonality [26], [27], [16].

Figure (2.8) shows the output of ACF of the time series of monthly wind speed. The results are compared to those for FFT in Figure (2.2b). The ACF plot illustrates a sine wave with minimal reduction in length as the lag increases, which results in a tailing off. The spikes at lags 1, 12, and 24 for monthly data indicate that seasonality repeats itself every 12 months. This result supports the FFT technique.

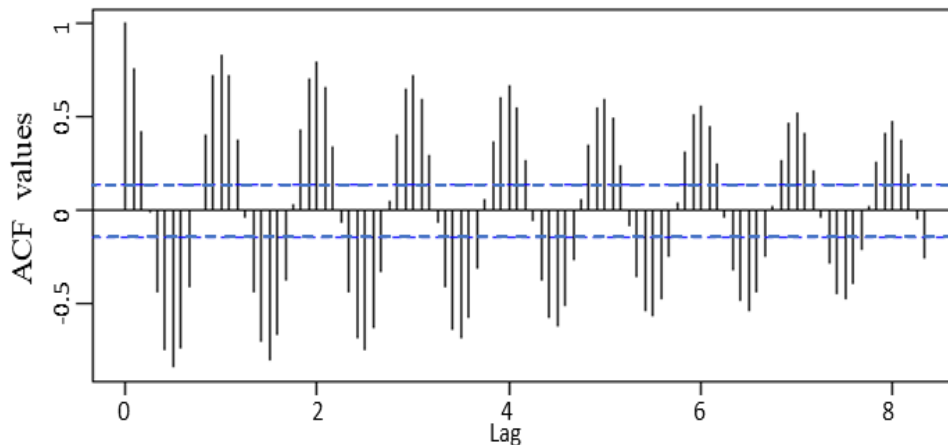


Figure 2.8 Output of ACF for the time series of monthly wind speed.

Figure (2.9) shows the output of ACF for the time series of electrical load. ACF has significant positive spikes at lags 24, 48, and 72 for hourly data. In comparing these results to those for FFT

presented in [16], we found that the ACF results indicate that the time series of the electrical load has a seasonality of 24 hours, while the FFT indicates a seasonality of 12 and 24 hours.

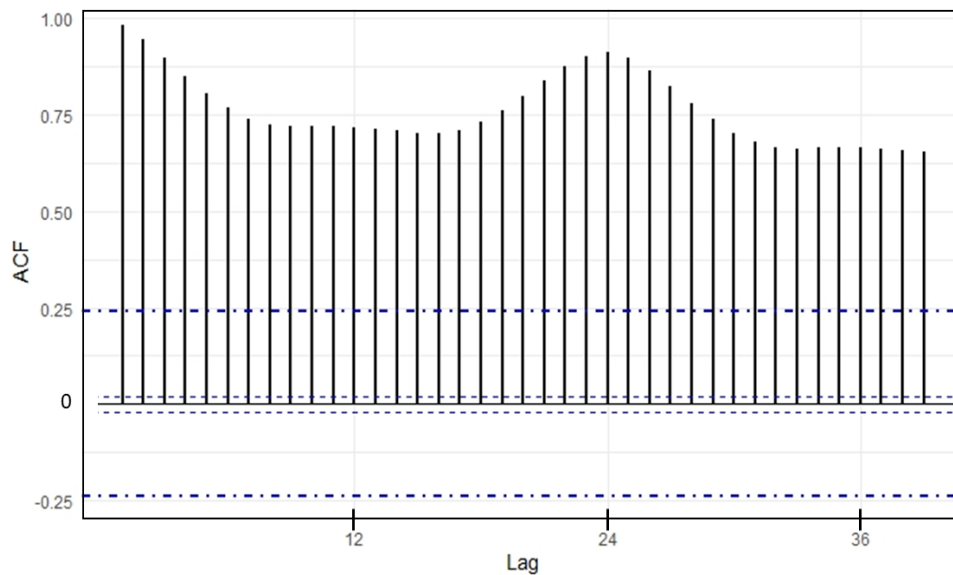


Figure 2.9 Output of ACF for the time series of an electrical load.

2.5 Conclusion

Many sets of time series have been analyzed by applying FFT to determine the seasonal component. It also allows for the identification of any trends, whether upward or downward, in the time series. FFT results have displayed good performance in detecting seasonality. The output of this technique shows promising results in determining a trend. Correspondingly, FFT outperformed ACF, as ACF has restrictions in identifying the exact time of the repeated seasonality. The seasonality must be significant before ACF can detect it.

2.6 SARIMA Forecasting Model of Short-Term Electric Load Data Enhanced by Fast Fourier Transform-based Seasonality Detection [16]

Abstract

The Seasonal Autoregressive Integrated Moving Average (SARIMA) model forecasts short-term electric load data. These types of data are affected by weather conditions, which means they have a seasonal component. For this reason, representing the data in the frequency spectrum domain will reflect the exact seasonal time. FFT has been used to detect the existence of the seasonal component in a time series of hourly electrical load data. This technique gives a clear view of the behavior of the time series in frequency domain, which shows the three main components at frequencies $f_1=3.17e^{-8}$ Hz, $f_2=1.157e^{-5}$ Hz, and $f_3=2.315e^{-5}$ Hz. These frequencies have been converted into time which are $t_1 = 8760h$, $t_2 = 24h$, and $t_3 = 12 h$, respectively. The model that has been selected to forecast the electrical load data is SARIMA (6,1,1) (4,1,1). Most of the predicted values fall into the 95% confidence interval.

2.7 Introduction

Forecasting helps designers in planning and decision-making, since it gives an insight into future uncertainty using the past and current behavior of given observations. Furthermore, load forecasting plays a vital role in the energy system, as inaccurate forecasting could cost power companies both money and time. Therefore, choosing a reliable and effective load forecasting method is important.

For this purpose, several approaches have been employed to study and forecast electrical load. These approaches can be divided into three groups [30]: traditional approaches, artificial intelligence approaches, and support vector regression approaches. The Seasonal Autoregressive Integrated Moving Average (SARIMA) model, based on the Box-Jenkins approach, is one of the more popular traditional methods. Due to the reliability of the Box-Jenkins, several researchers have used this model, confirming its importance in the forecasting literature [31]. In the present dissertation, SARIMA was applied to hourly electrical load data from January 2017 to December 2017 to achieve a short-term prediction of electrical load data for the given data.

When studying and analyzing a time series, it is important to identify its pattern to ensure accurate predictions. The seasonal component of the time series affects the accuracy of the prediction. Usually, the seasonal component is easily identified by visual inspection of graphing techniques

such as run sequence plots, seasonal sub-series plots, multiple box plots, or the autocorrelation plot [27]. However, in some cases, when the time series is very long and there is a large concentration of observed data, the detection of seasonality is difficult. To the best of our knowledge, most studies of electrical load forecasting use visual inspection of graphing techniques to detect seasonality. Therefore, we use FFT to detect seasonality in electrical load data.

To forecast short-term electricity demand in Singapore, two-time series models were suggested in [32]: the multiplicative decomposition model, and the SARIMA model. The authors stated that the multiplicative decomposition model had slightly higher accuracy than SARIMA. The autoregressive integrated moving average (ARIMA) model was applied to forecast seven years of domestic, commercial, and industrial electricity demand in Tamale, Ghana [33]. The selected models showed that the industrial electricity demand did not rise faster than either the domestic or commercial electricity demand. For forecasting load demand in distribution substations, [34] conducted a study comparing the ARIMA model, Artificial Neural Networks (ANN), and Adaptive Neuro-Fuzzy System techniques. Their study shows that ANN outperformed the ARIMA model and Adaptive Neuro-Fuzzy System techniques. In [30], energy consumption was predicted using the ARIMA model and a non-linear autoregressive neural network (NAR) model. Even though both models are considered adequate, comparing the predictive error value favors the performance of the ARIMA model. The study found that the two methods performed well, but they preferred the ARIMA model because of its simple structure.

2.8 Methodology and Material

A. Autoregressive Integrated Moving Average (ARIMA) Model

The ARMA model consists of Autoregression (AR) and Moving Average (MA). The addition of “I”, turning the model into ARIMA, indicates that it has the ability to convert a time series from non-stationary to stationary. The ARIMA model has been further expanded into SARIMA, or the seasonal autoregressive integrated moving average model, giving it the ability to deal with seasonal time series. SARIMA can be written as:

$$\phi_p(B)\phi_P(B^S)(1-B)^d(1-B^S)^D X_t = \theta_q(B)\theta_Q(B^S)\epsilon_t \quad (2.3)$$

where B is the backward shift operator; $\phi_p, \phi_P, \theta_q, \theta_Q$ are the polynomials of p, q, P, Q ; and $p, d,$ and q are the order of the non-seasonal AR model, ordinary differencing and non-seasonal MA

model, respectively. P, D, and Q represent the seasonal SAR model, seasonal differencing and seasonal SMA model, respectively.

B. Box-Jenkins Approach

In 1970, Box and Jenkins proposed a new approach to forecast data from historical data. The Box and Jenkins Approach can analyze and predict several types of time series. The Box-Jenkins strategy, as indicated in [26], is suitable for both short- and medium-term prediction. This approach is based on four basic steps:

- Model Identification: The number of orders p and q are identified using the autocorrelation function (PACF) and partial autocorrelation (ACF) plots, respectively. The number of orders can be determined by counting the first spikes that cross the significance limit in the PACF and ACF plot. A lower number of orders is preferable, as it makes the model simple.
- Estimation of model parameters: Determining which ARIMA model to choose depends on the Akaike Information Criterion (AIC) and Bayesian information criterion (BIC) value that make a trade-off between the fit statistics of the model and its complexity. Therefore, the one with the minimum AIC value should be chosen as the appropriate model.
- Diagnostic of the model: The final model is chosen using two factors: residuals and estimated parameters.
- Forecasting: The chosen and tested model is ready for forecasting.

C. Stationary and Non-stationary Data

When the mean, covariance, and autocorrelation are constant over time, the data becomes stationary. Non-stationary data can never be modeled and forecasted due to their unpredictable nature. This indicates that all non-stationary data should be converted to a stationary form before performing any forecasting.

D. Fast Fourier Transforms (FFT)

A time series consists of several signals that have different amplitudes and periods. FFT converts these time series from time domain to frequency domain, and clearly shows for each signal the individual frequencies and the dominant frequency. This can help in identifying the seasonality in the time series, especially when the seasonality is not shown in the time series. An FFT algorithm can be written as follows:

$$F(n) = \sum_{k=0}^{N-1} f(k)e^{-2j\pi nk/N} \quad (2.4)$$

Where N is the number of samplings.

2.9 Results and Discussion

Before applying the Box-Jenkins approach, the stationarity of the data must first be examined. It is very clear from figure (2.10) that the mean and variance of the data do not look constant over time, which results in the non-stationarity of the data. Also, the Augmented Dicker-Fuller (ADF) test and the Kwiatkowski–Phillips–Schmidt–Shin (KPSS) test with p-values of 0.6522 and 0.01, respectively, confirm that the data are not stationary. Therefore, differencing is mandatory to make the series stationary [26]. Since the time series of electrical load data might be affected by different factors such as weather conditions, we can assume that the time series of electrical load data is seasonal. Hence, the time series has been converted from the time domain to the frequency domain by Fourier Transformation to check the seasonality.

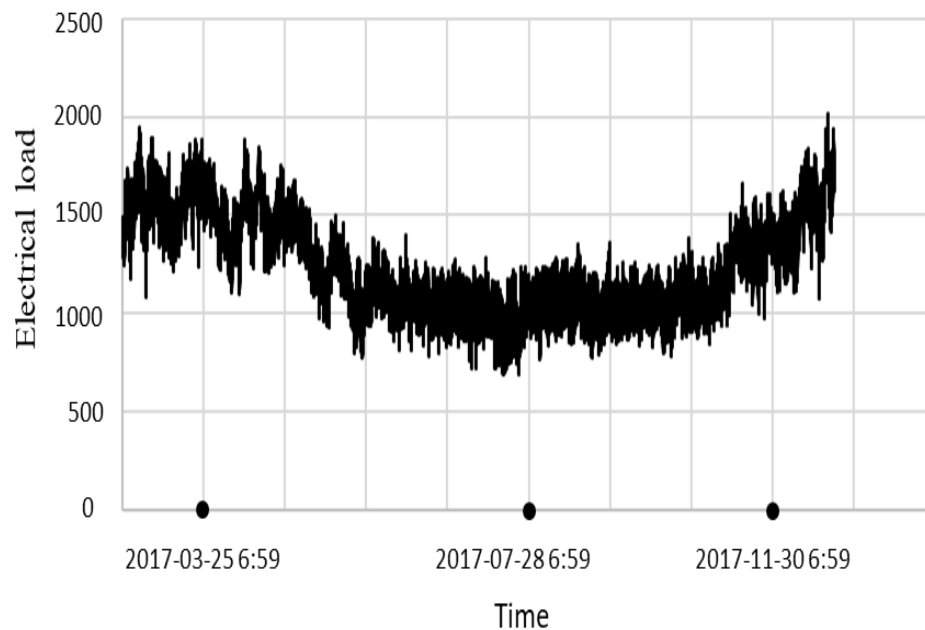


Figure 2.10 Hourly electrical load data.

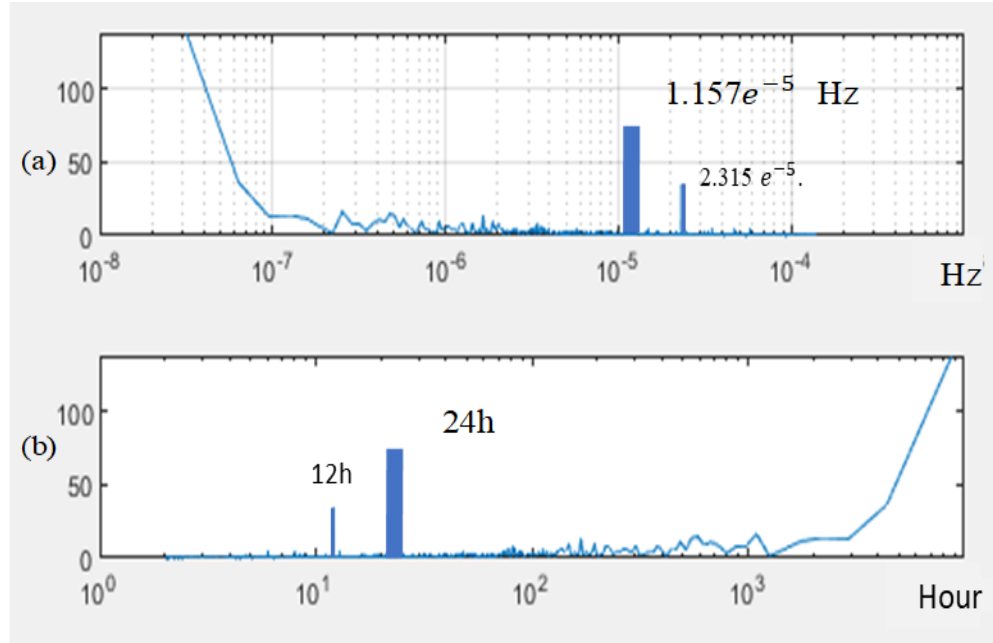


Figure 2.11 Time series of electric load data in frequency domain.

The frequency spectrum of the time series of electric load data for Figure (2.11a) shows there are three components at frequencies $f_1=3.17e^{-8}$ Hz, $f_2= 1.157 e^{-5}$ and $f_3= 2.315 e^{-5}$. These frequencies were converted into time to gain a clear understanding of the frequency domain. Therefore, f_1, f_2 and f_3 correspond to the times $t_1 = 8760$ h , $t_2 = 24$ h and $t_3 = 12$ h, as shown in Figure (2.11b). We obtained these values by using the following equation:

$$t = 1/f \text{ (h)} \quad (2.5)$$

Where f is a frequency and t is a time.

These components form the time series of electric load data. The component at $t_1 = 8760$ h represents the whole pattern of the time series of electric load data, which we are not interested in. Meanwhile, the component at $t_2 = 24$ h, which has the strongest significance in its amplitude, represents the day pattern and it tends to repeat itself every 24 hours. The component at $t_3 = 12$ h represents the half day pattern and it tends to repeat itself every 12 hours.

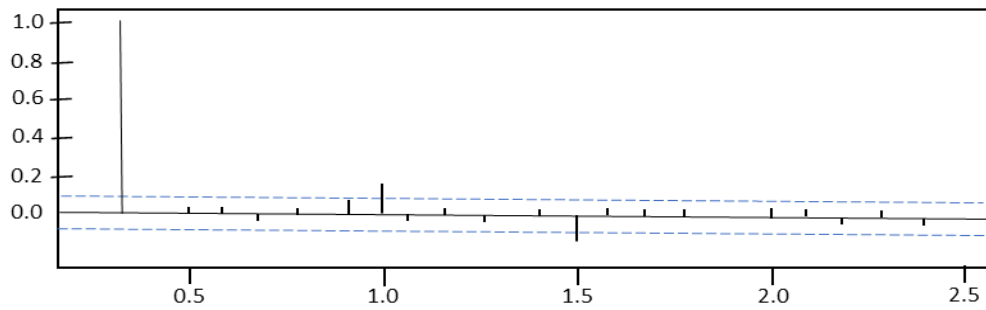
The auto.arima function in R Studio was employed to fit the ARIMA model to the electrical load time series. This function selects the model with the lowest AIC (Akaike Information Criterion) value. Table (2.1) shows the selected model, SARIMA (6,1,1) (2,1,1), as well as other suggested models.

Table 2.21 Suggested Models and Their AIC and BIC

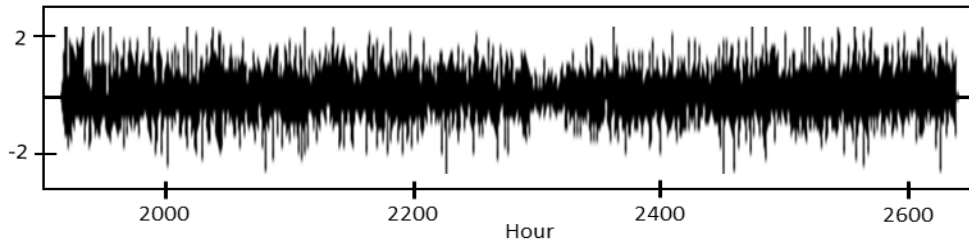
Model	AIC	BIC
SARIMA (1,1,1) (1,1,1)	82552.29	82587.67
SARIMA (6,1,1) (2,1,1)	81208.21	81286.05
SARIMA (6,1,1) (0,1,1)	82755.18	82818.87
SARIMA (7,1,1) (1,1,1)	82101.56	82179.4

- Estimation of model parameters

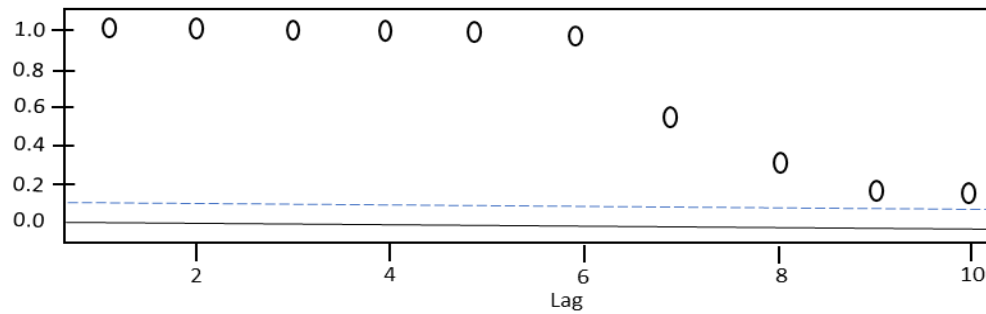
The model selected based on the minimum AIC and BIC values is SARIMA (6,1,1) (2,1,1).



(a). ACF of Residual



(b). Standardized Residuals



(c). P value for Ljung-Box statics

Figure 2.12 Residual plots of electrical load data.

- Diagnostic of the model:

The standardized residual is used to evaluate the goodness of fit of the ARIMA model by checking whether there are any pattern or significant correlation. Figure (2.12.a) shows the standardized residual has no specific pattern with zero mean and constant variance between -2 to 2, which means there is no outliers. In addition, the ACF of the residual and the P-values for the Ljung-Box test are used to evaluate the goodness of fit of the ARIMA model. The ACF of the residual in figure (2.12.b) shows that there are a few spikes at different lags that exceed the confidence limits, which means the model is well fitted. The P-values for the Ljung-Box test shows that all P-values are higher than 5%, so we accept the null hypothesis that says it is a good model, figure (2.12.c).

- Forecasting

SARIMA (6,1,1) (2,1,1) has been used to forecast one day ahead for the electrical load data. Figure (2.13) shows the time series of the electrical load followed by the forecasts as a blue line. Note that the upper and lower portion of 80% and 95% are in light blue and blue colors.

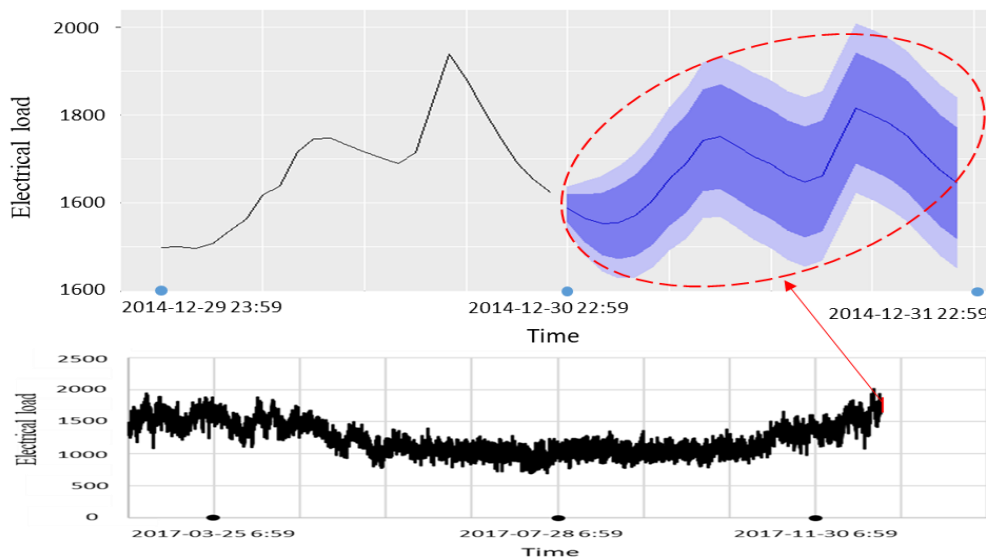


Figure 2.13 Forecasting 24 hours of electrical load data.

2.10 CONCLUSION

In this chapter, the time series of electrical load data was studied, and the stationarity was checked using ADF and KPSS tests. The results show that the series is not stationary. In addition, the seasonality of the series was determined by converting the time series of an electrical load from the time domain to the frequency domain using the adopted technique. The technique shows the

main components that form the series and the significant component that tends to repeat itself. The best model was selected based on AIC and BIC and has high order, increasing the complexity. The model was used to forecast the time series of electrical load data one day ahead. Most of the forecasted data fell into the 95% confidence interval. We can determine from these results that it is possible to employ the SARIMA models to forecast hourly electrical load data.

Chapter3. A Proposed Novel Adaptive DC Technique for Non-Stationary Data Removal

(The material presented in this chapter is based on a paper published in the journal Elsevier, Heliyon, 2023.[17])

Abstract

The stationarity of a time series is an important assumption in the Box-Jenkins methodology. Removing the non-stationary feature from a time series can be done using a differencing technique or a logarithmic transformation approach, but it is not guaranteed to be accomplished in one step. This paper proposes a new adaptive DC technique for removing a non-stationary time series at the first step. The technique involves transferring non-stationary data into another domain that deals with it as a stationary time series, because it is much easier to be forecasted in that domain. The adaptive DC technique has been applied to different time series, including gasoline and diesel fuel prices, temperature, load, and the number of internet users time series. The performance of the proposed technique is evaluated using several statistical tests, including Augmented Dickey-Fuller (ADF), Kwiatkowski-Phillips-Schmidt-Shin (KPSS), and Phillips Perron (PP). Additionally, the technique is validated by comparing it with a differencing technique. The results show that the proposed technique slightly outperforms the differencing method. The importance of the proposed method is its capability to get the stationarity data from the first step, whereas the differencing approach sometimes needs more than one step.

3.1 Introduction

Various studies have used different models to forecast electricity prices, load, and stock market prices. As presented in the previous chapter, one of the most popular techniques is the Autoregressive Integrated Moving Average (ARIMA) due to its simplicity and accuracy [35]. The ARIMA model is typically used for estimation if the time series of the data is stationary. The term “stationary data” indicates that data mean, variance, and autocorrelation are constant for a time period of the time series [36]. Figures (3.1a) and (3.1b) show different cases of non-stationarity, namely the mean and variance changing, respectively, in the time series over time. For prediction purposes, stationary data are much easier to predict than non-stationary data. Trend and seasonality are two main components that can convert stationary to non-stationary data and vice versa. These two components play an important role in varying the mean and the variance [37].

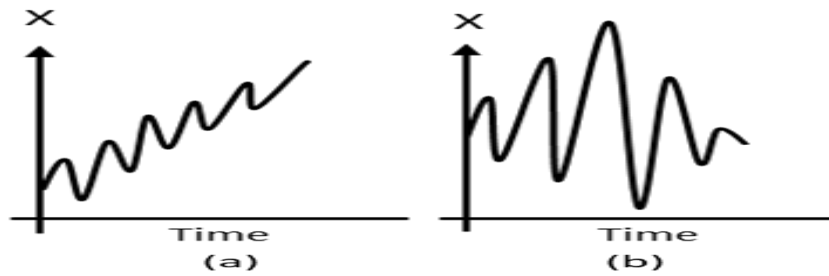


Figure 3.1 Various cases of non-stationary data. a) Time dependent mean. b) Time dependent variance.

More specifically, the trend controls the mean, and the seasonality controls the variance. Numerous studies have been conducted to understand whether the data has a trend or seasonal component. The Box-Jenkins approach, as shown in Figure (3.2), assumes in the first step that the time series should be stationary [36][19]. Checking for stationarity is presented separately in Figure (3.3). There are two main processes in the stationarity step: detection and transformation. The detection process includes aspects such as autocorrelation function (ACF), statistical tests [38], and Fast Fourier Transform (FFT) [16]. This process is concerned with checking whether the time series is stationary. In a case where the time series is stationary, we proceed to the Box-Jenkins approach. Otherwise, the time series is transformed into stationary, which is called the transformation process. Transformation can be done using a differencing technique or a logarithmic transformation approach, but these sometimes require several steps to convert non-stationary data into stationary data. Additional steps potentially increase the error, particularly if the converted data will be used for prediction after the conversion.

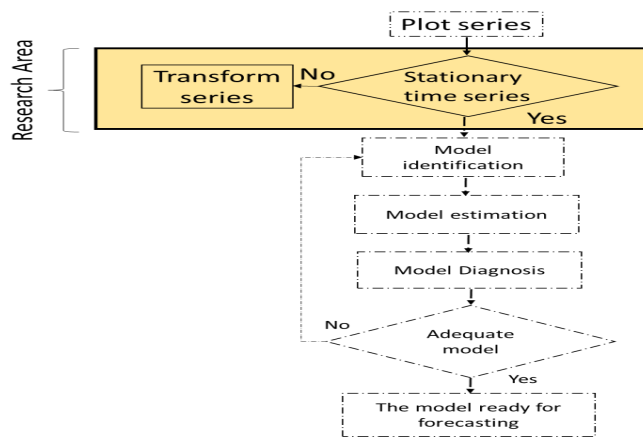


Figure 3.2 Flowchart of Box-Jenkins steps.

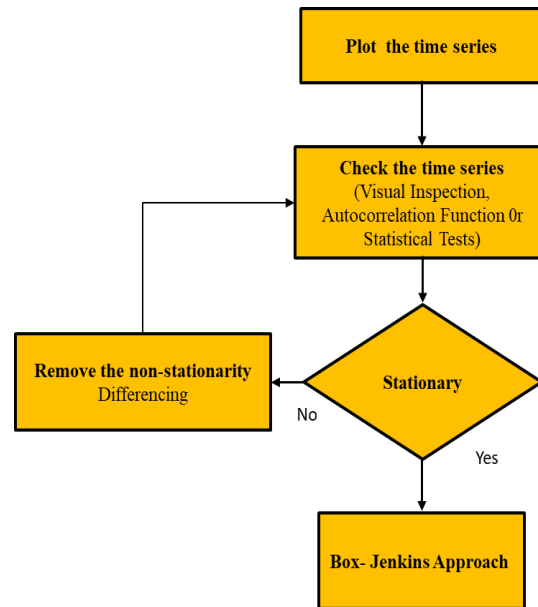


Figure 3.3 Flowchart showing the first stage in the Box-Jenkins approach.

In this chapter, a novel technique known as an Adaptive DC Technique is proposed to remove the non-stationarity from the different time series of gasoline and diesel fuel prices, temperature, load, and the number of internet users. The advantage of this technique is its capability to remove the non-stationarity from the first step for any kind of data compared to other techniques. The results of the adaptive DC technique are compared to the differencing technique using statistical tests such as the Augmented Dickey-Fuller (ADF), Kwiatkowski-Phillips-Schmidt-Shin (KPSS), and Phillips Perron (PP). The proposed technique has proved its effectiveness.

The aim of this chapter is:

1. To propose an Adaptive DC technique that will improve the forecasting of nonlinear datasets of most renewables, resulting in the enhancement of reliability.
2. To validate the proposed technique by comparing it with benchmark work done in that area.

3.2 Literature Review

In [39], a hybrid model consisting of Auto-Regressive Integrated Moving Average (ARIMA) and Artificial Neural Network (ANN) methods is examined over several datasets. As the Augmented Dickey-Fuller (ADF) test shows, Turkey's intraday electricity market price and the exchange rate between the British pound and the U.S. dollar dataset are non-stationary, so a natural logarithmic

function is used to transform them into stationary datasets. The results indicate that the ARIMA performs well when the dataset is stationary, and ANN models work well with non-stationary data; however, if the dataset is stationary, the performance is improved.

The ARIMA model was used to forecast a small-scale agricultural load in [40]. A small-scale agricultural load is non-stationary, so the transformation can potentially be done using differencing, deflating, or logging. Furthermore, in [41], the authors claimed that log transformation and differencing are suitable approaches to remove the non-stationarity, but that more than one step may be needed, which is time-consuming and increases the error profile. They used a differencing technique to convert the Johns Hopkins epidemiological data from non-stationary to stationary. Four graphical techniques are employed in [21] to detect seasonality in time series: a run sequence plot, a seasonal sub-series plot, multiple box plots, and an autocorrelation plot. The authors mentioned that seasonal subseries and box plots have limitations in identifying the seasonal. In addition to the graphical techniques, there are other statistical tests, such as the Chi (χ^2) goodness-of-fit, the Kolmogorov-Smirnov goodness-of-fit, and the non-parametric test, all of which can be used to identify seasonality [38]. Different types of tests are applied to the row variances of the Buys Ballot table in [21], using the Student T-test and Wilcoxon Signed-Ranks test. These showed promising results in detecting seasonality.

In [42], various signal processing techniques were used to detect the seasonality of winter and summer time series wind speed by applying Continuous Wavelet Transform. One of the most common spread tools employed in the literature to identify seasonality is the Auto-Correlation Function (ACF) tool. Researchers utilized the Box-Jenkins algorithm for forecasting, which focuses on building a statistical model for forecasting the monthly average surface temperature in the Brong Ahafo region of Ghana to understand the dynamics of events. For determining seasonality, they used the ACF and decomposing the monthly average surface temperature into various components. All these approaches confirmed the presence of seasonality.

Table (3.1) presents some studies that have been conducted to check and remove stationarity. Time series forecasting techniques, Neural networks, Wavelet, and a Kalman filtering estimator are the commonly used techniques for forecasting. Many hybrid techniques are proposed in the literature to improve the accuracy of the forecasting models, especially for nonlinear data[43] [44].

3.3 Removing Non-Stationarity

The stationarity in a time series is a potential condition in the Box-Jenkins approach. For this reason, many methods such as differencing and de-trending have been used to achieve this condition. In the present thesis, the differencing technique is the main tool used in the Box-Jenkins approach for the removing a trend. A proposed technique, called the Adaptive DC technique, is also presented here. Figures (3.4), (3.5), (3.6), (3.7) and (3.8) show the time series of hourly diesel prices, hourly gasoline prices, daily temperature, hourly load and the number of internet users, respectively.

Table 3.1 Sampling of Studies That Apply Common Tools to Identify and Remove Stationarity

Reference	Year	Time series dataset	Checking / Removing stationarity	Comments
[45]	2009	Load demand time series	Differencing method.	<ul style="list-style-type: none"> • Hard to detect stationarity in a long time series, but gives a clear view in a short time series. • Two and one non-seasonal and seasonal differentiation, respectively.
[46]	2012	Weekly rainfall	Autocorrelation Function (ACF) and / Logarithmic transformation and differencing method.	<ul style="list-style-type: none"> • The seasonality must be significant; otherwise, the ACF tool cannot detect it. • The stationarity in mean and variance are done by performing log transformation and differencing of the original data.
[47]	2015	Wind speed	the Augmented Dickey-Fuller (ADF) / Differencing method.	<ul style="list-style-type: none"> • ADF tends to reject the null hypothesis. One non-seasonal and one seasonal differentiation, respectively.
[48]	2016	Wind speed	Autocorrelation Function (ACF) / Differencing method.	<ul style="list-style-type: none"> • Seasonality must be significant, or the ACF tool cannot detect it. • Only one differencing.
[49]	2017	Temperature	ACF and ADF/ Differencing method.	<ul style="list-style-type: none"> • ADF tends to reject the null hypothesis. • One seasonal differentiation.
[50]	2020	solar power generation	KPSS/ Differencing method.	<ul style="list-style-type: none"> • KPSS tend to reject the null hypothesis. • the first difference
[51]	2021	Electricity Consumption	ADF/ Differencing method.	<ul style="list-style-type: none"> • ADF tends to reject the null hypothesis. • Differencing method.
[52]	2022	Somalia GDP growth rates	ADF and PP/ Differencing method.	<ul style="list-style-type: none"> • The first difference

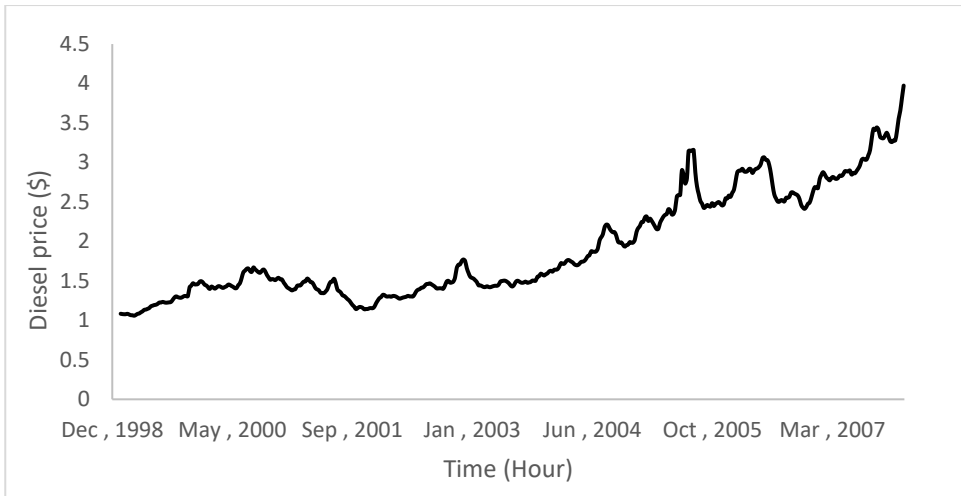


Figure 3.4 Hourly diesel prices.

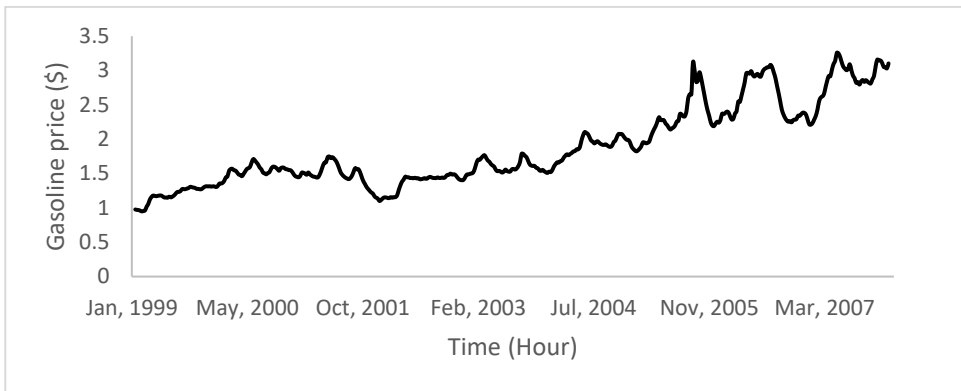


Figure 3.5 Hourly gasoline prices.

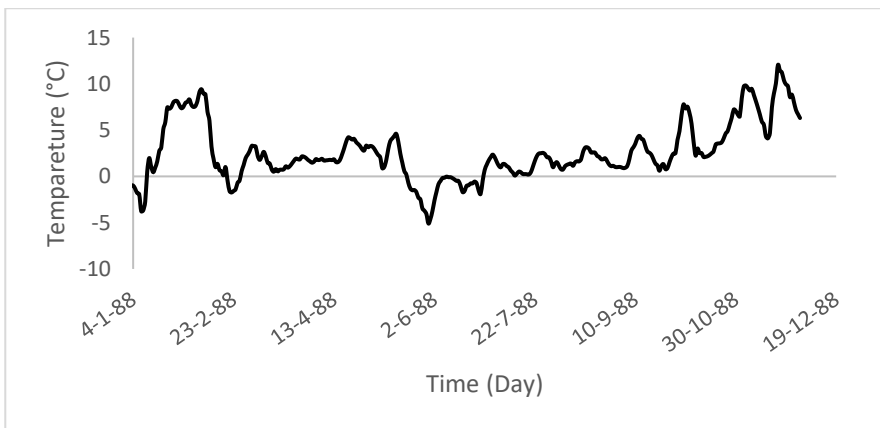


Figure 3.6 Daily temperature.

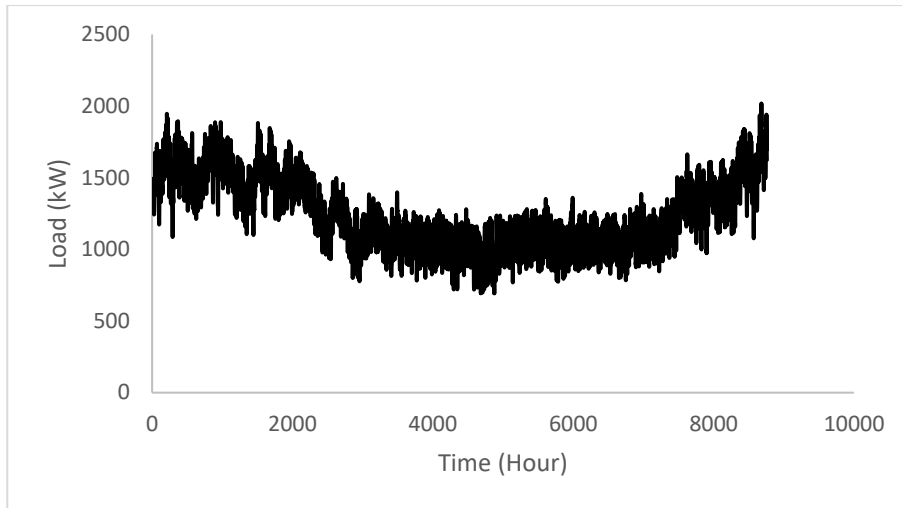


Figure 3.7 Hourly load.

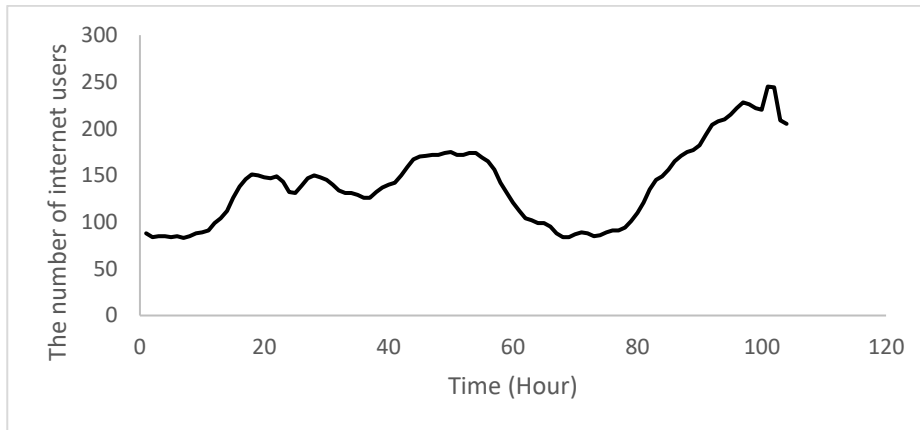


Figure 3.8 The number of internet users

3.3.1 Differencing Technique

This technique is easy to use but needs to be applied more than once to remove the non-stationary part. The differencing equation is written as follows:

$$\text{Difference}(t) = X_t - X_{t-1} \dots\dots\dots (8)$$

where

X_t : The current observation.

X_{t-1} : Previous observation.

Figures (3.9), (3.10), (3.11), (3.12) and (3.13) show the time series of hourly diesel prices, hourly gasoline prices, daily temperature, hourly load and the number of internet users, respectively, after applying the first differencing consecutively.

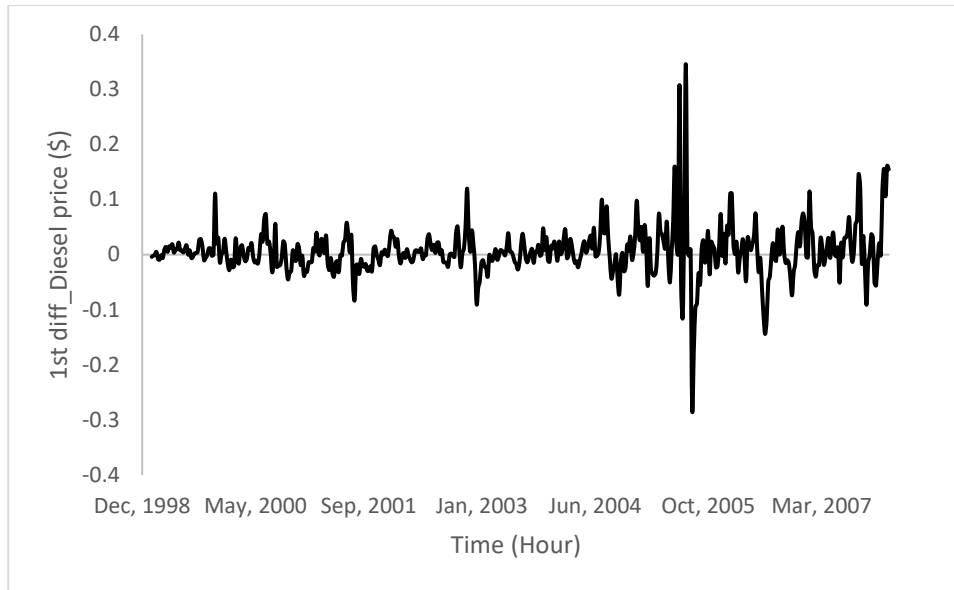


Figure 3.9 Differencing of the time series of diesel price.

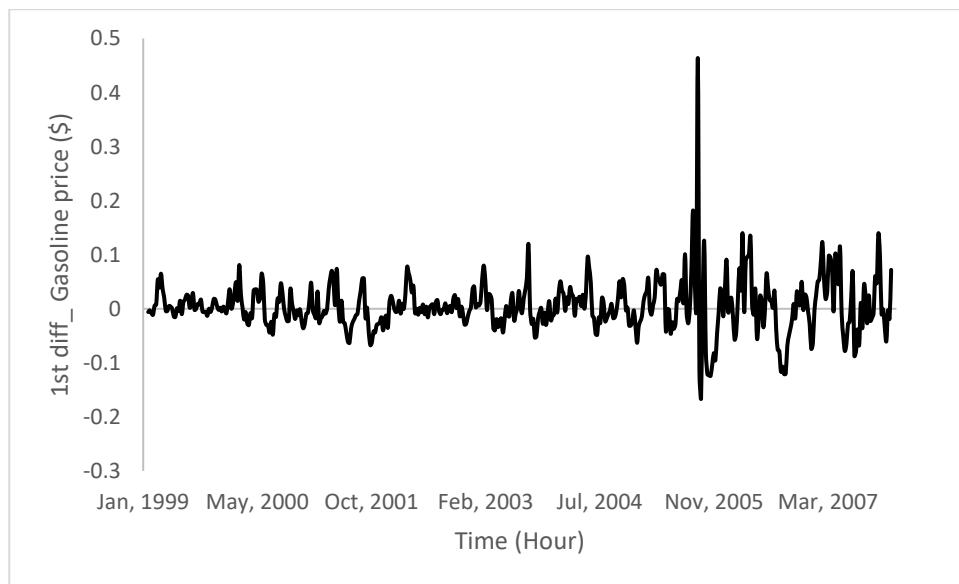


Figure 3.10 Differencing of the time series of diesel price.

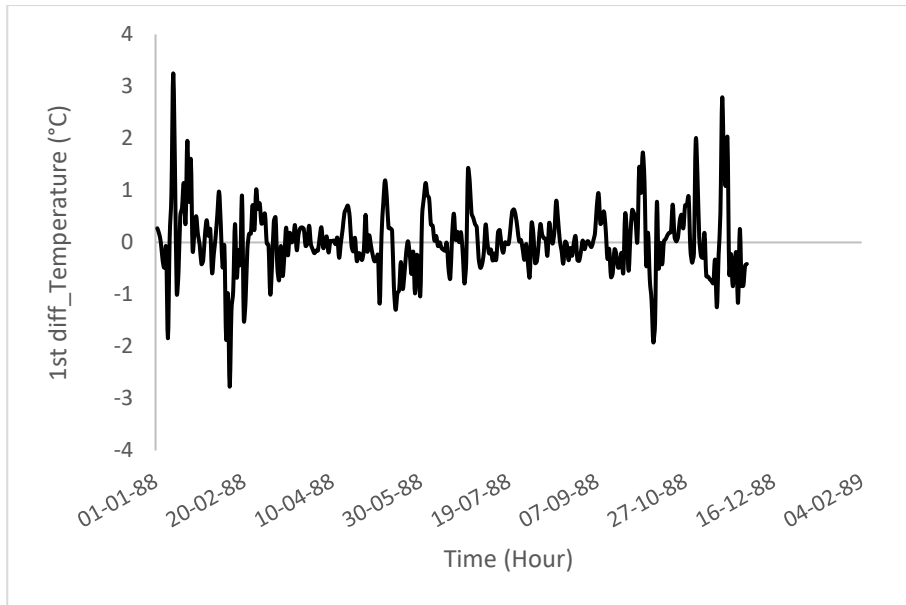


Figure 3.11 Differencing of the time series of temperature.

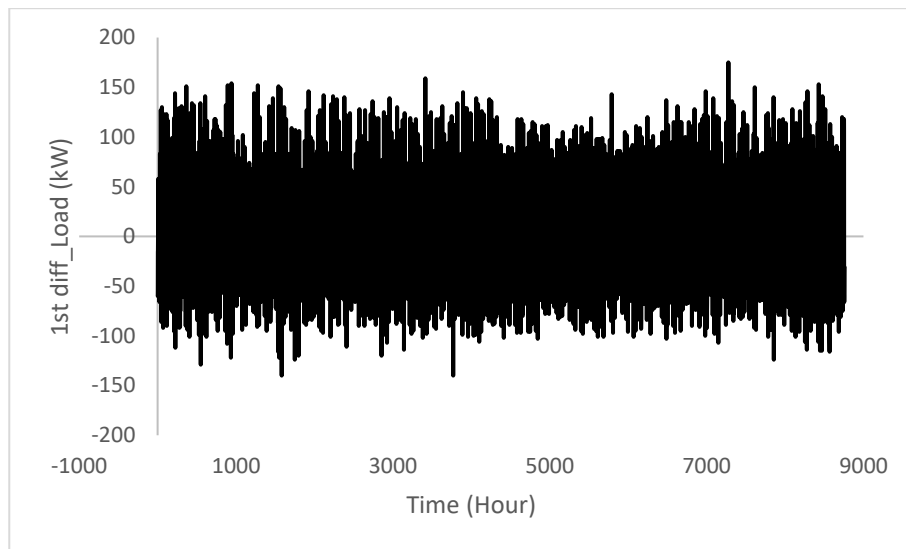


Figure 3.12 Differencing of the time series of load.

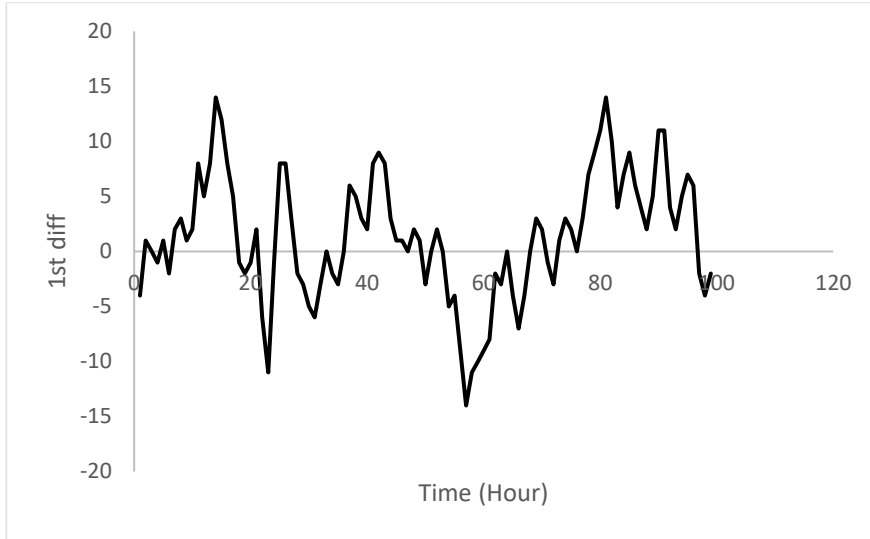


Figure 3.13 Differencing of the time series of the number of internet users.

3.3.2 Proposed Adaptive DC Technique

The proposed Adaptive DC technique is a novel approach that can be used to remove trend from a time series. The proposed technique has been inspired by DC offset removal in electrical signals. In the Adaptive DC technique, the time series is divided into groups of three points. The mean of the groups is calculated, and every three points are subtracted from the mean. Figure (3.14) explains the procedure of the Adaptive DC technique flowchart, and the following equation describes it:

$$y_i = x_i - \sum_j^{j+2} (x_j/3) \dots\dots\dots(9)$$

where x_i indicates the input data; y_i denotes the proposed converted data; $i = 1; n, j = 1, 4, 7 \dots n - 2$; n is the data size; and j changes for each $3i$. After performing thousands of runs of the proposed strategy, we found that the best size of j is a pattern of 1,4,7, and so on. The proposed method could work well with different cases of j , but the best performance is found to be when j is defined based on the above pattern. The Adaptive DC technique has been applied to the time series of hourly diesel prices, hourly gasoline prices, daily temperature, hourly load and the number of internet users, as shown in Figures (3.15), (3.16), (3.17), (3.18) and (3.19), respectively.

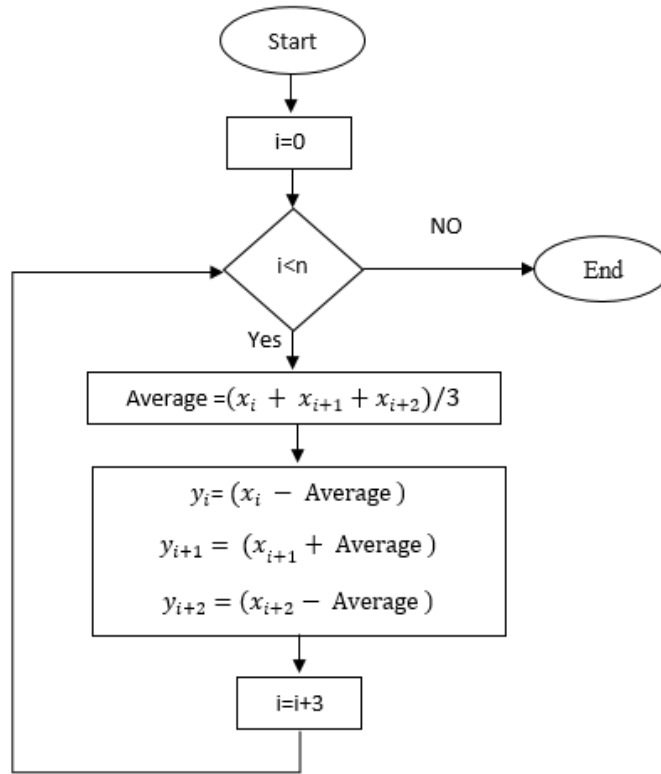


Figure 3.14 Adaptive DC technique flowchart.

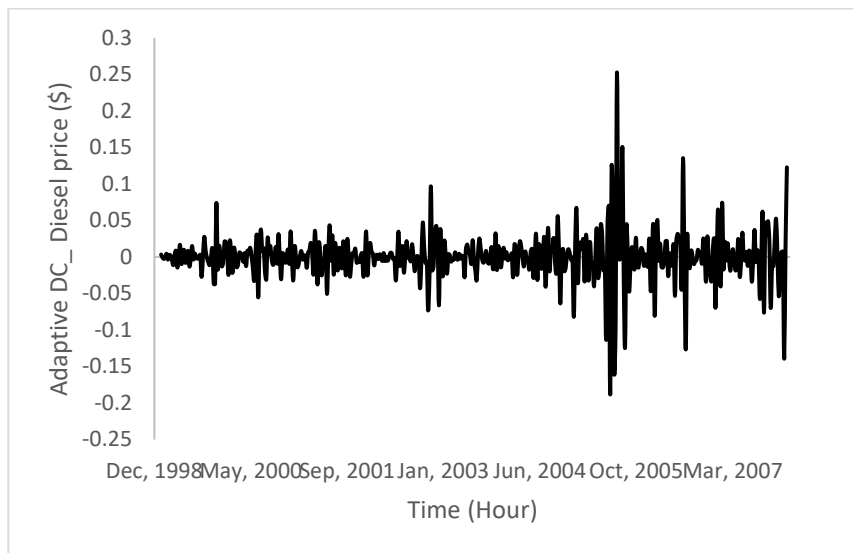


Figure 3.15 Adaptive DC technique of diesel.

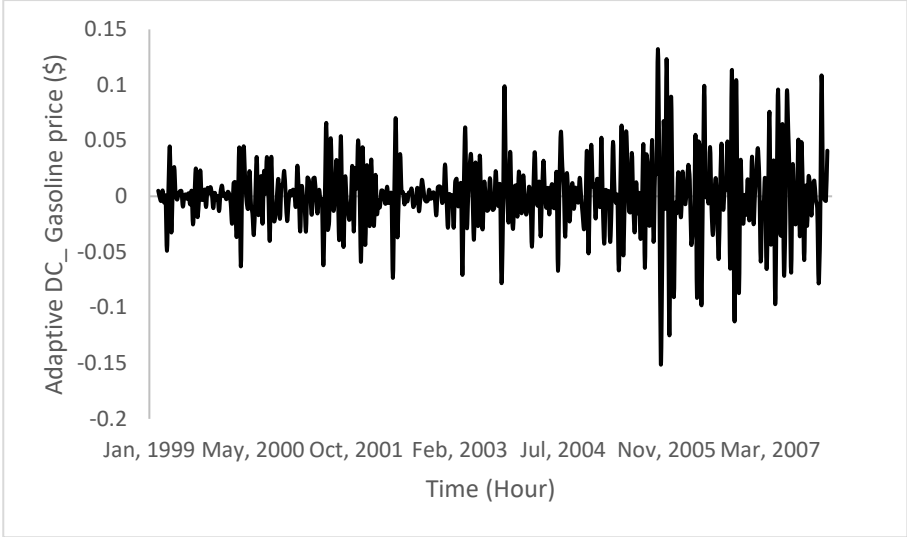


Figure 3.16 Adaptive DC technique of gasoline.

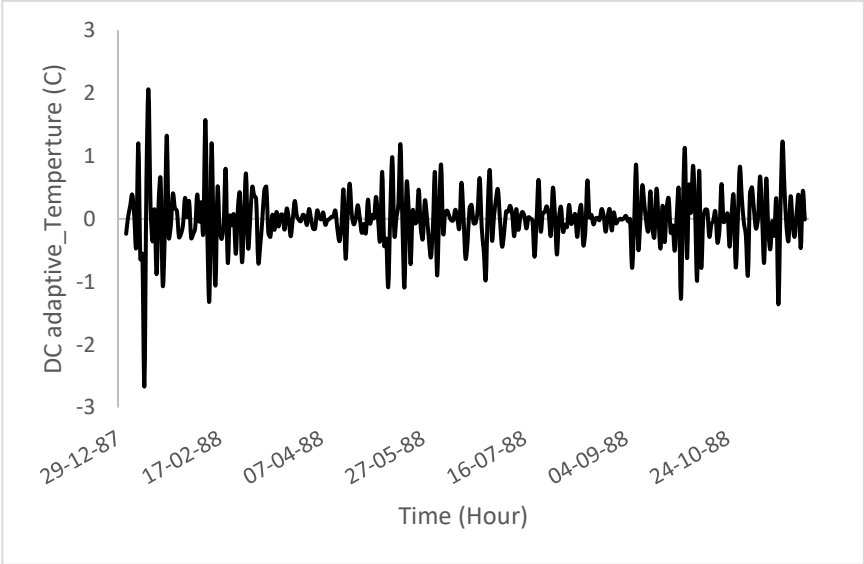


Figure 3.17 Adaptive DC technique of temperature.

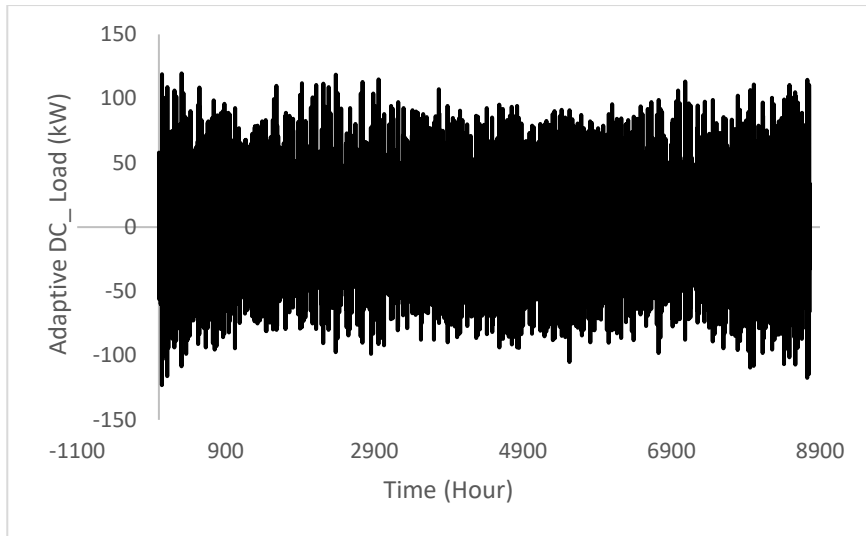


Figure 3.18 Adaptive DC technique of load.

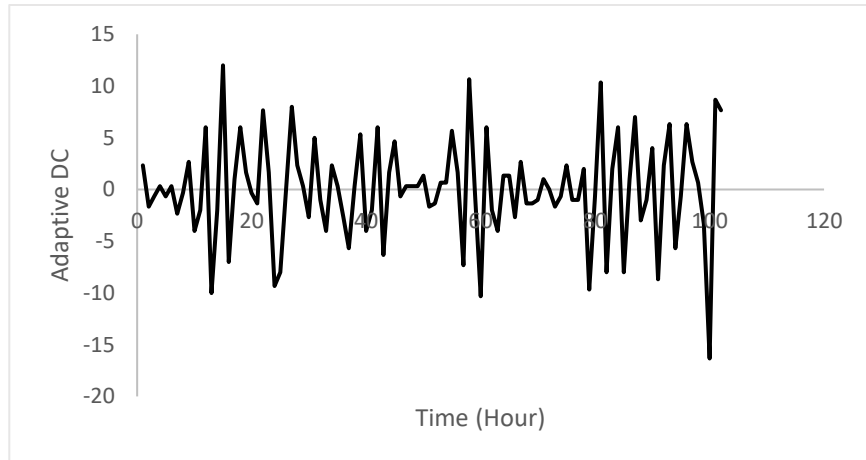


Figure 3.19 Adaptive DC technique of the number of internet users.

3.4 Results and Discussion

Statistical tests, including ADF, KPSS and PP, are widely used for checking the stationarity of a time series [27]. The p -values of the tests are compared to 0.05 to decide whether to reject or accept the null hypothesis, where the null hypothesis is non-stationary. In ADF and PP, if $p \geq 0.05$, the null hypothesis is true. For $p < 0.05$, the value is significant enough to reject the null. A key difference between the ADF test and the KPSS test is that the null hypothesis of the KPSS test in the series is stationary. Table (3.2) shows that the five-time series are non-stationary. The ability of the statistical tests to identify the stationarity in the time series depends on the time series length [53]. ADF and PP are appropriate tests when the time series length is 25 observations.

Table 3.2 Results of Statistical Tests of Time Series

Time series	Length of time series	P- value of ADF test	P- value of KPPSS test	P- value of PP test	Status of time series
Diesel prices	467	0.8839	0.01	0.9069	Non-stationary
Gasoline prices	467	0.14	0.01	0.2051	Non-stationary
Temperature	336	0.176	0.01	0.138	Non-stationary
Load	8760	0.656	0.01	0.1	Non-stationary
Number of internet users	105	0.44	0.1	0.9	Non-stationary

Table (3.3) shows statistical test results after applying the differencing method. The ADF, KPPSS, and PP tests indicate that diesel prices, gasoline prices, and temperature time series are stationary, while the results of the KPPSS, ADF and PP tests show that the number of internet users time series is non-stationary. Therefore, the second differencing is mandatory. For more investigation in regarding the stationarity of the number of internet users time series, the series in figure (3.13) is split into three contiguous sequences, then we can calculate the mean of each group of numbers and compare the values. The results clearly imply that the mean of the three contiguous sequences is considerably different from each other describing the series is non-stationary. Figure (3.20) shows the number of internet users time series after applying the second differencing. From Table (3.4), it is obvious that the five-time series are stationary after applying the Adaptive DC technique. Compared to the results from Table (3.3), it is clear that the proposed technique outperforms the differencing technique.

Table 3.3 Results of Statistical Tests After Applying Differencing Technique

Time series	Length of time series	P- value of ADF test	P- value of KPPSS test	P- value of PP test	Status of time series
Diesel prices	467	0.01	0.1	0.01	Stationary
Gasoline prices	467	0.01	0.1	0.01	Stationary
Temperature	336	0.01	0.1	0.01	Stationary
Load	8760	0.01	0.1	0.01	Stationary

Time series	Length of time series	P- value of ADF test	P- value of KPPSS test	P- value of PP test	Status of time series
Number of internet users	105	0.4	0.022	0.8	Non-Stationary

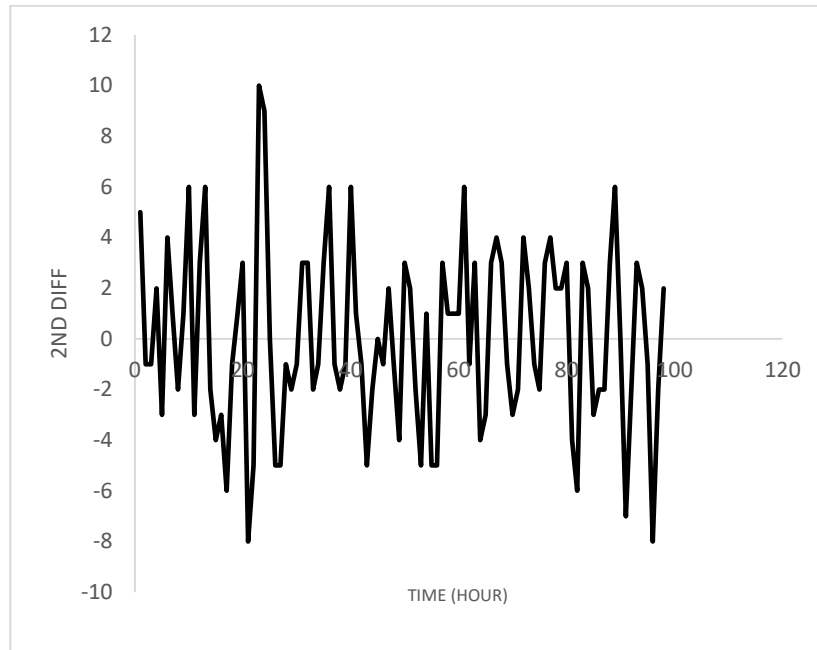


Figure 3.20 2nd Differencing of the time series of the number of internet users.

Table 3.4 Results of Statistical Tests After Applying the Adaptive DC technique.

Time series	Length of time series	P- value of ADF test	P- value of KPPSS test	P- value of PP test	Status of time series
Diesel prices	467	0.01	0.1	0.01	Stationary
Gasoline prices	467	0.01	0.1	0.01	Stationary
Temperature	336	0.01	0.1	0.01	Stationary
Load	8760	0.01	0.1	0.01	Stationary
Number of internet users	105	0.01	0.1	0.01	Stationary

3.5 Conclusion

In this work, we propose a novel Adaptive DC technique to convert a non-stationary time series into a stationary one in the first step. The adaptive DC technique was applied to various time series of different lengths. The differencing technique was also applied to the same series to validate the results using the ADF, KPSS, and PP tests. The results of the Adaptive DC technique and differencing technique were compared. When applying both techniques to gasoline and diesel fuel price, temperature, and load time series, the small comparison did not show any significant difference. However, when applying them to the number of internet users time series, the Adaptive DC technique was found to eliminate the non-stationary portion from the first step compared to the differencing technique.

In comparison, the differencing technique may need more than one step. This makes the Adaptive DC technique superior to the differencing technique, because the proposed technique reduces the number of steps, thus minimizing the processing time. As the data becomes more complicated, the other techniques required more steps for the conversion compared to the proposed technique. The additional steps will increase the total error for the forecasted data.

Chapter4. Energy Management of Hybrid Energy System Sources Based on Machine-Learning Classification Algorithms

(The material presented in this chapter is based on a paper published in the journal *Elsevier* [7].)

Abstract

Hybrid energy systems (HES) that contain renewable energy sources, such as wind and solar energy, help to minimize CO₂ emissions. Therefore, studying these systems to improve their performance has become especially important these days due to the global environmental crisis. Within HES, energy management (EM) is an essential topic that has been covered in detail by numerous studies, showing that errors in EM can lead to HES blackouts. Recent research has experimented with energy management strategy (EMS) to achieve optimal EM.

This chapter introduces a robust one-hour-ahead forecasting model. The research has two main objectives. The first is to determine which energy source should supply the demand-side, using different machine-learning algorithms such as Random Forest (RF), Decision Tree (DT), Gaussian Naive Bayes (Gaussian NB), and K-Nearest Neighbors (KNN). The second objective is to compare the results of these algorithms in order to choose the one with the best performance and rank them based on performance and accuracy. The results show that the DT algorithm achieves the best performance compared to the RF and Gaussian NB algorithms, whereas the KNN algorithm has the lowest accuracy, especially over class 3 that represents solar and diesel generator. The results prove that the RF, DT, and Gaussian NB algorithms are reliable.

4.1 Introduction

Forecasting plays a vital role in the electrical engineering industry, as it gives designers a clear idea about energy system configuration over short-term periods. Such forecasts can help plan and manage generated renewable energy as an alternative power source to reduce overall costs and CO₂ emissions stemming from conventional energy sources. If the forecasting is inaccurate, the energy system can break down. Hybrid energy systems (HES) consist of intermittent renewable energy sources such as wind and solar, so they need accurate forecasting models. The performance of HES depends on several variables that need to be considered, such as the load, power production, weather conditions, fuel prices, and power management [54]. A proper load forecast allows designers to determine power production capacity. Additionally, knowing weather

conditions enables designers to predict optimum solar and wind energy availability. These variables can either enhance or reduce the performance of HES.

To date, numerous studies have been conducted on forecasting and energy management, and several methods have been applied to achieve better results [44], [55]. EMS and optimization usually work side by side to guarantee load electrification and minimize energy production costs. A successful EMS gives the hybrid energy system stability and protects its components from damage caused by overloading [56].

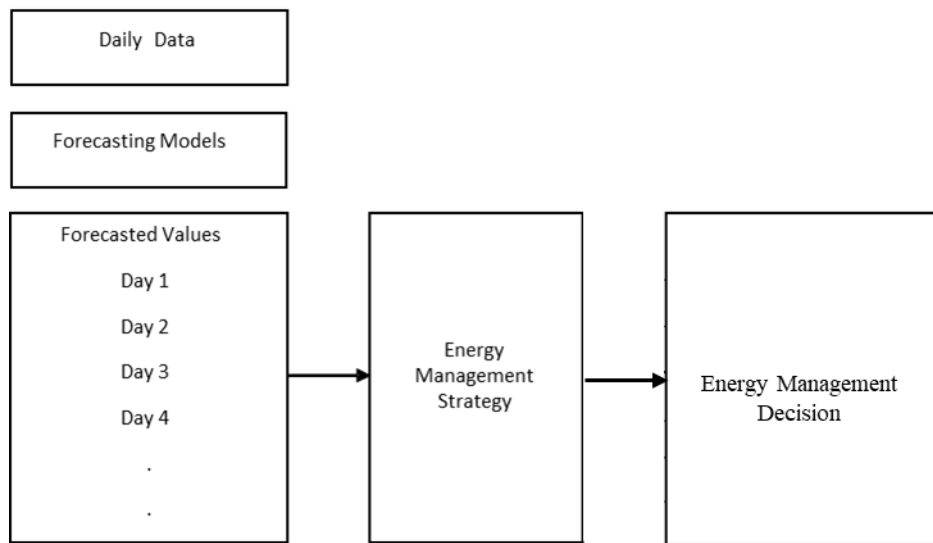


Figure 4.1 Common methodology.

As HES potentially includes solar and wind energy, EMS is mandatory, because solar and wind power are intermittent and oftentimes insufficient. Figure (4.1) represents the schematics of the traditional energy management methodology in a HES that contains solar and wind. In the first step, which involves forecasting the variable historical datasets for a day ahead, the results are used to create an EM using a genetic algorithm (GA), differential evolution (DE), neural network, fuzzy logic, or neuro-fuzzy techniques. In the proposed methodology, information obtained from the energy management technique is used to generate a dataset. Consequently, the dataset is used to forecast the source that should run in the HES. To the best of our knowledge, no previous study has investigated this topic. This study has two main objectives: 1. to forecast the scheduling of the

energy sources using machine-learning algorithms such as Random Forest (RF), Decision Tree (DT), Gaussian Naive Bayes (Gaussian NB), and K-Nearest Neighbors (KNN); and 2. to compare the results of the algorithms named above. The novelty of the proposed work is:

1. To propose a model for scheduling prediction.
2. To validate the proposed work by using different intelligent approaches.

4.2 Literature Review

One of the factors that should be considered when building a HES is the load problem. This problem can be solved by applying different methods and techniques, such as regression analysis, time series analysis, artificial neural networks, genetic algorithms, support vector machine, fuzzy logic, and adaptive network-based fuzzy inference. Recently, hybrid methods and intelligent approaches have been attractive to researchers in solving the load problem [57].

In [16], hourly short-term electric load data were predicted by applying the Seasonal Autoregressive Integrated Moving Average (SARIMA) model. The authors used the Fast Fourier Transformation algorithm (FFT) to detect the existence of seasonality in the time series of electrical load data. In [58], a fuzzy logic and adaptive neuro-fuzzy inference system (ANFIS) was used to forecast hourly short-term load in Turkey, with Artificial Intelligence (AI) being described as a powerful technique for determining the load problem. In addition, the researchers stated that using Artificial Neural Networks (ANNs) with Particle Swarm Optimization (PSO), Back Propagation Algorithm (BPA) or Fuzzy Logic (FL) as hybrid methods would increase the accuracy of solving this problem [59]. Several different ANN architecture performances in forecasting the load were evaluated in [60]. The authors affirmed that intelligent forecasting methods are superior to conventional methods with regard to accuracy. Multivariate adaptive regression splines (MARS), artificial neural network (ANN) and linear regression (LR) methods were used to determine short, mid-, and long-term load forecasting [61]. Several factors that affect HES indirectly were summarized in detail in [62].

Knowing in advance the amount of energy produced from renewable and traditional energy sources in a HES is recognized as a fundamental process in HES design. Forecasting the power production has received considerable attention in recent years, with many researchers applying

various approaches and techniques to achieve high forecasting accuracy. In [63], a multi-layer perceptron (MLP) model was employed to forecast wind power production 24 hours in advance. Meanwhile, the authors in [64] used Recurrent Neural Network (RNN) to forecast solar power production from a photovoltaic power plant. The researchers in [65] employed three different methods to forecast photovoltaic power production, namely, Auto Regressive Integrated Moving Average (ARIMA), Radial Basis Function Neural Network (RBFNN), and Least Squares Support Vector Machine (LS-SVM). In [66], solar power production was forecast using a hybrid Wavelet-PSO-SVM forecasting model based on SCADA.

Weather conditions, wind speed, solar irradiation, and temperature all directly affect the amount of power produced in a HES[54]. Wind speed was predicted in [67] using a novel hybrid forecasting system containing three modules (a data preprocessing module, an optimization module, and a forecasting module). The authors in [68] applied an autoregressive moving average with echo state network compensation to improve the accuracy of short-term wind speed forecasting. A hybrid deep learning model that contains a gated recurrent unit (GRU), a neural network and an attention mechanism was used to forecast the solar irradiance changes in four different seasons [69]. Meanwhile the authors in [70] demonstrated that forecasting solar irradiance is vital to renewable energy generation.

An intelligent hybrid clustered for wind speed forecasting model was proposed based on different combinations of ANN, WNN, and the least- square methods. The model is based on two different steps of forecasting using back-to-back results to increase the number of inputs in the second stage to improve system accuracy. The model uses preprocessed data based on clustering techniques; at the end, the forecasted data are aggregated [55]. A hybrid model consisting of Neuro Wavelet (WNN), Time Series, and Recurrent Kalman filter for wind speed forecasting was proposed based on two different stages. The model depended on using the error from the first stage as an input for the second stage to improve the system accuracy and reduce the training time [56]. Hybrid Models of ANN, WNN, and a Kalman filter based on clustering techniques for smart grid integration were proposed for short-term load forecasting. The model convergence in this approach is very fast but it is also more complicated and if there is any error at any stage, the error will be accumulated [71]. An adaptive method based on a multi-model partitioning algorithm (MMPA) was developed to forecast a short-term electricity load using historical data. Different real cases derived from

measurement loads taken at the Hellenic Public Power Cooperative Company were studied. The obtained results showed that the proposed method could determine the component of the electricity load time series [72]. Several ANN models have been built based on different combinations of learning algorithms and transfer functions. Real data were divided into three stages: training, validation and testing stages. The models' outputs were compared to each other to identify the most reliable one. The selected model was then used to forecast energy consumption a year ahead [73]. HOMER software was used to analyze the technical and economic viability of hybrid energy systems in the Masirah Island power system in Oman. They evaluated different scenarios using package DIgSILENT. The authors stated that the hybrid energy system containing diesel, photovoltaic, and a wind turbine is a good choice, as it reduces operational costs [74]. A comprehensive study was done to predict the hourly energy from a solar thermal collector system. The authors used random forest (RF), extra trees (ET), decision trees, and support vector regression (SVR). These models were evaluated based on ability (stability), accuracy and computational cost. The obtained results showed that RF and ET performances are equal, and that they are more accurate than DT [75]. The daily total energy generation of an installed photovoltaic system was predicted using the Naïve Bayes classifier. The classifier applied to a one-year historical dataset such as daily average temperature, daily total sunshine duration, daily total global solar radiation and daily total photovoltaic energy generation parameters. The results proved that the Naïve Bayes classifier effectively predicts the total energy generation, giving an accuracy of 82.1917% [76]. The authors in [27] claimed that many machine-learning algorithms, such as linear regression (LR), K nearest neighbor regression (KNN), support-vector machine regression (SVMR), and decision-tree regression (DTR), are used in renewable-energy predictions. They stated that the most used machine-learning algorithms were for solar energy and wind-energy predictions. The following section summarizes the different algorithms encountered in machine learning.

4.3 Machine Learning

Machine learning (ML) is an application of artificial intelligence (AI). It is widely used in every sphere of human life because of its ability to solve real-life problems. Figure (4.2) shows the two main steps in achieving ML algorithms. The two stages of the dataset are divided into two unequal groups—training and testing datasets—to designate training and testing stages. In the training

stage, the dataset is used as input in the selected algorithm to train it. The trained selected algorithm is then fed by testing the dataset to evaluate the selected algorithm performance in the testing stage.

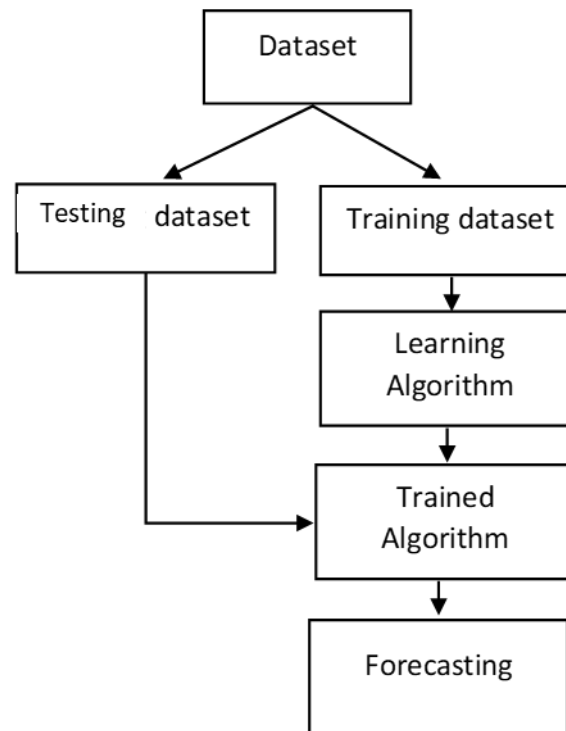


Figure 4.2 Two main steps in achieving ML algorithms

ML problems can be divided into three types: supervised, unsupervised and reinforcement. No specific algorithm can solve ML problems due to their complexity, which sometimes requires a unique algorithm [77]. The main reason for selecting Random Forest (RF), Gaussian Naive Bayes (Gaussian NB), Decision Tree (DT) and K-Nearest Neighbor (KNN) is the type of problem that needs to be solved. These algorithms can solve the classification problem. The second reason is the number of data points and features, as different algorithms can handle different sized datasets. Also, these algorithms do not require normalization of data and easy to implement.

4.3.1 Random Forest (RF)

Breiman [78] introduced Random Forest in 2001. RF is a supervised ML algorithm that is widely used due to its robust performance [79]. However, because the most practical classification problems are imbalanced, many algorithms cannot accurately handle them. RF can overcome this

challenge by applying a cost-sensitive learning and sampling technique [80]. Figure (4.3) presents the main steps of RF.

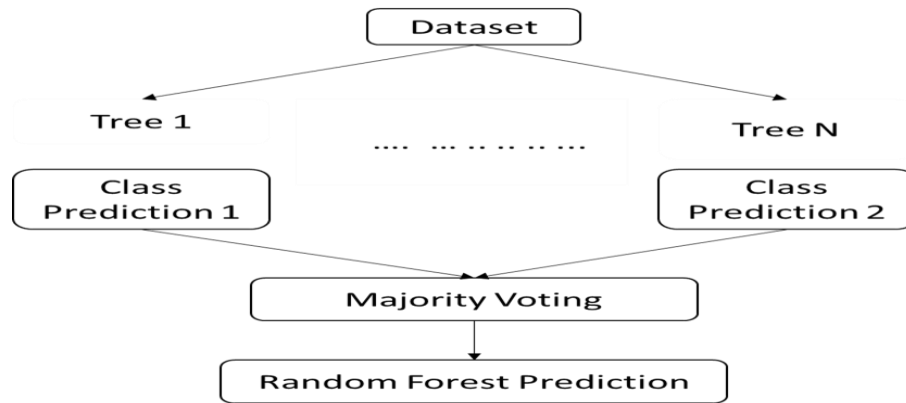


Figure 4.3 Main steps involved in the Random Forest (RF) algorithm.

4.3.2 Gaussian Naive Bayes (Gaussian NB)

Gaussian Naive Bayes is a simple probabilistic algorithm. It is one of the most well-known of the Naive Bayes (NB) algorithms that uses the Bayes’ theorem. The approach is designed to handle continuous attributes associated with each class that is distributed according to Gaussian distribution [81]. The significant advantages of the NB family are that it can be applied to practical classification problems, it requires less training data, and it can be trained very effectively in supervised learning. A significant drawback of the NB family is that the attributes are assumed to be independent, which is almost impossible [82]. Figure (4.4) illustrates the primary stages involved in the Gaussian NB algorithm.

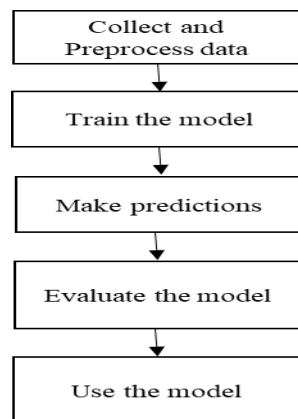


Figure 4.4 Gaussian Naive Bayes algorithm flowchart.

4.3.3 Decision Tree (DT) algorithm

Decision Tree algorithms were first introduced by Ho in 1995. Later, a multiple DT algorithm was used to form the RF algorithm [83]. The DT approach can be employed to solve classification or regression problems. Unlike many other algorithms, DT can handle a wide range of attributes and does not require scale normalization before model building and application. Furthermore, regarding data preparation, the DT algorithm is not affected by missing data [84]. Figure (4.5) shows the flowchart of DT.

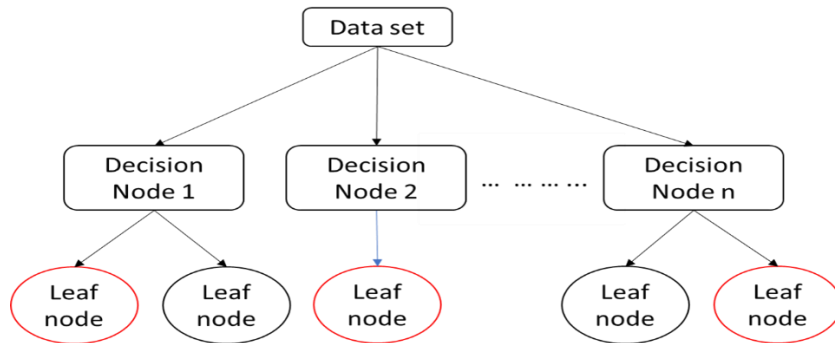


Figure 4.5 the flowchart of DT algorithm.

4.3.4 K-Nearest Neighbor (KNN)

K Nearest Neighbor (KNN) is one of the most frequently used algorithms in machine learning due to its ease of use and versatility [85]. However, because KNN uses all the training data, it requires time to read it and memory to store it. The authors in [86] provide a good summary of the advantages and disadvantages of KNN techniques. The letter “K” indicates the number of nearest neighbors. In contrast, the term “nearest neighbor” indicates that the algorithm is searching for the closest point needed for the classification and labeling of the nearest point assigned to it. The nearest neighbor distance between two points can thus be calculated using a Euclidean distance function, as shown in Equation (4.1):

$$D = \sqrt{\sum_{i=1}^n (b_i - a_j)^2} \dots\dots\dots (4.1)$$

where D is the distance between the two points a and b.

Algorithms such as KNN and support vectors that use distance measures between input variables could face some issues, one of which is the differences in input variable scales. This issue could lead to difficulty during model creation, and their performance could be poor during learning. Therefore, standardizing or normalizing data on the same scale is

highly recommended [87]. Equations (4.2) and (4.3) can be used to standardize or normalize the data.

$$\text{normalization value} = \frac{(x-\mu)}{\sigma} \dots\dots\dots (4.2)$$

where μ is the mean of the feature values and σ is the standard deviation of the feature values.

$$\text{standardization value} = \frac{=(x-x_{min})}{(x_{max}-x_{min})} \dots\dots\dots (4.3)$$

where X_{max} and X_{min} are the maximum and the minimum values of the feature, respectively.

4.4 Evaluating Metrics

An essential step in building a machine-learning model is evaluating its performance. Various metrics can be used for this purpose as well as for comparative purposes. Accuracy, which is a common evaluation metric for classification problems, is calculated as shown in Equation (4.4):

$$\text{Accuracy} = \frac{TP+TN}{T_o} \dots\dots\dots (4.4)$$

Where TP is true positive, TN is true negative, and T_o is total number of predictions. TP is when the predicted value is yes and the actual output is also yes, while TN is when the predicted value is no and the actual output is also no.

Overall classification accuracy is often not an appropriate metric for evaluating model performance in the case of a dataset with imbalanced data [88]. In addition, sometimes the algorithm understands only one or two classes, which means the algorithm could be biased towards one class over the others. A few of the more powerful metrics that can provide a clear idea about model performance when dealing with imbalanced data are given below:

- Precision

The precision metric can be calculated as shown in Equation (4.5) by the number of true positives (TPs) divided by the number of TPs and False Positives (FPs).

$$\text{Precision} = \frac{TP}{TP+FP} \dots\dots\dots (4.5)$$

- Recall

Recall is another important metric, which is defined as the number of TPs divided by the number of TPs and the number of FNs, as expressed in Equation (4.6):

$$\text{Recall} = \frac{TP}{TP+FN} \dots\dots\dots (4.6)$$

- F1 Score

The F1 Score metric shows the robustness and precision of the model and seeks to find the balance between precision and recall. Mathematically, it can be expressed as:

$$\text{F-Score} = \frac{2}{\frac{1}{\text{Precision}} + \frac{1}{\text{Recall}}} \dots\dots\dots (4.7)$$

4.5 Data Analysis and Hybrid Energy System Description

The scheduling dataset includes 336 instances and 5 attributes: 4 inputs and 1 output variable. The inputs are hourly load, temperature, and availability of solar and wind, while the output is the scheduling of the hybrid energy sources. The inputs are numeric and have values across various ranges. The last attribute is the class output variable. The class output type is nominal and has six values. These values are encoded as presented in Table (4.1). Figures (4.6), (4.7), (4.8), and (4.9) display the graphical distribution of the temperature, load, solar availability, and wind availability attributes, respectively. Each color represents the class and number of attributes. As can be seen, there is a different overlap distribution for the class values on each attribute. The temperature and load attributes have a Gaussian-like distribution and a nearly Gaussian distribution with a skew, respectively. The sun and wind attribute values are 0 and 1, where 0 means there is no wind or solar and 1 means there is wind or solar. The classes are imbalanced, indicating an unequal number of instances in each class.

Table 4.1 Encoded Values for Different Classes.

Class	Class Encoding
Solar and Wind 16	1
Gasoline Generator 90	2
Solar and Gasoline Generator 13	3
Wind and Gasoline Generator 152	4
Solar, Wind and Gasoline Generator 27	5
Gasoline Generator and Diesel Generator 39	6

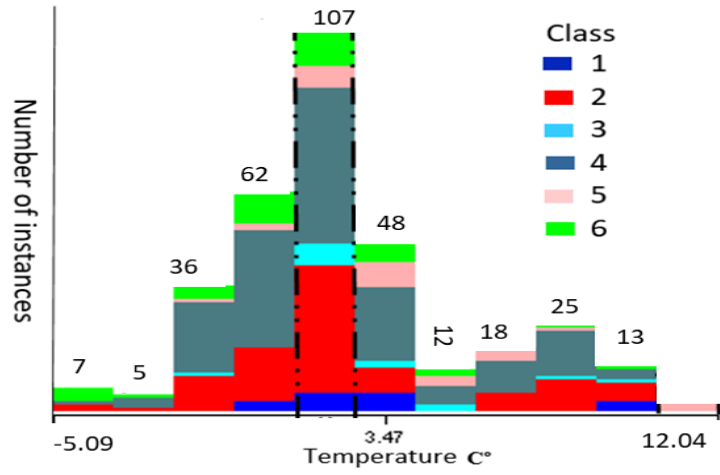


Figure 4.6 Graphical distribution of temperature.

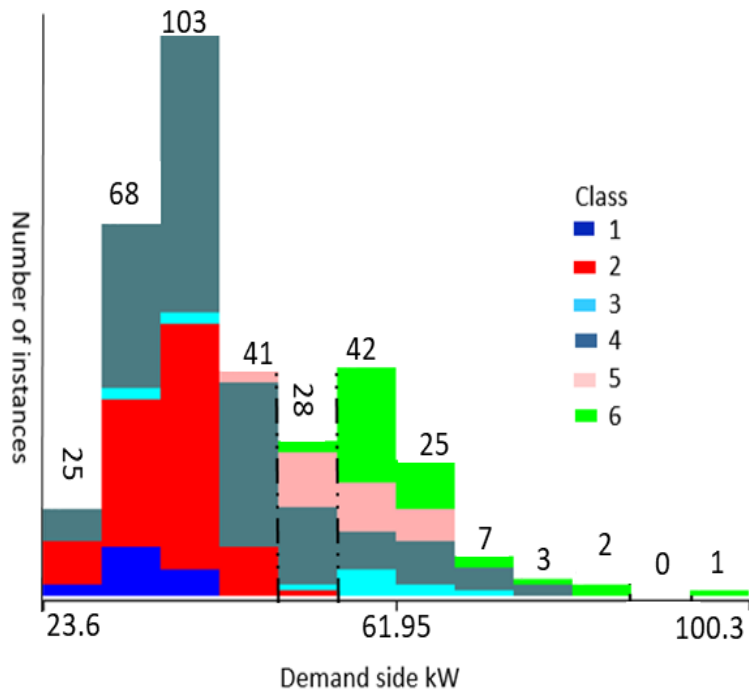


Figure 4.7 Graphical distribution of load.

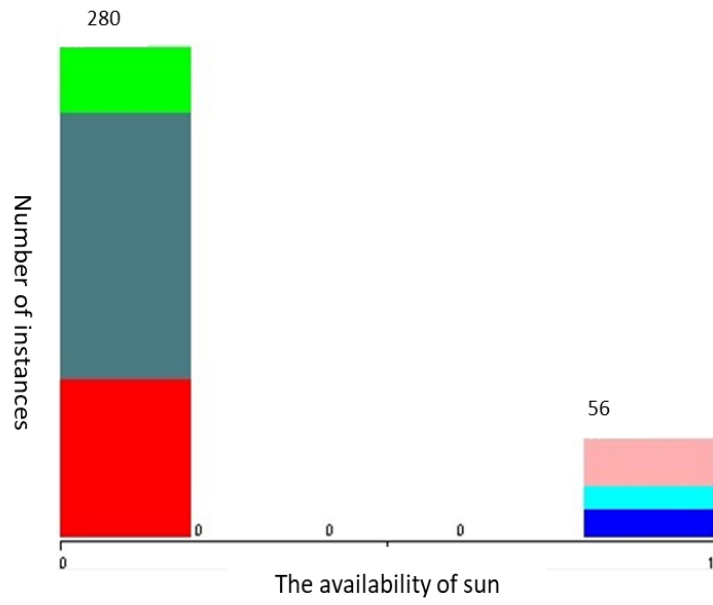


Figure 4.8 Graphical distribution of the availability of sun.

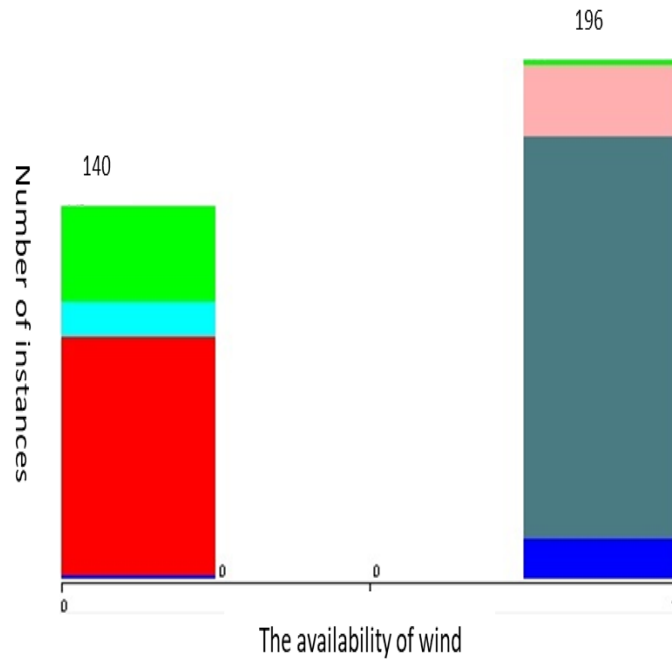


Figure 4.9 Graphical distribution of the availability of wind.

4.6 Focus of the Present Research

A HES consisting of two renewable energy sources (solar and wind energy) and two traditional energy sources (gasoline and diesel generators) is studied in this thesis. The power output of the solar and wind turbine is 20 kW and 25 kW, respectively, while the output for the gasoline and diesel generators is 50 kW and 55 kW, respectively. The system is used to supply a remote community. The maximum load in the remote community is 100 kW, and the minimum load is 23.6 kW. The sources of the HES have been scheduling more than 336 hours over two weeks. ML algorithms are employed to predict the scheduling of the HES sources. Specifically, the scheduling dataset is divided into two groups: 70% is for training the machine-learning algorithms, and the rest is for testing the algorithms.

4.7 Results and Discussion

Predicting a source that will meet the demand is one of the essential factors that should be considered when designing a hybrid energy system. As we stated in the literature review, many studies paid attention to power consumption, power generation, and weather prediction, but not scheduling prediction. The results of schedule prediction for a hybrid energy system were successfully obtained in the present study. Table (4.2) shows the overall accuracy of the algorithms applied to the scheduling dataset. RF, Gaussian NB, and DT algorithms resulted in reliable percentages. The accuracy can be used for evaluating binary and multiclass classifiers.

However, because the data are imbalanced, the overall accuracy cannot be a reliable metric to evaluate the algorithms, as the overall accuracy treats all classes equally and does not give attention to minority classes. This problem has been solved by using precision, recall, and F1-score metrics. These metrics show how the algorithms deal with individual classes.

Table 4.2 Overall Accuracy of Algorithms

Algorithm	Accuracy of training data	Accuracy of testing data
RF	99.5	95.05
Gaussian NB	95	95
DT	100	95
KNN	32.34	38.61
KNN Standard Scaler	97	95

Figure (4.10) presents the use of precision metric for evaluating the algorithms over the classes. As can be seen, the DT algorithm shows overall excellent performance, followed by the RF and Gaussian NB algorithms. The KNN algorithm shows the worst performance, especially in class 3. Figure (4.11) shows the use of recall metric for assessing the algorithms over classes 1, 2, 3, 4, 5, and 6. As shown in the figure, it is clear that the DT algorithm has the highest performance of the classes, while the RF and Gaussian NB algorithms and the KNN have the lowest.

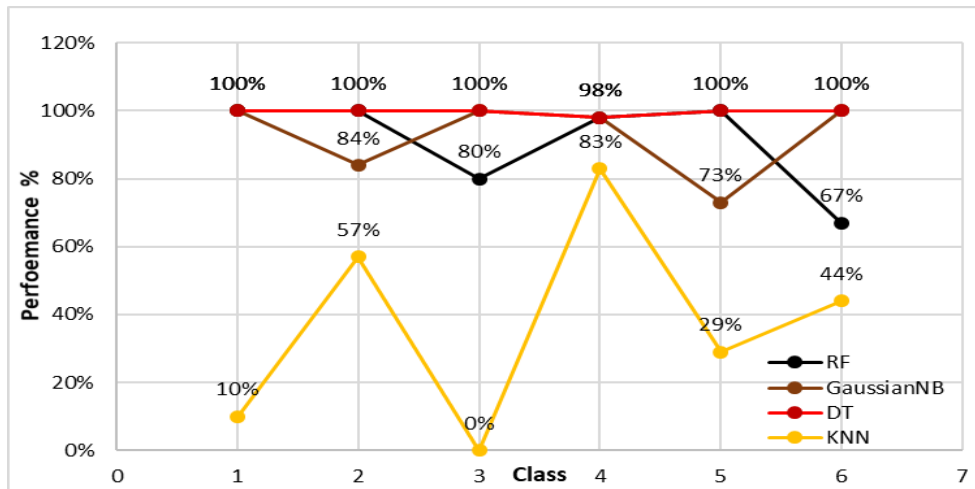


Figure 4.10 Precision metric.

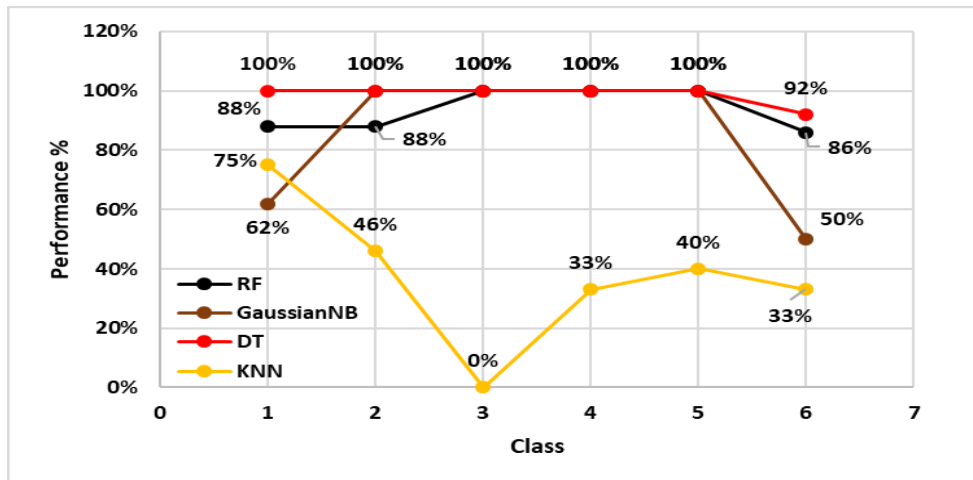


Figure 4.11 Recall metric.

Figure (4.12) depicts that utilizing the F1-score metric gives nearly the same results as the precision and recall metrics regarding performance. Even though class 3 occurs only 13 times in the dataset, RF, Gaussian NB and DT have a robust performance at every performance stages. The obtained results from the precision, recall, and F1-score metrics show the algorithm's real performances. Moreover, they show how the overall accuracy gives misleading results due to imbalanced data. In general, it is noticeable that the RF, Gaussian NB and KNN algorithms are biased to specific classes, whereas the DT algorithm understands all classes.

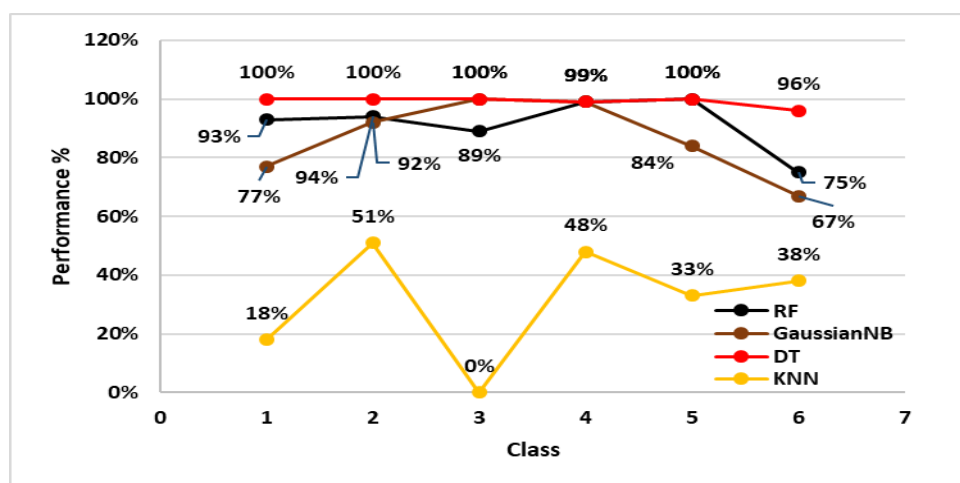


Figure 4.12 F1-score metric.

Standardizing the dataset is an amendment to the performance of the KNN algorithm. Figures (4.13), (4.14), and (4.15) manifest the performance of the KNN algorithm after standardizing the dataset. It is noticeable that there is a significant change in the KNN performance in cases where the KNN algorithm could understand all the classes. Due to the amendment, the KNN algorithm competed with the RF and Gaussian NB in only some of the classes.

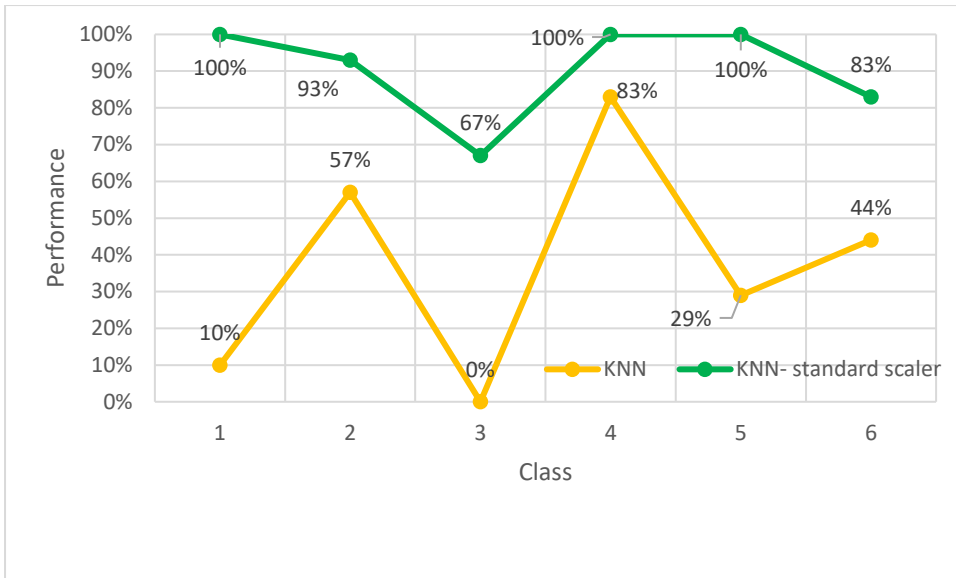


Figure 4.13 Precision metric: KNN algorithm performance post-dataset standardizing.

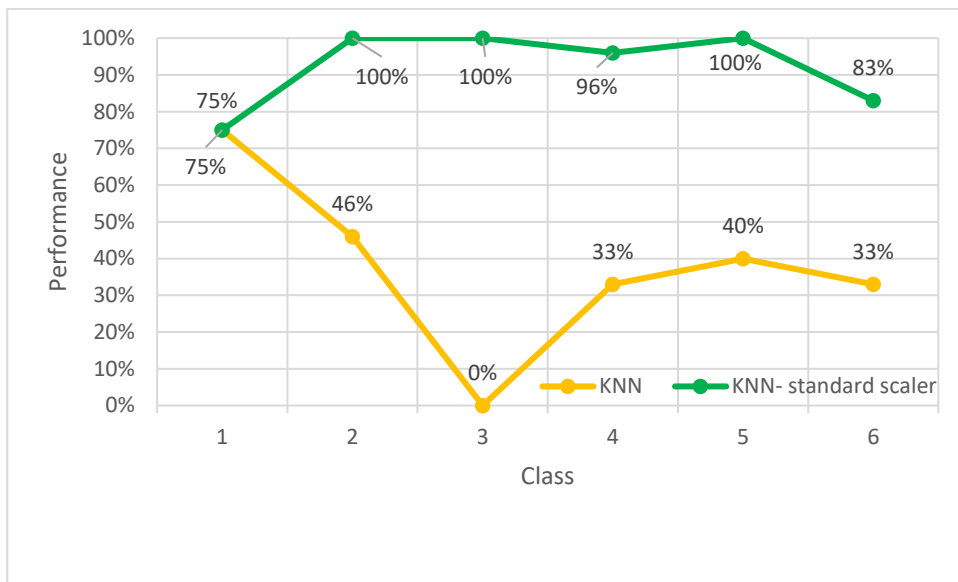


Figure 4.14 Recall metric: KNN algorithm performance post-dataset standardizing.

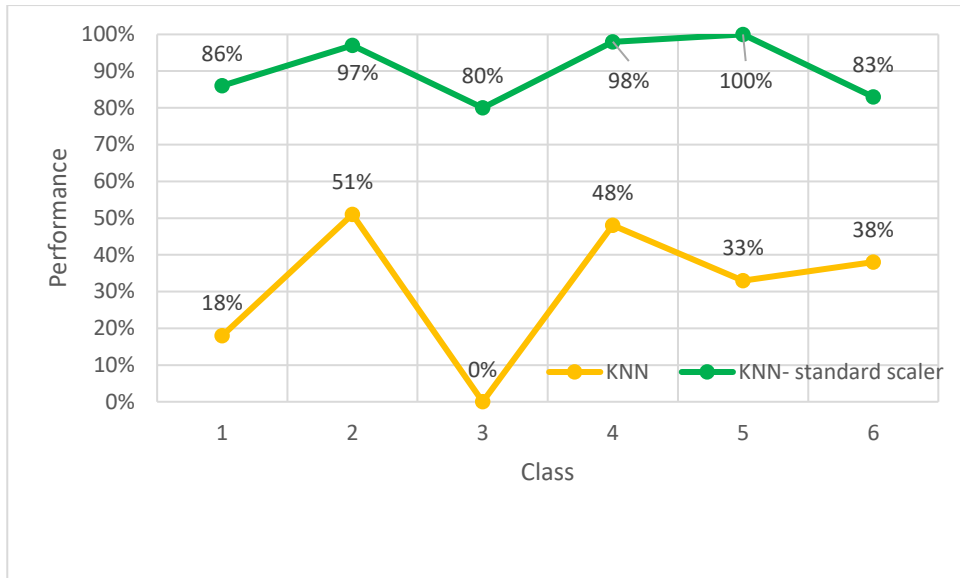


Figure 4.15 F1 score metric: KNN algorithm performance post-dataset standardizing.

The confusion matrix was generated to summarize the algorithms' performances, as shown in Figure (4.16). The columns represent the actual results, while the rows represent the predicted results; the correct predictions are highlighted in red. As can be seen, seven values were correctly classified as class 1. Reading down the class 3 column, one value that should be class 3 was classified as class 1. Also, 23 values were correctly classified as class 2. Reading down the class 6 column, three values that should be class 6 were classified as class 2. The RF algorithm correctly classified the other values, namely classes 4 and 5, figure (4.16a).

Class	1	2	3	4	5	6
1	[7 0 1 0 0 0]	[3 0 1 0 0 0]				
2	[0 23 0 0 0 3]	[0 28 0 0 0 0]				
3	[0 0 4 0 0 0]	[0 0 2 0 0 0]				
4	[0 0 0 52 0 0]	[0 0 0 43 0 2]				
5	[0 0 0 0 4 0]	[0 0 0 0 10 0]				
6	[0 0 0 1 0 6]	[0 2 0 0 0 10]				

a. Random Forest b. KNN Standard scaler

Class	1	2	3	4	5	6
1	[5 0 0 0 3 0]	[5 0 0 0 0 0]				
2	[0 27 0 0 0 0]	[0 27 0 0 0 0]				
3	[0 0 5 0 0 0]	[0 0 4 0 0 0]				
4	[0 0 0 41 0 0]	[0 0 0 43 0 0]				
5	[0 0 0 0 8 0]	[0 0 0 0 10 0]				
6	[0 5 0 1 0 6]	[0 0 0 1 0 11]				

c. Gaussian Naive Bayes d. DecisionTree

Figure 4.16 Confusion matrix of the algorithms.

4.8 Conclusion

This chapter proposed a novel technique for next-hour forecasting in order to optimize the energy management of hybrid energy systems. Machine-learning algorithms, such as RF and DT, were applied to energy management datasets to forecast which sources should supply the demand-side. The work was validated by comparing the two algorithms to Gaussian NB and KNN. The results from the overall accuracy metric indicate that the algorithms are reliable in forecasting energy management. However, these results are somewhat misleading, as the algorithms demonstrate biases to specific classes. Thus, a classification report was used instead of the overall accuracy metric. In utilizing classification, it was found that the DT algorithm achieved excellent performance compared to the RF and Gaussian NB algorithms. In contrast, the KNN algorithm presented a weak performance compared to the RF, DT, and Gaussian NB algorithms, especially over class 3. Finally, after standardizing the energy management dataset, the KNN algorithm was able to compete with the RF and Gaussian NB algorithms in some of the classes.

Chapter5. Energy Management Using Multi-Criteria Decision Making and Machine-Learning Classification Algorithms for Intelligent Systems

(The materials presented in this chapter are based on a journal paper published in *Elsevier* [18].)

Abstract

A hybrid energy system (HES) is one of the most effective solutions for power demand, especially in remote areas. It is well known that a HES usually includes renewables like solar or wind energy sources. However, as renewables can be intermittent, effective energy management plays an essential role in organizing the power flow in hybrid energy sources. In this chapter, a HES composed of wind, gasoline, and a diesel generator is used to electrify a specific remote area. The sources of the HES are categorized in different arrangements to select the best combination from all available six energy source combinations, based on five criteria. The technique for the order of preference by similarity to find the ideal solution (TOPSIS) is used. This work is divided into two stages. In the first stage, a historical load dataset is used to model and calculate the five criteria. TOPSIS results are combined with the five criteria and the load to form a dataset. In the second stage, machine-learning algorithms, namely random forest (RF) and light gradient boosted machine (LightGBM) algorithms, are used to predict the combination of the energy sources as a means of validating the proposed strategy. The evaluations show the superiority of the RF algorithm (with an accuracy of 81.81%) over the LightGBM algorithm (with an accuracy of 68.6%). The behavior of both algorithms is explained using the confusion matrix. RF classifies the classes G1G2 and G2 correctly but misclassifies some values of the other classes. LightGBM, on the other hand, classifies G2 correctly, but misclassifies values for other classes.

5.1 Introduction

Most remote communities suffer from a lack of essential services, including sufficient access to a power grid. Connecting these communities to the grid is possible, but the cost and transmission power losses can be high. A hybrid energy systems (HES) that contain renewable energy sources combined with more conventional energy sources is an ideal solution in such cases. However, because renewables, like solar and wind, are considered intermittent energy sources, a HES require a highly accurate energy management strategy (EMS) to organize energy flow from the HES sources to the load. An EMS is considered efficient if it protects HES components from damage

and ensures energy flow under all conditions. As well, an EMS is important for optimizing the size and cost of an energy system [43] [44] [56] [55] [89].

Energy management in a HES is usually done with software such as MATLAB, Simulink, HOMER and TRNSYS, or with artificial intelligence such as differential evolution algorithm, fuzzy logic quasi-steady-state time-series models, particle swarm optimization, genetic algorithm and artificial neural networks [89]. In this chapter, the energy management plan is forecasted using a dataset created with TOPSIS.

The novelty of the work is:

1. To propose an optimal HES based on TOPSIS using different combinations to minimize fossil fuel emission and overall costs as well as to increase the penetration of renewable energy resources. The results of this hybrid model will be used for the next stage.
2. To calculate five criteria based on time series load data to evaluate different sources combinations.
3. To create a dataset from TOPSIS method results that can be used in forecasting the sources that should be connected to the load.
4. To forecast energy management based on machine-learning algorithms.
5. To validate the proposed work by comparing the forecasted dataset with a different approach like LightGBM.

The hybrid energy system in this work consists of wind, gasoline and diesel generators and is used to electrify a remote area. The authors assume that the wind speed is sufficient to generate energy from the wind farm. The sources of the HES are categorized in different combinations (alternatives in the TOPSIS method) to select the best hybrid energy source from all possible available sources based on five criteria, using TOPSIS. The work is divided into two stages. In the first stage, a historical load dataset is used to model and calculate the five criteria. The TOPSIS method results are combined with the five criteria and the load to form a dataset. In the second stage, machine-learning algorithms, specifically RF and LightGBM, are used to predict possible alternatives to the energy sources.

5.2 Literature Review

5.2.1 Power Management

An electrical power management system provides precise information about power flow in an electrical power system. It records and provides the power system's data, which will be used to manage the power system components. In [90], a promising smart-grid system configuration was introduced with a tree-like node classification to ease the distributed generation strategies management based on load management, distributed storage, and renewable sources. The authors in [91] analyzed forty variables connected to industry power management using factor analysis. The factors were considered from behavioral, change, contingency, economic and technological perspective. A novel optimization model to evaluate the contribution of vehicle-to-grid V2G systems to assist power management within realistic configurations of small electric power systems, including green energy, was proposed in [92].

In [93], the authors proposed an EMS for a sustainable stand-alone HES composed of wind farm, solar arrays, and bioethanol. A genetic algorithm technique is introduced to size the stand-alone system optimally. To validate the introduced technique, various load scenarios were tested. Researchers in [94] suggested sizing HES using different EMS. The EMS applied in the proposed model are cycle-charging strategy (CCS), load-following strategy (LFS), and peak-shaving strategy (PSS). Genetic algorithm (GA), particle swarm optimization (PSO) and biogeography-based optimization techniques (BBO) are applied to size the HES by keeping energy index ratio at 1. Net present cost (NPC), cost of energy (COE), renewable fraction (RF), and emissions of CO₂ from diesel generator were also considered in the study.

Meanwhile, the authors in [95] proposed various hybrid power generation technology management options. Some well-known algorithms have been applied to manage the load sharing and to improve the performance of the hybrid system. The results obtained show that a combination of fuzzy logic controller with quantum behaved particle swarm optimization (QPSO) gives the best performance among other combinations, which including ant colony optimization (ACO), cuckoo optimization algorithm (COA), imperialist competitive algorithm (ICA), and particle swarm optimization (PSO). In [96], a hybrid power system composed of solar cells, fuel cells and a battery, along with an electrolyzer and H₂ tank, was presented. A control logic technique was introduced and then verified with SIMULINK. The simulation results obtained depict the efficiency of the model. In [97], a hybrid energy system composed of 1 MW wind farm, 1.1 MW

solar array, 300 kW fuel cell, 300 kW diesel generator and 72 kWh batteries, and designed its management strategy, was debuted. The load profile was estimated, and the system was sized using HOMER software. SIMULINK was then applied to obtain the simulation results. The results proved the feasibility of the power management strategy of the proposed hybrid power system. The authors in [98] showcased an autonomous stand-alone hybrid power system composed of solar panels energy and a backup fuel cell. A Simulink model was developed to test the effectiveness of the system presented. The obtained results proved the feasibility of their model.

5.2.2 Multi-Criteria Decision-Making (MCDM)

Multiple-criteria decision-making (MCDM) or multiple-criteria decision analysis (MCDA) is used to evaluate multiple conflicting criteria in decision-making in a variety of disciplines. MCDM is applied when multiple criteria (or objectives) must be considered together to rank or choose among the evaluated alternatives. The study in [99] proposed an MCDM technique based on AHP to evaluate five renewable power generation sources: biomass, geothermal, concentrated solar power, solar photovoltaic, and wind energy. The results obtained from the case study show that the best power generation techniques are solar photovoltaic and concentrated solar power, respectively. In [100], 13 renewable and non-renewable power sources for generating electricity in the United States using MCDM techniques were compared. The attained results conclude that biopower and geothermal energies are the optimal sustainable energy sources in the US. In most scenarios, renewable energy sources are more sustainable than fossil fuels, and nuclear ones are more favorable than fossil fuels. Renewable energy sources in Turkey were ranked in [101] using Fuzzy TOPSIS, based on the amount of energy produced, capacity installed, efficiency, job creation, investment cost, land use, operation and maintenance cost, payback period, and value of CO₂ emissions. The results showed that hydropower is the best energy source option in Turkey, followed by geothermal power, regulator and wind power, respectively.

In [102], the VIKOR method was combined with the AHP technique to select the optimal option of different renewable energy sources in Spain. The results showed that biomass energy is the best option, followed by wind power and solar thermo-electric alternatives. The researchers in [103] proposed a modified fuzzy TOPSIS approach to choose the best energy technology from various energy sources. A fuzzy AHP technique was applied to determine the weights of each criterion in order to build pairwise comparisons. The findings showed that wind energy is the optimal energy

source option in the studied area. A MCDM technique to select the optimal sustainable power generation technology was presented in [104]. MULTIMOORA (Multi-Objective Optimization on the basis of a Ratio Analysis plus Full Multiplicative Form) [105] and TOPSIS were applied, with the results showing that hydro and solar thermal energies are the best sustainable energy options in the studied area, followed by wood CHP and wind power. The fuzzy TOPSIS technique was employed in [106] to select the engine flywheel material.

In [107], the TOPSIS method determined investment opportunities in the Mokran coasts region in Iran by specifying the important infrastructures for entrepreneurial activities. Among 22 investment options, and by asking some experts and applying the best-worst MCDM [108], the researchers found commercial centers, loading, private port sites, particular areas of fisheries, and warehouses more attractive to investors. Other researchers [109] applied the fuzzy TOPSIS technique to determine the best combat response in case of oil spill accident in the Brazilian sea. Ten combat options, two decision criteria, and three decision-makers were applied, while in [110], the authors a fuzzy TOPSIS technique to determine the best location to build an urban distribution center.

A comprehensive state of the art review of the most recent advances in methodologies and applications of fuzzy MCDM in the energy field was investigated in [111], and in [112], the authors presented a new divergence measure to rank and choose the RES in MCDM techniques based on fuzzy TOPSIS; they then compared it with some existing algorithms. The results showed that the ranking outcomes were almost similar to the existing MCDM techniques. A state-of-the-art review for optimizing different manufacturing processes using the TOPSIS method was conducted in [113]. Some areas reviewed included milling, drilling, turning, electric discharge machining, abrasive jet machining, and micromachining. The authors in [114] introduced an optimal mapping of HES composed of wind farm, solar arrays, storage, and a diesel generator for households in southern Nigeria. The research considered technical, economic, environmental, and sociocultural criteria and was done based on HOMER software and the TOPSIS method. 7.23 kWh/day per household's electrical power demand was met either with the wind/solar/battery model or with the wind/solar/battery/diesel generator model.

In [115], the researchers introduced Social, Technical, Economical, Environmental, and Political STEEP-fuzzy AHP-TOPSIS techniques to determine thermal power plants and suggest their

locations in India. Fuzzy AHP is used to specify the weights of qualitative and quantitative criteria affecting the location selection process. The TOPSIS method is used to rank the alternative locations according on their overall performance. The authors in [116] applied TOPSIS to rank the significance and attractiveness of the stack of fuel cells as a sub-system in the automotive industry and to evaluate the labor and equipment needed in the laboratory and industry scale, while [117] introduced an AHP method in combination with benefits, opportunities, costs, and risks (BOCR) to determine an optimal wind farm project.

5.2.3 Machine Learning

Machine learning is a technology that belongs to artificial intelligence, which is applied to analyze the data automatically with minimal human interaction. A model was showcased in [118] to enhance the currently low-rate prediction accuracy of heart failure (HF). The results showed that the developed method could perform with 93.33% prediction accuracy. In [119], the authors investigated and tested a hybrid machine-learning technique that deals with big data analysis to optimize energy harnessing in the field of smart energy management. The manipulated data were taken from different conventional and green energy sources. A study in [120] reviewed the famous novel and classical algorithms that are applied in renewable energy technology. The study also provided a comprehensive literature review for various classification techniques, including support vector machines and artificial neural networks.

In [121], a model was presented that forecasted the climate for daily power generation at the Zhonghe PV station in North China using a random forest algorithm. The results showed a good outcome compared to the other three methods applied for comparison. A hybrid model of machine-learning algorithms to optimize power consumption in residential buildings was debuted in [122], with the results showing that the applied model could enhance building energy prediction accuracy. The authors in [123] looked at various machine-learning techniques applied in renewable power generation and renewable energy planning according to available data. They also investigated PV modules and wind farm sizing. In [124], state-of-the-art machine-learning models were applied in power systems. A novel taxonomy of the models was first applied, and then their applications were discussed. The authors concluded that hybrid ML models are robust, precise, and more effective for renewable power systems. Researchers in [125] presented a new forecasting algorithm based on a convolution neural network (CNN) combined with LightGBM to improve the forecasting accuracy and robustness of wind power data.

Fidelity and computational costs, along with the solidity of extra trees (ET) and random forest for forecasting hourly PV power output, were examined and compared in [126]. The comparison of ET and RF's performance was done via the supervised machine-learning technique called support vector regression (SVR). From the computational cost viewpoint, ET outperformed RF and SVR and was found to be an ideal candidate for PV output forecasting. Finally, in [127], the authors used five machine-learning techniques to perform long-term wind energy forecasting. Various scenarios were taken into consideration to determine the performance of the machine-learning algorithms. Promising results were obtained, especially for long-term wind power forecasting.

5.3 Methodology

5.3.1 TOPSIS

The Technique for Order Preference by Similarity to Ideal Solution (TOPSIS) method was developed in 1981 by Hwang and Yoon [19]. The researchers' aim in creating TOPSIS was to find the closest and farthest alternatives to the ideal and negative solutions [99]. In consequence, the designer can exclude farthest alternative from the system. Also, TOPSIS is suitable for situations with many alternatives and attributes. The steps in TOPSIS are simple and fixed, regardless of the criteria or number of alternatives [7]. However, one of the main drawbacks of the method is that there is no equation to derive the weight values, so only decision-makers can assign these values [95]. Only the decision-maker's subjective weights are considered, while the end-user's evaluation is disregarded.

However, involving end-users in evaluating the weight of the criteria and taking their judgments into consideration is essential to overcome issues that may arise from adding or deleting an alternative [128]. This can be done using the AHP or FAHP methods. Rank reversal phenomenon is another disadvantage may occur in MADM methods, such as the Borda–Kendall (BK) method for aggregating ordinal preferences and the simple additive weighting (SAW) method. This paper does not need to address the rank reversal phenomenon issue, because the case study that the paper dealt with is fixed. TOPSIS has proved its ability to solve selection problems with a finite number of alternatives. Due to its advantages [129], this method has been widely used in many fields, like manufacturing systems and engineering, environmental management, marketing management, design, business, water, and human resources management.

The TOPSIS method is described by the following steps:

- Constructing the decision matrix: A decision-making problem has m alternatives, and each alternative has n criteria. The decision matrix X_{ij} can be written as follows:

$$X_{ij} = \begin{bmatrix} x_{11} & x_{12} & \dots & x_{1n} \\ x_{21} & x_{22} & \dots & x_{2n} \\ \vdots & \vdots & \vdots & \vdots \\ x_{m1} & x_{m2} & \dots & x_{mn} \end{bmatrix} \quad (5.1)$$

where j^{th} is the criterion of the i^{th} alternative, $i=1,2, \dots, m$ and $j=1,2, \dots, n$.

- Calculating normalized matrix: The different criteria are converted from dimensional criteria into non-dimensional criteria to compare them. Equation (5.2) is used to normalize the decision matrix X_{ij} :

$$\bar{x}_{ij} = \frac{x_{ij}}{\sqrt{\sum_{i=1}^m x_{ij}^2}} \quad (5.2)$$

- Calculating the weighted normalized decision matrix by Equation (5.3):

$$V_{IJ} = \bar{X}_{ij} \times W_j \quad (5.3)$$

where W_j is the relative weight of the j^{th} criterion. The summation of criterion weight must be equal to 1.

- Determining the positive-ideal and negative-ideal solutions: Identifying beneficial and non-beneficial criteria. The beneficial criteria are the higher criteria value that are desired, while the non-beneficial criteria are the lower criteria values that are desired.
- Calculating the Euclidean distance from the ideal best and worst by Equations (5.4) and (5.5)

$$S_i^+ = \left[\sum_{j=1}^n (V_{ij} - V_j^+)^2 \right]^{-0.5} \quad (5.4)$$

$$S_i^- = \left[\sum_{j=1}^n (V_{ij} - V_j^-)^2 \right]^{-0.5} \quad (5.5)$$

where S^+ is the ideal best and S^- is the ideal worst

- Calculating Performance Score using Equation (5.6):

$$P_i = \frac{S_i^-}{S_i^+ + S_i^-} \quad (5.6)$$

Using TOPSIS, the weight values of the criteria are assigned randomly, because there is no equation to derive the weight values. This issue is considered the main weakness in the method [100]. To calculate the weight values of a criteria, other methods like AHP and FAHP can be used.

5.3.2 Analytic Hierarchy Method (AHP)

The analytic hierarchy method (AHP), developed by Saaty, is a powerful multi-criteria decision-making tool that has been applied in numerous applications in various fields such as economics, politics, and engineering [130]. It is a powerful method for analyzing and solving complex decision problems. The foremost step in the AHP method is creating a hierarchical structure that contains the goal at the top level, the criteria at the middle level, and the alternatives at the bottom level, as shown in Figure (5.1).

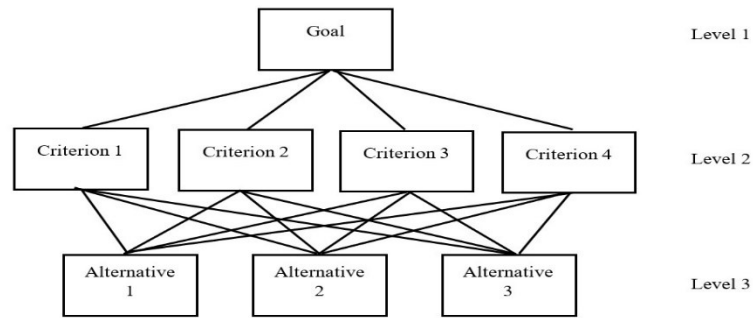


Figure 5.1 Hierarchical tree of criteria for AHP analysis.

The second step is creating a pairwise comparison matrix. This matrix contains the decision-maker's judgments, which show the relative importance of various criteria with respect to the goal. The judgments are evaluated in a scale of relative importance developed by Saaty, as presented in Table (5.1). The judgments must be consistent; otherwise, they will lead to a wrong decision [101].

Table 5.1 Scale of Relative Importance

Scale	Definition
1	Equal importance
3	Moderate importance
5	Strong importance
7	Very strong importance
9	Extreme importance
2, 4, 6, 8	Intermediate value

The third step is to calculate the normalized pairwise comparison matrix, followed by calculating the relative priority weights for the criteria.

The fourth step is to compute a Consistency Index, which is given by Equation (5.7):

$$Consistency\ Index\ (CI) = \frac{\lambda\ max - n}{n - 1} \tag{5.7}$$

where $\lambda\ max$ is an approximated eigenvector, and n is the number of criteria.

The final step is checking the consistency, which can be difficult to achieve. Consistency is measured by the Consistency Ratio (CR), as shown in Equation (5.8).

$$Consistency\ ratio = \frac{CI}{RI} \tag{5.8}$$

where RI is random index of random consistency of a randomly generated pairwise comparison matrix, as presented in Table (5.2) [131].

Table 5.2 Random Consistency of a Randomly Generated Pairwise Comparison Matrix

n	2	3	4	5	6	7	8	9	10	...
RI	0.00	0.58	0.9	1.12	1.24	1.32	1.41	1.45	1.49	...

The pairwise comparison matrix is considered consistent if the consistency ratio is less than 10 %. If it is greater than 10%, the pairwise comparison matrix needs to be re-evaluated. The authors in [132] explain how to identify inconsistent judgments and make them consistent.

5.3.3 Fuzzy Analytic Hierarchy Method (F-AHP)

The Fuzzy Analytic Hierarchy Process (F-AHP) was developed based on AHP, so F-AHP's uses are very similar to AHP's uses; the main difference is that F-AHP uses a range of values, whereas

AHP uses crisp values. Using a range of values allows the F-AHP method to remove the vagueness and uncertainty in decision-making. This benefit makes F-AHP superior to AHP. The procedure for executing the F-AHP method is as follows [103]:

- Create a pairwise comparison matrix using fuzzy numbers.
- Calculate the fuzzy geometric mean for each criterion (\tilde{r}_i), as shown in Equation (5.9), where \tilde{a}_{1n} is a fuzzy value of the pair-wise comparison of criterion i to criterion n.

$$\tilde{r}_i = (\tilde{a}_{i1} \otimes \dots \otimes \tilde{a}_{in})^{1/n} \quad (5.9)$$

-
- Compute the fuzzy weight of the i th criterion using Equation (5.10).

$$\tilde{w}_i = \tilde{r}_i \otimes (\tilde{r}_1 \oplus \tilde{r}_2 \dots \oplus \tilde{r}_n)^{-1} \quad (5.10)$$

- De-fuzzify the fuzzy weight by using Equation (5.11).

$$COA = \frac{l + m + u}{3} \quad (5.11)$$

Where: COA is center of area, and l, m and u are lower, middle and upper values of the fuzzy number.

5.3.4 LightGBM Algorithm

The LightGBM algorithm was developed by G. Ke and his colleagues in 2017. It implements the Gradient Boosting Decision Tree (GBDT) algorithm. LightGBM is widely used for solving classification and regression problems [133]. It is more powerful than many other machine-learning algorithms like XGBoost. The advantages of LightGBM are that it occupies less memory and has less training speed. Many parameters and settings are adjusted manually, which makes the algorithm complicated. The algorithm performance can be improved by optimizing the algorithm parameters using the Bayesian hyper-parameter optimization algorithm [134]. The theory of LightGBM algorithm's objective function can be written as:

$$obj^{(t)} = \sum_{i=1}^n l(y_i, \hat{y}_i^{(t)}) + \sum_{i=1}^t \Omega(f_i) \quad (5.12)$$

$$L(\theta) = \sum_i [y_i \ln(1 + e^{-\hat{y}_i}) + (1 - y_i) \ln(1 + e^{\hat{y}_i})] \quad (5.13)$$

where y_i is the objective value, i is the predicted value, t represents the number of leaf nodes, f_i is a decision tree, and $L(\theta)$ is Logistic loss.

5.3.5 Random Forest

The random forest (RF) algorithm is an ensemble learning technique that contains numerous decision trees. Leo Breiman introduced the algorithm in 2001 to overcome the main decision trees disadvantage, which is overfitting. Compared to other state-of-the-art algorithms like XGBoost and Gradient Boosting Machines (GBM), tuning the RF setting is simple, as it has a small number of parameters. RF is widely used to deal with regression and classification problems [78]. The random forest classifier consists of several decision tree models and is expressed as follows [135]:

$$\{DT(x, \theta_k)\}_{T_{k=1}} \quad (5.14)$$

Where x is the input vector, θ_k denotes the parameters that define the decision tree constructed using the k th bootstrap sample, and T is the number of bootstrap samples that derived from the training data. K represents how many samples were taken from the training dataset. The curly brackets indicate the use of multiple decision trees, and the indexing of the trees from 1 to T is shown by the subscript $T_{k=1}$. To classify the input vector x , the equation, in other words, describes the ensemble of T decision trees that are being employed.

Several metrics, such as the confusion matrix, were used to evaluate the performance of the algorithms. The confusion matrix is utilized to summarize an algorithm's performance when dealing with classification problems [136]. The performance of the algorithms is shown by the confusion matrix's four measures, which are true positive (TP), true negative (TN), false positive (FP), and false negative (FN) [60]. The matrix rows represent actual classes, while the columns represent their predicted classes. The confusion matrix could deal with a $n \times n$ classification problem.

Generally, LightGBM is a robust algorithm that shows superiority in solving multi-classification problems when compared to Random Forest, Decision Tree, Xgboost, Catboost, Extra Trees, Neural Network, Baseline and Linear algorithms, as presented in Table (5.3) [137]. LogLoss metric has also been used for evaluating the performance of the algorithm. RF performs well when compared to the same algorithms, as presented in Table (5.4).

Table 5.3 Comparison Between LightGBM and Other Classification Algorithms

Dataset \ Algorithm	Amazon-commerce-reviews	Car	Cnae-9	Connect-4	Mfeat-factors	Segment	Vehicle
Decision Tree	Lightgbm	Lightgbm	Lightgbm	Lightgbm	Lightgbm	Lightgbm	Lightgbm
Xgboost	Lightgbm	Lightgbm	Lightgbm	Lightgbm	Xgboost	Xgboost	Xgboost
Catboost	Lightgbm	Lightgbm	Lightgbm	Lightgbm	Catboost	Catboost	Catboost
Extra Trees	Lightgbm	Lightgbm	Lightgbm	Lightgbm	Lightgbm	Lightgbm	Lightgbm
Neural Network	Lightgbm	Lightgbm	Lightgbm	Lightgbm	Neural Network	Lightgbm	Neural Network
Baseline	Lightgbm	Lightgbm	Lightgbm	Lightgbm	Lightgbm	Lightgbm	Lightgbm
Linear	Linear	Lightgbm	Linear	Lightgbm	Linear	Lightgbm	Linear

Table 5.4 Comparison Between Random Forest and Other Classification Algorithms.

Dataset \ Algorithm	Amazon-commerce-reviews	Car	Cnae-9	Connect-4	Mfeat-factors	Segment	Vehicle
Decision Tree	RF	RF	RF	RF	RF	RF	RF
Xgboost	Xgboost	Xgboost	Xgboost	Xgboost	Xgboost	Xgboost	Xgboost
Lightgbm	Lightgbm	Lightgbm	Lightgbm	Lightgbm	Lightgbm	Lightgbm	Lightgbm
Catboost	Catboost	Catboost	Catboost	Catboost	Catboost	Catboost	Catboost
Extra Trees	RF	RF	Extra Trees	RF	RF	RF	RF
Neural Network	RF	Neural Network	Neural Network	Neural Network	Neural Network	Neural Network	Neural Network
Baseline	RF	RF	RF	RF	RF	RF	RF
Linear	Linear	RF	Linear	RF	Linear	RF	Linear

5.4 Case Study

A single source or combination of various sources has been proposed to form a HES to provide electricity load in a remote community. Table (5.5) shows sizing of single source or combination of various sources, where the sizing of the combination of various sources are calculating by

summing the single sources. A three-day dataset was used to comprise the hourly load of a remote community. The minimum and maximum values of the load of the remote community are 8 kW and 89.1 kW, respectively. Energy management of the hybrid energy system has been done using the TOPSIS method. Selecting the best alternative was achieved based on the following five criteria:

1. Efficiency of the energy sources.

$$\text{Efficiency} = \frac{\text{output of the source power kW}}{\text{size of the source power Kw}} \times 100 \quad (5.15)$$

2. CO₂ emissions.

$$\text{CO}_2 \text{ emission (Kg)} = \text{emission rate} * \text{Liter (L)} \quad (5.16)$$

The CO₂ emissions of gasoline and diesel generators are 2.29 kg/L and 2.66 kg/L, respectively.

3. Gasoline and diesel fuel prices

$$\text{Fuel Price} = \text{Fuel consumption (liter)} * \text{Liter Price (\$)} \quad (5.17)$$

The gasoline and diesel fuel prices are CAD \$0.981 and CAD \$0.896/ kW, respectively.

4. Labor

$$\text{Labour} = \text{Rate Maintenance} * \text{output of the source power} \quad (18)$$

The rate maintenance for gasoline and diesel generators is CAD \$0.015 and CAD \$0.01, respectively.

5. Consumption of fuels

The reference in [138] is used to determine the consumption of fuels.

These five criteria are divided into two categories: positive-ideal and negative-ideal solutions. The efficiency of the energy sources criterion is a beneficial criterion, while the other criteria are desired to be non-beneficial.

Table 5.5 Different Alternatives of Hybrid Energy Sources

Sources	Size of Sources
Wind farm (W)	25 kW
Gasoline generator (G1)	50 kW
Diesel generator (G2)	55 kW
Wind farm and gasoline generator (WG1)	75 kW
Wind farm and diesel generator (WG2)	80 kW
Gasoline and diesel generator (G1G2)	105 kW

5.5 Proposed Model Framework

The overall process of the proposed energy management of the HES model is depicted in Figure (5.2). In the first stage, the load dataset is used as input to calculate the five criteria. Then the alternative energy sources are evaluated based on these five criteria, using the TOPSIS method. The best combinations are saved as a dataset, which is called a pre-processed dataset. In the second stage, the dataset is used as input to the classification machine-learning algorithms.

5.6 Results and Discussion

Based on the TOPSIS method, the decision matrix has been constructed using Equations (5.15), (5.16), (5.17) and (5.18), as shown in Table (5.6).

Table 5.6 Decision Matrix at 34.2 kw

Sources	Fuel consumption (Liter)	Price(\$)	Efficiency (%)	CO ₂ (Kg)	Labor (\$/Kw)
G1	14.17239	13.90311	68.4	32.45477	0.513
G2	11.30805	10.13201	62.18182	30.07942	0.342
G1G2	16.08765	15.19662	17.1	39.3888	0.4275
WG1	5.900244	5.788139	18.4	13.51156	0.138
WG2	4.052453	3.630998	16.72727	10.77953	0.092
W	0	0	0	0	0

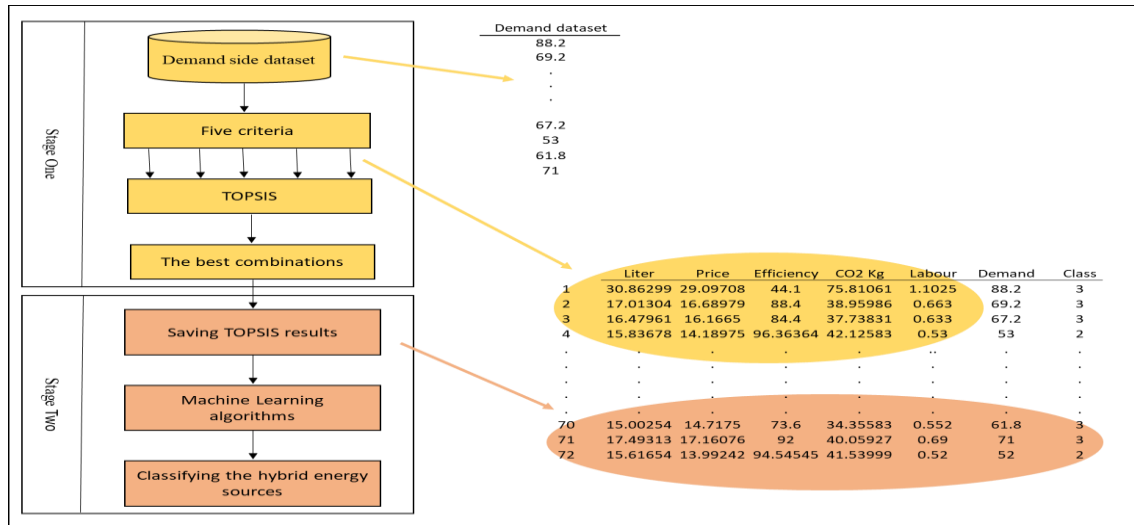


Figure 5.2 Overall process of proposed EM of the HES model.

The decision matrix values were calculated based on the first value of the load, which is 34.2 kW. The second step is, applying Equation (5.2) to convert the data in Table (5.6) from dimensional criteria into non-dimensional criteria. The aim in doing this is to make them comparable, as shown in Table (5.7).

Table 5.7 Normalized Matrix

Sources	Fuel consumption (Liter)	Price(\$)	Efficiency (%)	CO ₂ (Kg)	Labor (\$/Kw)
G1	0.390179	0.39994	0.7034	0.52591	0.0486
G2	0.31132	0.29146	0.6394	0.4874	0.032
G1G2	0.442908	0.43715	0.1758	0.638	0.0405
WG1	0.162439	0.16650	0.1892	0.2189	0.0130
WG2	0.11156	0.104450	0.1720	0.1746	0.008

The calculations of the weights of the criteria were done based on the following methods:

1. APH method
2. F-APH method
1. Calculating the weights of the criteria using AHP method

Table (5.8) shows the pairwise comparison matrix that was written according to the scale of relative importance. The relative importance of the five criteria to each other was collected based on the directors' judgments of the remote community.

Table 5.8 Pairwise Comparison Matrix

	Efficiency (%)	CO ₂ (kg)	Price(\$)	Labor(\$/Kw)	Fuel consumption (Liter)
Efficiency (%)	1	2	3	4	7
CO ₂ (kg)	0.5	1	5	4	9
Price (\$)	0.33333	0.2	1	3	3
Labor (\$/Kw)	0.25	0.25	0.333	1	4
Fuel consumption (Liter)	0.1428	0.111	0.333	0.25	1

Table (5.9) presents the normalized pairwise comparison matrix, whose results were obtained from the Table (5.6), using Equation (5.2). Table (5.9) also shows the weights of the criteria. The consistency was checked by applying Equation (5.7). The consistency equals 0.08, which means that the directors' judgments are acceptable.

Table 5.9 Normalized Pairwise Comparison Matrix

	Efficiency (%)	CO ₂ (kg)	Price(\$)	Labor(\$/Kw)	Fuel consumption (Liter)
Efficiency (%)	0.4491	0.5616	0.3	0.326531	0.29
CO ₂ (kg)	0.22	0.281	0.51	0.321	0.35
Price (\$)	0.1	0.056	0.10	0.24	0.1
Labor (\$/Kw)	0.1	0.070	0.03	0.081	0.166
Fuel consumption (Liter)	0.06	0.031	0.03	0.020	0.04
Weight	0.38	0.34	0.13	0.09	0.03

The results obtained from Table (5.7) were used to calculate the weighted normalized matrix. These results were then applied to calculate the Euclidean distance from the ideal best and worst using Equations (5.3) and (5.4). Finally, the performance score of the HES was identified using Equation (5.5) and Table (5.10).

Table 5. 10 Performance Score of Hybrid Energy Sources Based on AHP

Sources	Fuel consumption (Liter)	Price(\$)	Efficiency (%)	CO ₂ (Kg)	Labor (\$/Kw)	Si+	Sj-	Pi	Rank
G1	0.148	0.1375	0.0914	0.048	0.0014	0.154	0.193	0.55	4
G2	0.118	0.1002	0.0831	0.045	0.00097	0.109	0.232	0.67	3
G1G2	0.168	0.1503	0.0228	0.059	0.00121	0.192	0.148	0.43	5
WG1	0.0617	0.0572	0.0245	0.020	0.0003927	0.075	0.29	0.79	2
WG2	0.042	0.035	0.02236	0.016	0.00026	0.070	0.319	0.81	1

2. Calculating the weights of the criteria using the F-AHP method

The pairwise comparison matrix in Table (5.10) is rewritten in fuzzy numbers, as shown in Table (5.11).

Table 5.11 Pairwise Comparison Matrix in Fuzzy Numbers

	Efficiency (%)	CO ₂ (kg)	Price(\$)	Labor(\$/Kw)	Fuel consumption (Liter)
Efficiency (%)	(1,1,1)	(1,1,1)	(2,3,4)	(3,4,5)	(6,7,8)
CO ₂ (kg)	(1,1,1)	(1,1,1)	(4,5,6)	(3,4,5)	(9,9,9)
Price (\$)	(1/4,1/3,1/2)	(1/6,1/5,1/4)	(1,1,1)	(2,3,4)	(2,3,4)
Labor (\$/Kw)	(1/5,1/4,1/3)	(1/5,1/4,1/3)	(1/4,1/3,1/2)	(1,1,1)	(3,4,5)
Fuel consump. (L)	(1/8,1/7,1/6)	(1/9,1/9,1/9)	(1/4,1/3,1/2)	(1/5,1/4,1/3)	(1,1,1)

Table (5.12) shows the fuzzy geometric mean for each criterion using Equation (5.9). The results presented in Table (5.12) are used to calculate the fuzzy weight of the *i*th criterion using Equation (5.10), as shown in Table (5.13). De-fuzzification of the fuzzy weight of the *i*th criterion can be done using Equation (5.11), as shown in Table (5.14). The process for calculating the Euclidean distance from the ideal best and worst using Equations (5.4) and (5.5), and then applying Equation (5.6) to calculate the performance score of the HES, can be seen in Table (5.15).

Table 5.12 Fuzzy Geometric Mean for Each Criterion

	Efficiency (%)	CO ₂ (kg)	Price(\$)	Labor(\$/Kw)	Fuel consumption (Liter)	Fuzzy geometric mean
Efficiency (%)	(1,1,1)	(1,1,1)	(2,3,4)	(3,4,5)	(6,7,8)	(2.04,2.4,2.75)
CO ₂ (kg)	(1,1,1)	(1,1,1)	(4,5,6)	(3,4,5)	(9,9,9)	(2.55,2.8,3)
Price (\$)	(1/4,1/3,1/2)	(1/6,1/5,1/4)	(1,1,1)	(2,3,4)	(2,3,4)	(0.69,0.9,1.14)
Labor (\$/Kw)	(1/5,1/4,1/3)	(1/5,1/4,1/3)	(1/4,1/3,1/2)	(1,1,1)	(3,4,5)	(0.4,0.6,0.77)
Fuel consumption (Liter)	(1/8,1/7,1/6)	(1/9,1/9,1/9)	(1/4,1/3,1/2)	(1/5,1/4,1/3)	(1,1,1)	(0.23,0.26,0.3)

Table 5.13 Fuzzy Weight of the ith Criterion

	Efficiency (%)	CO ₂ (kg)	Price(\$)	Labor (\$/Kw)	Fuel consumption (Liter)	Fuzzy geometric mean	Fuzzy weight
Efficiency (%)	(1,1,1)	(1,1,1)	(2,3,4)	(3,4,5)	(6,7,8)	(2.04,2.4,2.75)	(0.25,0.34,0.46)
CO ₂ (kg)	(1,1,1)	(1,1,1)	(4,5,6)	(3,4,5)	(9,9,9)	(2.55,2.8,3)	(0.3,0.4,0.5)
Price (\$)	(1/4,1/3,1/2)	(1/6,1/5,1/4)	(1,1,1)	(2,3,4)	(2,3,4)	(0.69,0.9,1.14)	(0.08,0.1,0.19)
Labor (\$/Kw)	(1/5,1/4,1/3)	(1/5,1/4,1/3)	(1/4,1/3,1/2)	(1,1,1)	(3,4,5)	(0.4,0.6,0.77)	(0.05,0.08,0.1)
Fuel consumption (Liter)	(1/8,1/7,1/6)	(1/9,1/9,1/9)	(1/4,1/3,1/2)	(1/5,1/4,1/3)	(1,1,1)	(0.23,0.26,0.3)	(0.028,0.08,0.5)

Table 5.14 De-fuzzification of the Fuzzy Weight of the ith Criterion

Fuzzy geometric mean	Fuzzy weight	De-Fuzzy weight
(2.04,2.4,2.75)	(0.25,0.34,0.46)	0.35
(2.55,2.8,3)	(0.3,0.4,0.5)	0.4
(0.69,0.9,1.14)	(0.08,0.1,0.19)	0.1
(0.4,0.6,0.77)	(0.05,0.08,0.1)	0.07
(0.23,0.26,0.3)	(0.028,0.08,0.5)	0.03

Table 5.15 Performance Score of Hybrid Energy Sources Based on F-AHP

Sources	Fuel consumption (Liter)	Price(\$)	Efficiency (%)	CO ₂ (Kg)	Labor (\$/Kw)	Si+	Sj-	Pi	Rank
G1	0.136	0.159	0.0914	0.0404	0.0017	0.158	0.199	0.55	4
G2	0.108	0.116	0.0831	0.0375	0.0011	0.109	0.242	0.68	3
G1G2	0.155	0.1748	0.02286	0.049	0.0014	0.1956	0.155	0.44	5
WG1	0.056	0.066	0.0245	0.0168	0.00047	0.075	0.301	0.79	2
WG2	0.039	0.041	0.0223	0.013	0.00031	0.070	0.33	0.82	1

The weighted normalized matrix results were used to calculate the Euclidean distance from the ideal best and worst using Equations (5.4) and (5.5). The performance score of the HES was identified using Equations (5.6) and Table (5.13).

It was found that the ranks are almost similar, as shown in Figures (5.3), (5.4), and (5.5). The reason for this finding is that the AHP and F-AHP methods used to calculate the criteria weight in the third step in the TOPSIS method gave almost equal results. Figure (5.3) shows that the wind and the combination of gasoline and diesel generator are the best and worst alternatives, respectively, when the load is 23 kW. However, when the load changed from 23 kW to 66 kW, the wind farm and gasoline generator combination are the best alternative, and the wind farm, diesel generator and gasoline generator become the worst alternative, as shown in Figure (5.4). Increasing the load value from 66 kW to 76 kW led to changes in the ranks of the HES, where the best alternative becomes the combination of the wind farm and diesel generator, as shown in Figure (5.5).

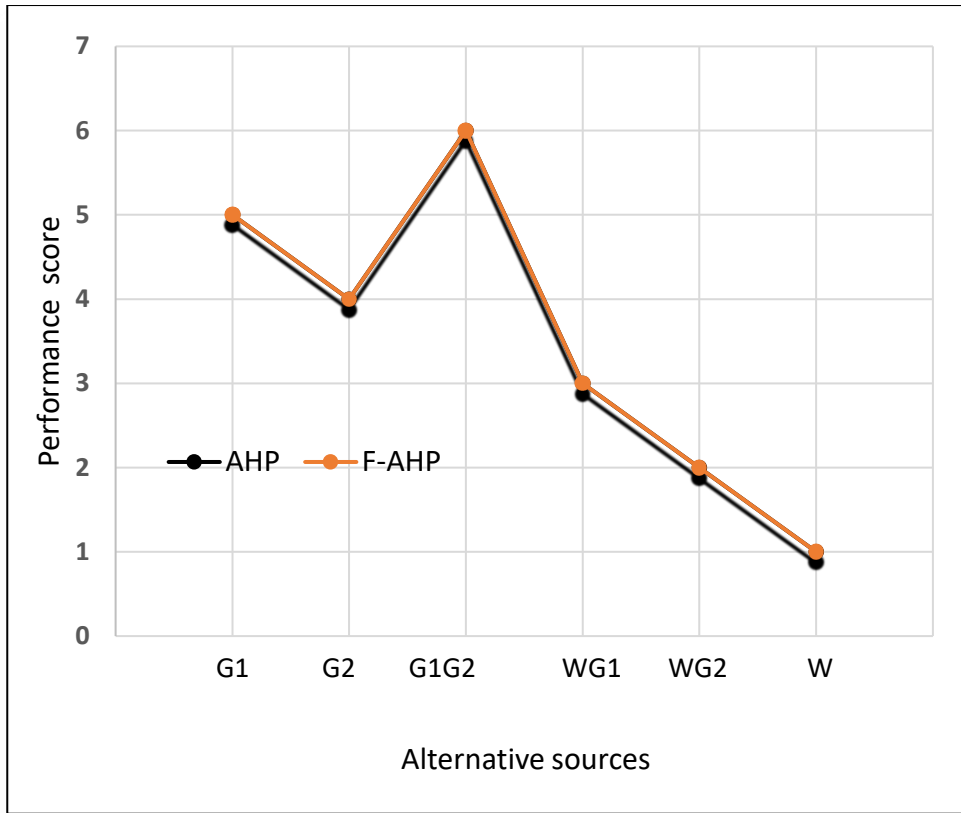


Figure 5.3 Rank of the HES at 23 kW.

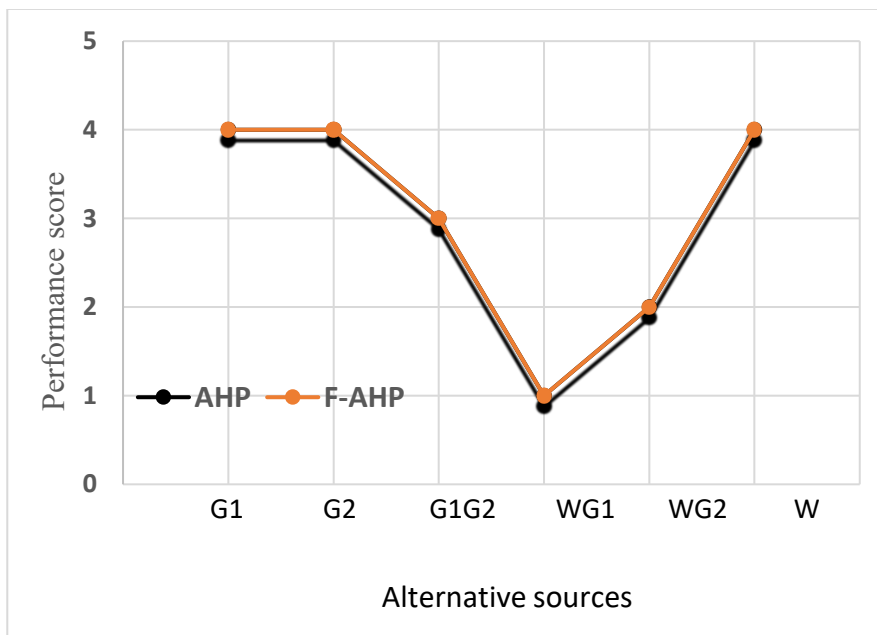


Figure 5.4 Rank of the HES at 66 kW.

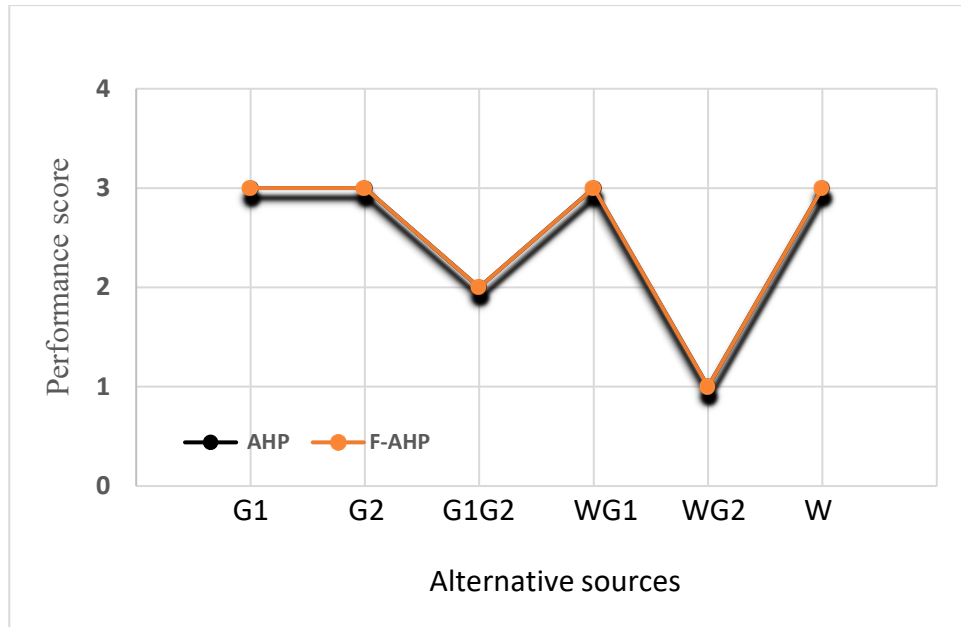


Figure 5.5 Rank of the HES at 76 kW.

The outputs of the TOPSIS method that employed the AHP method to calculate criteria weights are collected for use in the second stage as a dataset. The dataset contains 7 columns and 72 rows. The first 6 columns are liter, efficiency, price, labor, CO₂, and load, which are called attributes. Every 6 attributes belong to a class. The TOPSIS technique omitted the G1 class, which left us with 5 dataset classes, namely the G2, G1G2, W, WG1, and WG2 classes. The RF and LightGBM algorithms are applied to the new dataset, which is divided into training and testing datasets at 30% and 70%, respectively. The training dataset is used to train the algorithm, while the testing dataset is held out to measure the generalized performance of the algorithm. As an essential condition, this dataset must not be seen by the algorithm prior to its use in order to prevent it from contributing to the learning aspect of the algorithm[139], [140]. The performance of RF and LightGBM classifiers were evaluated using the accuracy metric. The results showed RF accuracy at 81.81 and LightGBM at 68.6. Because the dataset is almost balanced, the results are acceptable to some extent.

To summarize the algorithm's performance, a confusion matrix is derived, as shown in Figure (5.6). The rows in the confusion matrix correspond to what the machine-learning classifier predicted, and the columns correspond to the known true value. It is obvious from Figure (5.6a) that the RF classifier classified G1G2 and G2 classes correctly. However, the RF classifier

misclassified one value as W by saying it is WG1 and misclassified two values as G1G2 by saying they were W. Also, the RF classifier correctly classified two values as WG2, but misclassified two values as G1G2 by saying they were WG2.

Class	WG1	G1G2	W	WG2	G2
WG1	[4	0	1	0	0]
G1G2	[0	4	0	0	0]
W	[0	2	4	0	0]
WG2	[0	2	0	2	0]
G2	[0	0	0	0	4]

a. Random Forest Classifier

Class	WG1	G1G2	W	WG2	G2
WG1	[4	0	1	0	0]
G1G2	[0	3	1	0	0]
W	[0	2	3	0	1]
WG2	[0	1	2	1	0]
G2	[0	0	0	0	4]

b. lgb.LGBM Classifier

Figure 5.6 Confusion matrix.

Figure (5.6b) shows the confusion matrix for the LightGBM classifier. The confusion matrix illustrates that the LightGBM classifier classified the WG1 and WG2 classes correctly but misclassified the other classes. Improving LightGBM performance could be done by increasing the number of instances, or it could use a Bayesian hyper-parameter optimization algorithm to optimize the algorithm parameters, which may lead to improved LightGBM algorithm performance.

5.7 Conclusion

In this chapter, the TOPSIS method was used to create an energy management plan for a HES based on five criteria. These criteria are energy efficiency, CO2 emissions, gasoline and diesel fuel prices, labor, and consumption of fuel. A historical load dataset was used to determine the five criteria. Since no equation in the literature was found to derive the weight values in the TOPSIS method, the AHP method was utilized here to calculate the criteria weights. The AHP results were validated using the F-AHP method. It was noticed that the AHP and F-AHP results were almost the same. The outcome of the TOPSIS was then collected to create a new dataset. Two different machine-learning algorithms were applied to the new dataset to forecast the best alternative. The accuracy metrics showed that RF (81.81%) outperformed LightGBM (68.6%).

Chapter6. Conclusions & Future Work

6.1 Conclusions

This thesis studied hybrid energy systems (HES) and discussed forecasting as one of the most important aspects to be considered when operating these systems. Two types of forecasting – regression and classification – were investigated, with the intention of finding the best way to increase the reliability of HES. For regression forecasting, the thesis focused on the ARIMA model, and a deep study was conducted on non-stationary time series. For classification forecasting, the thesis dealt with two case studies that used several machine-learning algorithms to activate one or more sources that would be effective and reliable in a HES.

Chapter 2 presented the non-stationary time series concept and the problems that could occur between two variables if the time series remained non-stationary. Therefore, the Fast Fourier Transform (FFT) was proposed to identify the stationarity. FFT was used here to enhance the performance of the SARIMA model in forecasting short-term electric load data. Chapter 2 also provided a comparison between the FFT technique and the Autocorrelation Function (ACF), where it was found that FFT offered an acceptable performance for identifying trend and seasonality.

Chapter 3 proposed a new adaptive DC technique for converting a non-stationary time series to a stationary time series in one step. The adaptive DC technique was evaluated by applying it to several different time series. The results were compared with the results of the differencing technique using statistical tests, including Augmented Dickey-Fuller (ADF), Kwiatkowski-Phillips-Schmidt-Shin (KPSS), and Phillips Perron (PP). The comparison showed that the proposed technique slightly outperformed the differencing method, which shows the ability of the adaptive DC technique to achieve stationarity data in one step. In contrast, the differencing technique sometimes needed more than one step.

Chapters 4 and 5 presented a new perspective on energy management concepts. The two chapters suggested forecasting techniques as an alternative way of using energy management methods. In Chapter 4, a dataset was collected from the energy management method. The dataset was used as input in supervised machine-learning algorithms to forecast which energy source should supply

the demand-side. The results showed that the DT algorithm achieved the best performance compared to the other tested algorithms.

The results obtained in Chapter 4 provided motivation to conduct further investigations on a new dataset. For this purpose, the TOPSIS method was employed in Chapter 5 to achieve optimal forecasting using the machine-learning algorithms RF and LightGBM. The findings showed that RF outperformed LightGBM, with an accuracy of 81.81% compared to 68.6%, respectively.

6.2 Future Work

Based on the results presented in this research, further analyses and investigations are recommended for future work. In Chapter 4, a novel adaptive DC technique could be implemented with the ARMA function instead of a differencing method. Other suggestions come from Chapters 4 and 5, as they present a new idea and are rich in future work possibilities. The five criteria could be expanded to n criteria or could involve more than one level of criteria. The decision-maker judgments could be made by a questionnaire.

Also recommended as future research directions would be to evaluate other forecasting techniques and make a comparison between energy management methods. To implement the work in chapter 5, we would need to divide it into two stages: reading and process stages. The reading stage would involve reading the load measurement. To achieve this stage, a data acquisition system that contains a smart meter sensor, signal condition, and analog-to-digital circuits could be used. In the process stage, the TOPSIS method and machine learning could be employed to create a new dataset and to forecast which energy source should be connected to the load, respectively. This stage could be done using a personal computer or Arduino board. In addition, the accuracy of managing hybrid energy sources could be increased by building a hybrid forecasting system that consists of scheduling and fault forecasting models. The fault forecasting model can serve as closed-loop feedback to the scheduling forecasting model, and this will ensure the proper functioning of the hybrid system.

Bibliography

- [1] E. Muh and F. Tabet, “Comparative analysis of hybrid renewable energy systems for off-grid applications in Southern Cameroons,” *Renew Energy*, vol. 135, pp. 41–54, May 2019, doi: 10.1016/j.renene.2018.11.105.
- [2] H. H. H. Aly, “A hybrid optimized model of Adaptive Neuro-Fuzzy Inference System, Recurrent Kalman Filter and Neuro-Wavelet for Wind Power Forecasting Driven by DFIG” *Journal of Energy*, vol. 239, part E, 2022, <https://doi.org/10.1016/j.energy.2021.122367>.
- [3] J. Royer,” Status of remote/off-grid communities in Canada. *Natural Resources Canada*, 2011. 28, 4626-4639
- [4] R. Banik and P. Das, “A Review on Architecture, Performance and Reliability of Hybrid Power System,” *Journal of The Institution of Engineers (India): Series B*, vol. 101, no. 5. Springer, pp. 527–539, Oct. 01, 2020. doi: 10.1007/s40031-020-00473-6.
- [5] C. Ammari, D. Belatrache, B. Touhami, and S. Makhloufi, “Sizing, optimization, control and energy management of hybrid renewable energy system—A review,” *Energy and Built Environment*. KeAi Communications Co., 2021. doi: 10.1016/j.enbenv.2021.04.002.
- [6] P. Bajpai and V. Dash, “Hybrid renewable energy systems for power generation in stand-alone applications: A review,” *Renewable and Sustainable Energy Reviews*, vol. 16, no. 5. pp. 2926–2939, Jun. 2012. doi: 10.1016/j.rser.2012.02.009.
- [7] H. Musbah, H. H. Aly, and T. A. Little, “Energy management of hybrid energy system sources based on machine learning classification algorithms,” *Electric Power Systems Research*, vol. 199, Oct. 2021, doi: 10.1016/j.epsr.2021.107436.
- [8] A. Tascikaraoglu, O. Erdinc, M. Uzunoglu, and A. Karakas, “An adaptive load dispatching and forecasting strategy for a virtual power plant including renewable energy conversion units,” *Appl Energy*, vol. 119, pp. 445–453, 2014, doi: 10.1016/j.apenergy.2014.01.020.
- [9] Y. Li, Y. Su, and L. Shu, “An ARMAX model for forecasting the power output of a grid connected photovoltaic system,” *Renew Energy*, vol. 66, pp. 78–89, 2014, doi: 10.1016/j.renene.2013.11.067.

- [10] X. Wang, A. Palazoglu, and N. H. El-Farra, "Operational optimization and demand response of hybrid renewable energy systems," *Appl Energy*, vol. 143, pp. 324–335, 2015, doi: 10.1016/j.apenergy.2015.01.004.
- [11] J. Chen and C. Rabiti, "Synthetic wind speed scenarios generation for probabilistic analysis of hybrid energy systems," *Energy*, vol. 120, pp. 507–517, 2017, doi: 10.1016/j.energy.2016.11.103.
- [12] W. Zhang, A. Maleki, M. A. Rosen, and J. Liu, "Sizing a stand-alone solar-wind-hydrogen energy system using weather forecasting and a hybrid search optimization algorithm," *Energy Convers Manag*, vol. 180, no. November 2018, pp. 609–621, 2019, doi: 10.1016/j.enconman.2018.08.102.
- [13] P. Bento, H. Nunes, J. Pombo, M. do Rosário Calado, and S. Mariano, "Daily operation optimization of a hybrid energy system considering a short-term electricity price forecast scheme," *Energies (Basel)*, vol. 12, no. 5, 2019, doi: 10.3390/en12050924.
- [14] M. Hamza Zafar, N. Mujeeb Khan, M. Mansoor, A. Feroz Mirza, S. Kumayl Raza Moosavi, and F. Sanfilippo, "Adaptive ML-based technique for renewable energy system power forecasting in hybrid PV-Wind farms power conversion systems," *Energy Convers Manag*, vol. 258, Apr. 2022, doi: 10.1016/J.ENCONMAN.2022.115564.
- [15] H. Musbah, M. El-Hawary, and H. Aly, "Identifying seasonality in time series by applying fast fourier transform," *2019 IEEE Electrical Power and Energy Conference, EPEC 2019*, vol. 3, pp. 28–31, 2019, doi: 10.1109/EPEC47565.2019.9074776.
- [16] H. Musbah and M. El-Hawary, "SARIMA Model Forecasting of Short-Term Electrical Load Data Augmented by Fast Fourier Transform Seasonality Detection," In *IEEE Canadian Conference of Electrical and Computer Engineering (CCECE)* (pp. 1-4). IEEE. Edmonton, Canada, 2019.
- [17] H. Musbah, G. Ali, H. H. Aly, and T. A. Little. "A proposed novel adaptive DC technique for non-stationary data removal", *Heliyon Journal*, 2023. <https://doi.org/10.1016/j.heliyon.2023.e13903>.

- [18] H. Musbah, G. Ali, H. H. Aly, and T. A. Little, “Energy management using multi-criteria decision making and machine learning classification algorithms for intelligent system,” *Electric Power Systems Research*, vol. 203, no. June 2021, p. 107645, 2022, doi: 10.1016/j.epsr.2021.107645.
- [19] R. Manuca and R. Savit, “Stationarity and nonstationarity in time series analysis,” *Physica D: Nonlinear Phenomena*, vol. 99, no. 2–3, pp. 134–161, 1996, doi: 10.1016/S0167-2789(96)00139-X.
- [20] T. A. Chawsheen and M. Broom, “Seasonal time-series modeling and forecasting of monthly mean temperature for decision making in the Kurdistan Region of Iraq,” *J Stat Theory Pract*, vol. 11, no. 4, pp. 604–633, 2017, doi: 10.1080/15598608.2017.1292484.
- [21] E. C. Nwogu, I. S. Iwueze, and V. U. Nlebedim, “Some tests for seasonality in time series data,” *Journal of Modern Applied Statistical Methods*, vol. 15, no. 2, pp. 382–399, 2016, doi: 10.22237/jmasm/1478002920.
- [22] I. S. Iwueze, E. C. Nwogu, O. Johnson, and J. C. Ajaraogu, “Uses of the Buys-Ballot Table in Time Series Analysis,” *Appl Math (Irvine)*, vol. 02, no. 05, pp. 633–645, 2011, doi: 10.4236/am.2011.25084.
- [23] L. di Persio and M. Frigo, “Gibbs sampling approach to regime switching analysis of financial time series,” *J Comput Appl Math*, vol. 300, pp. 43–55, 2016, doi: 10.1016/j.cam.2015.12.010.
- [24] S. Mukhopadhyay, D. Dash, A. Mitra, and P. Bhattacharya, “A comparative study between seasonal wind speed by Fourier and Wavelet analysis,” vol. 1, no. 2011.
- [25] S. Bf and A. Of, “Investigating the Non-Stationarity of Historical Data on Rainfall at Ilorin, Available online www.jsaer.com *Journal of Scientific and Engineering Research*, pp. 537-548, 2016.
- [26] E. Afrifa-yamoah, “Application of ARIMA Models in Forecasting Monthly Average Surface Temperature of Brong Ahafo Region of Ghana,” October 2015, doi: 10.5923/j.statistics.20150505.08.

- [27] G. E. P. Box and G. M. Jenkins “Review Reviewed Work (s): Time Series Analysis Forecasting and Control “Palgrave Macmillan Journals on behalf of the Operational Research Society Stable URL : <https://>,” vol. 22, no. 2, pp. 2–5, 1977.
- [28] N. Mohamecl, M. H. Ahmad, and Suhartono, “Forecasting short term load demand using double seasonal arima model,” *World Appl Sci J*, vol. 13, no. 1, pp. 27–35, 2011.
- [29] E. A. Yfantis and L. E. Borgman, *Fast fourier transforms 2-3-5*, vol. 7, no. 1. 1981. doi: 10.1016/0098-3004(81)90041-8.
- [30] C. Nichiforov, I. Stamatescu, and F. Ioana, “Energy Consumption Forecasting Using ARIMA and Neural Network Models”, In *5th IEEE International Symposium on Electrical and Electronics Engineering (ISEEE)* (pp. 1-4), 2017.
- [31] E. El-Mallah and S. Elsharkawy, “Time-Series Modeling and Short Term Prediction of Annual Temperature Trend on Coast Libya Using the Box-Jenkins ARIMA Model,” *Adv Res*, vol. 6, no. 5, pp. 1–11, 2016, doi: 10.9734/air/2016/24175.
- [32] J. Deng and P. Jirutitijaroen, “Short-term load forecasting using time series analysis: A case study for Singapore,” *2010 IEEE Conference on Cybernetics and Intelligent Systems, CIS 2010*, pp. 231–236, 2010, doi: 10.1109/ICCIS.2010.5518553.
- [33] S. Katara, A. Faisal, and G. M. Engmann, “A Time Series Analysis of Electricity Demand in Tamale, Ghana,” vol. 4, no. 6, pp. 269–275, 2014, doi: 10.5923/j.statistics.20140406.03.
- [34] L. C. M. de Andrade and I. N. da Silva, “Very short-term load forecasting based on ARIMA model and intelligent systems,” *2009 15th International Conference on Intelligent System Applications to Power Systems, ISAP '09*, 2009, doi: 10.1109/ISAP.2009.5352829.
- [35] E. El-Mallah and S. Elsharkawy, “Time-Series Modeling and Short Term Prediction of Annual Temperature Trend on Coast Libya Using the Box-Jenkins ARIMA Model,” *Adv Res*, vol. 6, no. 5, pp. 1–11, 2016, doi: 10.9734/air/2016/24175.
- [36] O. O. Ochanda, “Time Series Analysis and Forecasting of Monthly Air Temperature Changes in Nairobi Kenya,” 2016, Accessed: Nov. 22, 2022. [Online]. Available: <http://erepository.uonbi.ac.ke/handle/11295/100003>

- [37] H. Musbah, H. H. Aly, and T. A. Little, "A Novel Approach for Seasonality and Trend Detection using Fast Fourier Transform in Box-Jenkins Algorithm," in Canadian Conference on Electrical and Computer Engineering, Aug. 2020, vol. 2020-August. doi: 10.1109/CCECE47787.2020.9255819.
- [38] C. Chatfield, "The Analysis of Time Series : An Introduction, Sixth Edition," The Analysis of Time Series, Jul. 2003, doi: 10.4324/9780203491683.
- [39] Ü. Ç. Büyükhahin and Ş. Ertekin, "Improving forecasting accuracy of time series data using a new ARIMA-ANN hybrid method and empirical mode decomposition," Neurocomputing, vol. 361, pp. 151–163, Oct. 2019, doi: 10.1016/J.NEUCOM.2019.05.099.
- [40] S. Noureen, S. Atique, V. Roy, and S. Bayne, "Analysis and application of seasonal ARIMA model in Energy Demand Forecasting: A case study of small scale agricultural load," 2019 IEEE 62nd International Midwest Symposium on Circuits and Systems (MWSCAS), 2019, doi: 10.1109/MWSCAS.2019.8885349.
- [41] D. Benvenuto, M. Giovanetti, L. Vassallo, S. Angeletti, and M. Ciccozzi, "Application of the ARIMA model on the COVID-2019 epidemic dataset," Data Brief, vol. 29, Apr. 2020, doi: 10.1016/J.DIB.2020.105340.
- [42] B. F. Sule, "Investigating the Non-Stationarity of Historical Data on Rainfall at Ilorin, North Central Nigeria Sustainable Sediment Management of Upstream Watershed of Jebba Hydropower Reservoir View project Development of Novel Hybrid Hydrokinetic Turbines View project," 2016. [Online]. Available: <https://www.researchgate.net/publication/305722503>
- [43] H. H. H. Aly, "A novel approach for harmonic tidal currents constitutions forecasting using hybrid intelligent models based on clustering methodologies," Renew Energy, vol. 147, pp. 1554–1564, Mar. 2020, doi: 10.1016/J.RENENE.2019.09.107.
- [44] H. H. H. Aly and M. E. El-Hawary "A proposed ANN and FLSM hybrid model for tidal current magnitude and direction forecasting," IEEE Journal of Oceanic Engineering, vol. 1, 2014, doi:10.1109/JOE.2013.2241934.

- [45] L. Carli Moreira de Andrade and I. Nunes da Silva, "Very Short-Term Load Forecasting Based on ARIMA Model and Intelligent Systems," 2009 15th International Conference on Intelligent System Applications to Power Systems, 2009, doi: 10.1109/ISAP.2009.5352829.
- [46] S. Zakaria, N. Al-Ansari, S. Knutsson, and T. Al-Badrany, "ARIMA Models for weekly rainfall in the semi-arid Sinjar District at Iraq," *Journal of Earth Sciences and Geotechnical Engineering*, vol. 2, no. 3, pp. 1792–9660, 2012.
- [47] Y. Min, W. Bin, Z. Liang-li, and C. Xi, "Wind speed forecasting based on EEMD and ARIMA; Wind speed forecasting based on EEMD and ARIMA," 2015 Chinese Automation Congress (CAC), 2015, doi: 10.1109/CAC.2015.7382700.
- [48] E. Grigonytė and E. Butkevičiūtė, "Short-term wind speed forecasting using ARIMA model," *Energetika*, vol. 62, no. 1–2, pp. 45–55, Jul. 2016, doi: 10.6001/ENERGETIKA.V62I1-2.3313.
- [49] L. Puka, D. K. Dwivedi, G. R. Sharma, and S. S. Wandre, "Forecasting mean temperature using SARIMA Model for Junagadh City of Gujarat," *IJASR*, 7(4), 2017, 183-194.
- [50] H. Sharadga, S. Hajimirza, and R. S. Balog, "Time series forecasting of solar power generation for large-scale photovoltaic plants," *Renew Energy*, vol. 150, pp. 797–807, May 2020, doi: 10.1016/j.renene.2019.12.131.
- [51] N. Guo, W. Chen, M. Wang, Z. Tian, and H. Jin, "Applying an Improved Method Based on ARIMA Model to Predict the Short-Term Electricity Consumption Transmitted by the Internet of Things (IoT)," *Wirel Commun Mob Comput*, vol. 2021, 2021, doi: 10.1155/2021/6610273.
- [52] A. O. Mohamed, "Modeling and Forecasting Somali Economic Growth Using ARIMA Models," *Forecasting*, vol. 4, no. 4, pp. 1038–1050, Dec. 2022, doi: 10.3390/forecast4040056.
- [53] M. Arltová, "Selection of Unit Root Test on the Basis of Length of the Time Series and Value of AR(1) Parameter," 2016, Accessed: Nov. 22, 2022. [Online]. Available: <https://www.researchgate.net/publication/308972405>

- [54] S. Ramaswamy, & P. K. Sadhu, "Forecasting PV power from solar irradiance and temperature using neural networks." IEEE International conference on infocom technologies and unmanned systems (ICTUS), (pp. 244-248), 2017.
- [55] H. H. H. Aly, "A novel deep learning intelligent clustered hybrid models for wind speed and power forecasting," Journal of energy,2020, doi: 10.1016/j.energy.2020.118773.
- [56] H. H. H. Aly, "An intelligent hybrid model of neuro Wavelet, time series and Recurrent Kalman Filter for wind speed forecasting," Sustainable Energy Technologies and Assessments journal,2020, doi: 10.1016/j.seta.2020.100802.
- [57] G. Aburiyana and M. E. El-Hawary, "An Overview of Forecasting Techniques for Load, Wind and Solar Powers". IEEE Electrical Power and Energy Conference, 2017 (EPEC) (pp. 1-7).
- [58] H. Hü, C. , Evik, • Mehmet, and C. , Unkas, receivedunkas, , "Short-term load forecasting using fuzzy logic and ANFIS," Neural Comput Appl journal, 2015 doi: 10.1007/s00521-014-1809-4.
- [59] A. Baliyan, K. Gaurav, and S. Kumar Mishra, "A review of short term load forecasting using artificial neural network models," Procedia Comput Sci, vol. 48, no. C, pp. 121–125, 2015, doi: 10.1016/J.PROCS.2015.04.160.
- [60] S. Talha Mehmood and M. El-Hawary Fellow, "Performance Evaluation of New and Advanced Neural Networks for Short Term Load Forecasting," IEEE Electrical power and energy conference, 2014, doi: 10.1109/EPEC.2014.45.
- [61] G. Nalcaci, A. Özmen, and G. W. Weber, "Long-term load forecasting: models based on MARS, ANN and LR methods," Cent Eur J Oper Res, vol. 27, pp. 1033–1049, 2019, doi: 10.1007/s10100-018-0531-1.
- [62] V. Gupta, S. Pal, and P. G. Student, "An Overview of Different Types of Load Forecasting Methods and the Factors Affecting the Load Forecasting," International Journal for Research in Applied Science & Engineering Technology, 2017, doi: 10.22214/ijraset.2017.4132.

- [63] J. Wasilewski and D. Baczynski, "Short-term electric energy production forecasting at wind power plants in pareto-optimality context," *Renewable and Sustainable Energy Review* 2016, doi: 10.1016/j.rser.2016.11.026.
- [64] T. Burianek, J. Stuchly, and S. Misak, "Solar power production forecasting based on recurrent neural network," *Advances in Intelligent Systems and Computing*, vol. 427, pp. 195–204, 2016, doi: 10.1007/978-3-319-29504-6_20/COVER.
- [65] Y. Zhang, M. Beaudin, H. Zareipour, S. Member, and D. Wood, "Forecasting Solar Photovoltaic Power Production at the Aggregated System Level," 2014, doi: 10.1109/NAPS.2014.6965389.
- [66] A. T. Eseye, J. Zhang, and D. Zheng, "Short-term photovoltaic solar power forecasting using a hybrid Wavelet-PSO-SVM model based on SCADA and Meteorological information," *Renew Energy*, vol. 118, pp. 357–367, Apr. 2018, doi: 10.1016/J.RENENE.2017.11.011.
- [67] P. Jiang, H. Yang, and J. Heng, "A hybrid forecasting system based on fuzzy time series and multi-objective optimization for wind speed forecasting," *Appl Energy*, vol. 235, pp. 786–801, Feb. 2019, doi: 10.1016/J.APENERGY.2018.11.012.
- [68] Z. Tian, G. Wang, and Y. Ren, "Wind Engineering 2020," vol. 44, no. 2, pp. 152–167, doi: 10.1177/0309524X19849867.
- [69] K. Yan, H. Shen, L. Wang, H. Zhou, M. Xu, and Y. Mo, "Short-Term Solar Irradiance Forecasting Based on a Hybrid Deep Learning Methodology", *Machine Learning on Scientific Data and Information*, 2020, doi: 10.3390/info11010032.
- [70] A. Alzahrani, P. Shamsi, C. Dagli, and M. Ferdowsi, "Solar Irradiance Forecasting Using Deep Neural Networks," *Procedia Comput Sci*, vol. 114, pp. 304–313, 2017, doi: 10.1016/J.PROCS.2017.09.045.
- [71] H. H. H. Aly, "A proposed intelligent short-term load forecasting hybrid models of ANN, WNN and KF based on clustering techniques for smart grid," *Electric Power Systems Research*, 2020, doi: 10.1016/j.epsr.2019.106191.

- [72] S. Sp PAPPAS, L. Ekonomou, V. C. Moussas, P. Karampelas, and S. K. Katsikas, "Adaptive load forecasting of the Hellenic electric grid," *J Zhejiang Univ Sci A*, vol. 9, no. 12, pp. 1724–1730, 2008, doi: 10.1631/jzus.A0820042.
- [73] P. Karampelas, V. Vita, C. Pavlatos, V. Mladenov, and L. Ekonomou, "Design of artificial neural network models for the prediction of the Hellenic energy consumption," 10th Symposium on Neural Network Applications in Electrical Engineering, 2010, doi: 10.1109/NEUREL.2010.5644049.
- [74] H. M. al Ghaithi, G. P. Fotis, and V. Vita, "Techno-Economic Assessment of Hybrid Energy Off-Grid System - A Case Study for Masirah Island in Oman," *International Journal of Power and Energy Research*, 2017, doi: 10.22606/ijper.2017.12003.
- [75] M. W. Ahmad, J. Reynolds, and Y. Rezgui, "Predictive modelling for solar thermal energy systems: A comparison of support vector regression, random forest, extra trees and regression trees," *J Clean Prod*, vol. 203, pp. 810–821, Dec. 2018, doi: 10.1016/J.JCLEPRO.2018.08.207.
- [76] R. Bayindir, M. Yesilbudak, M. Colak, and N. Genc, "A Novel Application of Naïve Bayes Classifier in Photovoltaic Energy Prediction", 16th IEEE International Conference on Machine Learning and Applications, 2017 doi: 10.1109/ICMLA.0-108.
- [77] P. Gupta and N. K. Sehgal, "Introduction to Machine Learning in the Cloud with Python," book, 2021, doi: 10.1007/978-3-030-71270-9.
- [78] L. Breiman, "Random Forests," *Machine learning book*, 2001, 45(1), 5-32
- [79] M. Fernández-Delgado, E. Cernadas, S. Barro, D. Amorim, and A. Fernández-Delgado, "Do we Need Hundreds of Classifiers to Solve Real World Classification Problems?," *Journal of Machine Learning Research*, vol. 15, pp. 3133–3181, 2014, Accessed: Nov. 22, 2022. [Online]. Available: <http://www.mathworks.es/products/neural-network>.
- [80] C. Chen and A. Liaw, "Using Random Forest to Learn Imbalanced Data," *University of California, Berkeley*, 2004, 110(1-12), 24.

- [81] B. M. Gayathri, C. P. Sumathi, A. Professor, and H. Sdnb, “An Automated Technique using Gaussian Naïve Bayes Classifier to Classify Breast Cancer,” *Int J Comput Appl*, vol. 148, no. 6, pp. 975–8887, 2016.
- [82] H. Kamel, D. Abdulah, and J. M. Al-Tuwaijari, “Cancer Classification Using Gaussian Naive Bayes Algorithm; ,” *IEEE International Engineering Conference*, 2019.
- [83] C. Reinders, H. Ackermann, M. Y. Yang, and B. Rosenhahn, “Chapter 4 - Learning Convolutional Neural Networks for Object Detection with Very Little Training Data,” *Book*, 2019, doi: 10.1016/B978-0-12-817358-9.00010-X.
- [84] V. Kotu, and B. Deshpande, “Predictive analytics and data mining: concepts and practice with rapidminer.” *Morgan Kaufmann*, 2014
- [85] L. Y. Hu, M. W. Huang, S. W. Ke, and C. F. Tsai, “The distance function effect on k-nearest neighbor classification for medical datasets,” *Springer plus*, vol. 5, no. 1, Dec. 2016, doi: 10.1186/s40064-016-2941-7.
- [86] N. Bhatia, “Survey of Nearest Neighbor Techniques,” *IJCSIS) International Journal of Computer Science and Information Security*, vol. 8, no. 2, 2010, Accessed: Nov. 22, 2022. [Online]. Available: <http://sites.google.com/site/ijcsis/>
- [87] I. H. Witten, E. Frank, M. A. Hall, and M. Kaufmann, “Practical Machine Learning Tools and Techniques,” *Data mining journal*, 2005, vol. 2, no. 4, pp.143-186.
- [88] J. S. Akosa, “Predictive Accuracy: A Misleading Performance Measure for Highly Imbalanced Data,” *In Proceedings of the SAS global forum, 2017 (Vol. 12, pp. 1-4)*.
- [89] H. H. H. Aly, “A Hybrid Optimized Model of Adaptive Neuro-Fuzzy Inference System, Recurrent Kalman Filter and Neuro-Wavelet for Wind Power Forecasting Driven by DFIG,” *Journal of Energy*, vol. 239, p. 122367, Jan. 2022, doi: 10.1016/J.ENERGY.2021.122367.
- [90] B. B. Alagoz, A. Kaygusuz, and A. Karabiber, “A user-mode distributed energy management architecture for smart grid applications,” *Journal of Energy*, 2012, doi: 10.1016/j.energy.2012.06.051.

- [91] A. V. H. Sola and C. M. M. Mota, “Influencing factors on energy management in industries,” 2019, *Journal of Cleaner Production*, 248, 119263. doi: 10.1016/j.jclepro.2019.119263.
- [92] C. Battistelli, L. Baringo, and A. J. Conejo, “Electric Power Systems Research Optimal energy management of small electric energy systems including V2G facilities and renewable energy sources,” *Electric Power Systems Research*, vol. 92, pp. 50–59, 2012, doi: 10.1016/j.epsr.2012.06.002.
- [93] D. Feroldi, L. Nieto Degliuomini, and M. Basualdo, “Energy management of a hybrid system based on wind–solar power sources and bioethanol,” *Chemical Engineering Research and Design journal*, 2013, doi: 10.1016/j.cherd.2013.03.007.
- [94] S. Upadhyay and M. P. Sharma, “Selection of a suitable energy management strategy for a hybrid energy system in a remote rural area of India,” *Journal of energy*, 2015, doi: 10.1016/j.energy.2015.10.134.
- [95] N. Bigdeli, “Optimal management of hybrid PV/fuel cell/battery power system: A comparison of optimal hybrid approaches,” *journal of renewable and sustainable energy reviews*, 2014, doi: 10.1016/j.rser.2014.10.032.
- [96] V. Dash and P. Bajpai, “Power management control strategy for a stand-alone solar photovoltaic-fuel cell-battery hybrid system”, *Journal of sustainable energy technologies and assessments* doi: 10.1016/j.seta.2014.10.001.
- [97] R. Cozzolino, L. Tribioli, and G. Bella, “Power management of a hybrid renewable system for artificial islands: A case study,” *Journal of energy* 2016, doi: 10.1016/j.energy.12.118.
- [98] S. Nasri, B. Slama Sami, and A. Cherif, “Power management strategy for hybrid autonomous power system using hydrogen storage,” *International Journal of Hydrogen Energy*, 2015, doi: 10.1016/j.ijhydene.2015.11.085.
- [99] H. al Garni, A. Kassem, A. Awasthi, D. Komljenovic, and K. Al-Haddad, “A multicriteria decision making approach for evaluating renewable power generation sources in Saudi Arabia”, *Journal of Sustainable Energy Technologies and Assessments*, 2016 doi: 10.1016/j.seta.05.006.

- [100] S. J. W. Klein and S. Whalley, "Comparing the sustainability of U.S. electricity options through multi-criteria decision analysis," *Journal of Energy Policy*, vol. 79, pp. 127–149, Apr. 2015, doi: 10.1016/J.ENPOL.2015.01.007.
- [101] Ü. Şengül, M. Eren, S. Eslamian Shiraz, V. Gezder, and A. B. Sengül, "Fuzzy TOPSIS method for ranking renewable energy supply systems in Turkey," *Renewable Energy journal*, vol. 75, pp. 617–625, Mar. 2015, doi: 10.1016/J.RENENE.2014.10.045.
- [102] J. R. San Cristóbal, "Multi-criteria decision-making in the selection of a renewable energy project in Spain: The VIKOR method," *Renewable Energy journal*, vol. 36, no. 2, pp. 498–502, Feb. 2011, doi: 10.1016/J.RENENE.2010.07.031.
- [103] T. Kaya and C. Kahraman, "Multicriteria decision making in energy planning using a modified fuzzy TOPSIS methodology," *Expert Syst Appl journal*, vol. 38, no. 6, pp. 6577–6585, Jun. 2011, doi: 10.1016/J.ESWA.2010.11.081.
- [104] D. Streimikiene, T. Balezentis, I. Krisciukaitien, and A. Balezentis, "Prioritizing sustainable electricity production technologies: MCDM approach," *Renewable and Sustainable Energy Reviews*, vol. 16, no. 5, pp. 3302–3311, Jun. 2012, doi: 10.1016/J.RSER.2012.02.067.
- [105] W. M. Karel Brauers and E. Kazimieras Zavadskas, "Project management by multimora as an instrument for transition economies," *Technological and Economic Development of Economy*, 2010, doi: 10.3846/tede.2010.01.
- [106] P. Purohitand and M. Ramachandran, "Selection of Flywheel Material using Multicriteria Decision Making Fuzzy TOPSIS," *Indian Journal of Science and Technology*, vol. 8, no. 33, 2015, doi: 10.17485/ijst/v8i33/80028.
- [107] K. Askarifar, Z. Motaffef, and S. Aazaami, "An investment development framework in Iran's seashores using TOPSIS and best-worst multi-criteria decision making methods," *Decision Science Letters*, 2018, vol. 7, no. 1, pp. 55–64, Jan., doi: 10.5267/J.DSL.4.004.
- [108] J. Rezaei, "Best-worst multi-criteria decision-making method: Some properties and a linear model," *Omega Journal*, 2016, vol. 64, pp. 126–130, Oct., doi: 10.1016/J.OMEGA.12.001.

- [109] R. A. Krohling and V. C. Campanharo, "Fuzzy TOPSIS for group decision making: A case study for accidents with oil spill in the sea," *Expert Syst Appl*, vol. 38, no. 4, pp. 4190–4197, Apr. 2011, doi: 10.1016/J.ESWA.2010.09.081.
- [110] A. Awasthi, S. S. Chauhan, and S. K. Goyal, "A multi-criteria decision making approach for location planning for urban distribution centers under uncertainty," *Math Comput Model Journal*, vol. 53, no. 1–2, pp. 98–109, Jan. 2011, doi: 10.1016/J.MCM.2010.07.023.
- [111] İ. Kaya, M. Çolak, and F. Terzi, "A comprehensive review of fuzzy multi criteria decision making methodologies for energy policy making," *Energy Strategy Reviews*, vol. 24, pp. 207–228, Apr. 2019, doi: 10.1016/J.ESR.2019.03.003.
- [112] P. Rani, A. R. Mishra, A. Mardani, F. Cavallaro, M. Alrasheedi, and A. Alrashidi, "A novel approach to extended fuzzy TOPSIS based on new divergence measures for renewable energy sources selection," *Journal of Cleaner Production*, vol. 257, Jun. 2020, doi: 10.1016/J.JCLEPRO.2020.120352.
- [113] A. Shukla, P. Agarwal, R. S. Rana, and R. Purohit, "Applications of TOPSIS Algorithm on various Manufacturing Processes: A Review," *Materials Today*, vol. 4, no. 4, pp. 5320–5329, 2017, doi: 10.1016/J.MATPR.2017.05.042.
- [114] E. O. Diemuodeke, A. Addo, C. O. C. Oko, Y. Mulugetta, and M. M. Ojapah, "Optimal mapping of hybrid renewable energy systems for locations using multi-criteria decision-making algorithm," *Renewable Energy*, vol. 134, pp. 461–477, Apr. 2019, doi: 10.1016/J.RENENE.2018.11.055.
- [115] D. Choudhary and R. Shankar, "An STEEP-fuzzy AHP-TOPSIS framework for evaluation and selection of thermal power plant location: A case study from India," *Energy*, vol. 42, no. 1, pp. 510–521, 2012, doi: 10.1016/J.ENERGY.2012.03.010.
- [116] K. Sadeghzadeh and M. B. Salehi, "Mathematical analysis of fuel cell strategic technologies development solutions in the automotive industry by the TOPSIS multi-criteria decision making method," *Int J Hydrogen Energy*, vol. 36, no. 20, pp. 13272–13280, Oct. 2011, doi: 10.1016/J.IJHYDENE.2010.07.064.

- [117] A. H. I. Lee, H. H. Chen, and H. Y. Kang, “Multi-criteria decision making on strategic selection of wind farms,” *Renewable Energy*, vol. 34, no. 1, pp. 120–126, Jan. 2009, doi: 10.1016/J.RENENE.2008.04.013.
- [118] L. Ali et al., “A Feature-Driven Decision Support System for Heart Failure Prediction Based on χ^2 Statistical Model and Gaussian Naive Bayes,” *Computational and Mathematical Methods in Medicine*, 2019, doi: 10.1155/2019/6314328.
- [119] P. Sharmila, J. Baskaran, C. Nayanatara, and R. Maheswari, “A hybrid technique of machine learning and data analytics for optimized distribution of renewable energy resources targeting smart energy management,” *Procedia Computer Science*, 2019, vol. 165, pp. 278–284, , doi: 10.1016/J.PROCS.2020.01.076.
- [120] M. Pérez-Ortiz, S. Jiménez-Fernández, P. A. Gutiérrez, E. Alexandre, C. Hervás-Martínez, and S. Salcedo-Sanz, “A Review of Classification Problems and Algorithms in Renewable Energy Applications,” *Energies*, 2016, doi: 10.3390/en9080607.
- [121] M. Meng and C. Song, “Daily Photovoltaic Power Generation Forecasting Model Based on Random Forest Algorithm for North China in Winter”, *Sustainability*, 2020 doi: 10.3390/su12062247.
- [122] S. Banihashemi, G. Ding, and J. Wang, “Developing a Hybrid Model of Prediction and Classification Algorithms for Building Energy Consumption,” *Energy Procedia*, 2017, vol. 110, pp. 371–376, 2017, doi: 10.1016/J.EGYPRO.03.155.
- [123] W. Lee Woon Zeyar Aung Stuart Madnick, “Data Analytics for Renewable Energy Integration,” *Book*, Springer, 2014, Accessed: Nov. 25, 2022. [Online]. Available: <http://www.springer.com/series/1244>
- [124] A. Mosavi, M. Salimi, S. F. Ardabili, T. Rabczuk, S. Shamshirband, and A. R. Varkonyi-Koczy, “State of the Art of Machine Learning Models in Energy Systems, a Systematic Review,” *Energies*, vol. 12, 2019, doi: 10.3390/en12071301.
- [125] Y. Ju, G. Sun, Q. Chen, M. Zhang, and H. Zhu, “A Model Combining Convolutional Neural Network and LightGBM Algorithm for Ultra-Short-Term Wind Power Forecasting” *IEEE Access*, doi: 10.1109/ACCESS.2019.2901920.

- [126] M. W. Ahmad, M. Mourshed, and Y. Rezgui, "Tree-based ensemble methods for predicting PV power generation and their comparison with support vector regression," *Energy*, vol. 164, pp. 465–474, Dec. 2018, doi: 10.1016/J.ENERGY.2018.08.207.
- [127] H. Demolli, A. S. Dokuz, A. Ecemis, and M. Gokcek, "Wind power forecasting based on daily wind speed data using machine learning algorithms," *Energy Conversion and Management*, 2019, vol. 198, Oct, doi: 10.1016/J.ENCONMAN.2019.111823.
- [128] Y. M. Wang and Y. Luo, "On rank reversal in decision analysis," *Mathematical and Computer Modelling*, 2009, vol. 49, no. 5–6, pp. 1221–1229, doi: 10.1016/J.MCM.2008.06.019.
- [129] A. Kumar et al., "A review of multi criteria decision making (MCDM) towards sustainable renewable energy development," *Renewable and Sustainable Energy Reviews*, vol. 69, pp. 596–609, Mar. 2017, doi: 10.1016/J.RSER.2016.11.191.
- [130] F. Ribeiro, P. Ferreira, and M. Araújo, "Evaluating future scenarios for the power generation sector using a Multi-Criteria Decision Analysis (MCDA) tool: The Portuguese case," *Energy*, 2013, vol. 52, pp. 126–136, Apr, doi: 10.1016/J.ENERGY.2012.12.036.
- [131] J. H. Lim, E. Hu, and G. J. Nathan, "Impact of start-up and shut-down losses on the economic benefit of an integrated hybrid solar cavity receiver and combustor," *Appl Energy*, 2016, vol. 164, pp. 10–20, doi: 10.1016/j.apenergy.2015.11.028.
- [132] M. Lei, J. Zhang, X. Dong, and J. J. Ye, "Modeling the bids of wind power producers in the day-ahead market with stochastic market clearing," *Sustainable Energy Technologies and Assessments*, 2016, vol. 16, pp. 151–161, doi: 10.1016/j.seta.2016.05.008.
- [133] C. Chen, Q. Zhang, Q. Ma, and B. Yu, "LightGBM-PPI: Predicting protein-protein interactions through LightGBM with multi-information fusion," *Chemometrics and Intelligent Laboratory Systems*, 2019, vol. 191, pp. 54–64, Aug. doi: 10.1016/J.CHEMOLAB.2019.06.003.
- [134] E. Al Daoud, "Comparison between XGBoost, LightGBM and CatBoost using a home credit dataset," *International Journal of Computer and Information Engineering*, 2019, 13(1), 6-10.

- [135] J. Magidi, L. Nhamo, S. Mpandeli, and T. Mabhaudhi, “Application of the random forest classifier to map irrigated areas using google earth engine,” *Remote Sens (Basel)*, 2021, vol. 13, no. 5, pp. 1–15, doi: 10.3390/rs13050876.
- [136] O. Caelen, “A Bayesian interpretation of the confusion matrix,” *Annals of Mathematics and Artificial Intelligence*, vol. 81, pp. 429–450, 2017, doi: 10.1007/s10472-017-9564-8.
- [137] “Compare Machine Learning Algorithms”, MLJAR, (accessed Nov. 25, 2022). <https://mljar.com/machine-learning/compare-ml-algorithms/>
- [138] “Fuel Consumption for Diesel Generators.” Green Mountain Generators (GMG). <https://greenmountaingenerators.com/2012/09/29/fuel-consumption-for-diesel-generators/> (accessed September 29, 2012).
- [139] G. Ali, H. N Musbah, H. H Aly, and T. Little “Hybrid Renewable Energy Resources Selection Based on Multi Criteria Decision Methods for Optimal Performance” *IEEE Access*, vol. 11, pp. 26773- 26784, 2023, doi: 10.1109/ACCESS.2023.3254532.
- [140] B. Genç and H. Tunç, “Optimal training and test sets design for machine learning,” *Turkish Journal of Electrical Engineering and Computer Sciences*, vol. 27, no. 2, p. 60, 2019, doi: 10.3906/elk-1807-212.

Appendix A

IEEE thesis competition

Dear Hmeda

On behalf of the Grid Edge Technologies Organizing Committee, it is my pleasure to inform you that after careful reviews, your dissertation titled "*Stationarity Analysis and Supervised Machine Learning Techniques for Energy Management Forecasting*" is selected for the final round of competition which will be held in San Diego.

Appendix B

I received this email from the editor of Electric Power System Research asking for a permission to use the papers that I published in the journal in my thesis.

epsr-thu@tsinghua.edu.cn

Hmeda Musbah

CAUTION: The Sender of this email is not from within Dalhousie.

Dear Hmeda:

For my understanding, the paper you published can be used in you thesis by default. This permission is naturally justified. Hope this letter helps. If not, you can draft one permission per the request of your University and I will sign it.

Best regards.

Chongqing

Chongqing Kang, FIEEE, FIET

Editor, Electric Power System Research

Professor & Dean, Department of Electrical Engineering

Tsinghua University,

Beijing, 100084, P. R. China

Tel: +86-10-62788166

Email: cqkang@tsinghua.edu.cn

epsr-thu@tsinghua.edu.cn

Appendix C

Published papers from this work

Journal papers:

1. H. Musbah, H. H. Aly, T. A. Little "A proposed novel adaptive DC technique for non-stationary data removal" Heliyon Journal, Elsevier publisher, 2023. (IF=3.7).
2. H. Musbah, G. Ali, H. H. Aly, T. A. Little "Energy management using multi-criteria decision making and machine learning classification algorithms for intelligent system" Electric Power Systems Research Journal, 2022. (IF=3.4).
3. H. Musbah, G. Ali, H. H. Aly, T. A. Little "Energy management of hybrid energy system sources based on machine learning classification algorithms" Electric Power Systems Research Journal, 2022. (IF=3.4).

Conference papers:

1. H. Musbah, H. H. Aly, T. A. Little "A Novel Approach for Seasonality and Trend Detection using Fast Fourier Transform in Box-Jenkins Algorithm" IEEE Canadian Conference on Electrical and Computer Engineering (CCECE), 2020.
2. H. Musbah, M. El-Hawary, H. Aly "Identifying seasonality in time series by applying fast Fourier transform" 2020 IEEE Canadian Conference on Electrical and Computer Engineering" IEEE Electrical Power and Energy Conference, 2019.
3. H. Musbah, M. El-Hawary "SARIMA model forecasting of short-term electrical load data augmented by fast Fourier transform seasonality detection" IEEE Canadian Conference of Electrical and Computer Engineering, 2019.